NTNU

Norwegian University of
Science and Technology

Reliable Power Cable Ground Screen Connections

Resistance of improper ground screen
connections exposed to heat cycles

Peder Severin Søndenå

Master of Energy and Environmental Engineering
Submission date: June 2018
Supervisor: Frank Mauseth, IEL
Co-supervisor: Hans Lavoll Halvorson, SINTEF Energi AS

Norwegian University of Science and Technology
Department of Electric Power Engineering

Project description

Several severe and costly service failures have occurred during the last years in the Norwegian distribution grid due to local overheating of power cables. The failures are believed to be related to the quality of the metallic ground screen and laminate connections close to cable accessories. The root cause of the failures are not fully understood. Today, no national or international standardized qualification test for such connections exist. The student project work is a part of a four-year research project on cable ground screen connections. The project is a co-operation between REN, Norwegian utilities, cable and equipment vendors and SINTEF Energy Research.

The work will be mainly experimental. For the study, samples will be obtained from the project participants.

It can be of interest to study the roll-spring connection equipment method. Parameters such as the transition resistance, resulting local temperature and the dimensional changes during constant load, load cycling and transient conditions can be studied. Also, the magnetic properties of the commercial available roll springs, impact of wrong installation and current distribution in the cable screen are interest to study.

Preface

The following report is the conclusion of my master's degree, completed during the spring of 2018. The thesis is credited with 30 credits, and has been carried out at the Department of Electrical Power Engineering at the Norwegian University of Science and Technology in co-operation with SINTEF Energy Research.

I would like to thank my supervisor Frank Mauseth and co-supervisor Hans Lavoll Halvorson for their support, guidance and help during this year. Further, I would like to thank Bård Almås, Svein Erling Norum, Aksel Andreas Reitan Hanssen and Morten Flå at the Department of Electrical Power Engineering for help with practical matters in the laboratory as well as production of necessary equipment. I also thank Horst Förster, Jørund Aakervik and Jan Arne Ervik at SINTEF Energy Research for their help and contribution with the experimental setup in the laboratory. Finally, I will also thank Oddgeir Rokseth for help with experimental equipment and Magne Runde for help and discussion on the theoretical matters of the project, both of SINTEF Energy Research.

Peder Severin Søndenå

Trondheim, Norway

June 2018

Abstract

The Norwegian power grid consists of an ever-increasing share of power cables. In Norway, the ground screen of the cable in distribution networks is usually grounded at each end of the cable length due to recommendations from the authorities. As a result, screen currents are allowed to flow through the ground screen due to the voltage induced in it by the current of the cable conductor and surrounding current carrying objects. The screen currents may vary from a few to several hundreds of amperes, depending on cable dimensions, load current and laying configurations. If this is not taken into consideration when designing the layout of the cable system, large screen currents may arise that can cause significant heating to occur in the cable screen and its connections.

Several breakdowns of power cables have occurred in the distribution grid, which are believed to be connected to the above mentioned topics. Because of this, a research project was initiated by REN AS with the goal of "establishing guidelines for testing and installation of ground screen connections to avoid future fault scenarios and to increase the reliability of the cable network" [1], and further use this knowledge as a basis to propose international standardization tests for ground screen connections.

The project has mainly been experimental, and focus has been to study the mechanisms of known fault scenarios in a typical ground screen connection.

Two types of ground screen connection designs were obtained from Norwegian equipment vendors. A test setup was built allowing six ground screen connections of each type to be tested. The cable ground screens and the ground screen connections were heat cycled by a DC current source. In addition, the cable conductors were heated by inducing current from a ring transformer and a variable voltage source. 25 heat cycles were conducted with the ground screen connections installed as explained in the installation manuals, before the same number of heat cycles were performed with the known improper installation on the two designs. The resistance of the ground screen connections was monitored with four-point resistance measurement before, during and between the heat cycles.

The results show that the improper installation of the ground screen connections increase the resistance drastically. With a screen current of 30 A, type I experienced a temperature increase close to that of the correct installation with 100 A. Type II saw an increased temperature with 30 A and improper installation compared to correct installation of the ground screen connection with 100 A.

Sammendrag

Det norske strømnettet består av en stadig økende andel av kraftkabler. I Norge er det vanlig at kabelens skjerm i distribusjonsnettet jordes i begge ender av kabelen på grunn av anbefalinger fra myndighetene. Som en konsekvens av dette vil en strøm flyte i kabelskjermen på grunn av spenningen indusert i skjermen av laststrømmen i kabelen og omliggende strømførende gjenstander. Skjermstrømmene kan ligge mellom noen få til flere hundre ampere, avhengig av kabeldimensjoner, laststrøm og hvordan kablene legges i kabelgrøften. Dersom dette ikke blir tatt hensyn til når kabelsystemet designes kan store skjermstrømmer oppstå, som vil kunne avgi vesentlig varme i kabelskjermen og dennes tilkoblinger.

Flere kabelfeil har funnet sted i distribusjonsnettet, hvor årsakene mistenkes å være i forbindelse med den overnevnte tematikken. Som et resultat av dette har REN AS iverksatt et forskningsprosjekt med hovedmål om "å etablere retningslinjer for testing og installasjon av skjermtilkoblinger i kraftkabler for å unngå fremtidige feilsituasjoner og for å øke kabelnettets pålitelighet" [1], og videre bruke dette som et grunnlag til å foreslå internasjonale kvalifikasjonstester for skjermforbindelser i denne typen kraftkabler.

Prosjektet som denne rapporten dekker har i hovedsak vært eksperimentelt, og fokuset har vært å undersøke mekanismene bak en kjent feilmontasje i skjermforbindelser.

To typer skjermforbindelsesdesign ble innhentet fra norske utstyrsleverandører. Et testoppsett ble lagd som tillot seks skjermforbindelser av hver type å bli testet. Kabelskjermene og skjermforbindelsene ble utsatt for varmesyklinger ved hjelp av en DC-kilde. I tillegg ble lederen i kablene varmet opp ved hjelp av en ringtransformator og en variabel spenningskilde. 25 varmesykluser ble gjennomført, først med skjermforbindelsene installert som forklart i installasjonsmanualene før the samme antallet varmesykluser ble gjennomført med den kjente feilinstallasjonen. Overgangsmotstanden i skjermforbindelsene ble overvåket med firepunkts motstandsmåling både før, under og etter varmesyklingene.

Resultatene viser at feilinstallasjonen i skjermforbindelsene gir en vesentlig økning i overgangsmotstanden. Med en skjermstrøm på 30 A oppnådde type I nesten tilsvarende temperaturøkning med feilinstallasjon som for den korrekte installasjon med 100 A påtrykt. Type II så en økning i temperatur med feilinstallasjon og skjermstrøm på 30 A, sammenliknet med korrekt installasjon og 100 A påtrykt.

Contents

Abbreviations

Abbreviation	Explanation	Unit
XLPE	Cross-linked polyethylene	
HDPE	High-density polyethylene	
LDPE	Low-density polyethylene	
PVC	Polyvinyl chloride	
PE	Polyethylene	
OSC	Outer semi-conductor	
T.O.	Test object	
EMI	Electromagnetic Interference	
a	Contact spot radius	[m]
A	Area	[mm^2]
A_a	Apparent contact area	[mm^2]
A_b	Load bearing area	[mm^2]
A_c	Contact area	[mm^2]
P	Mechanical load	[N]
H	Hardness	[N/mm^2]
U	Electrical voltage	[V]
ρ	Electrical resistivity	[Ωm]
ρ_0	Electrical resistivity at reference temperature 20 °C	[Ωm]
σ	Electrical conductivity	[S/m]
σ_f	Resistance per area of insulating film	[Ωm^2]
f	Power frequency, 50 Hz	[Hz]
ω	Angular frequency	[rad/second]
μ_0	Permeability in vacuum	[H/m]
μ_r	Relative permeability	[1]
ϵ_0	Permittivity in vacuum	[F/m]
ϵ_r	Relative permittivity	[1]
ϵ''	Imaginary part of permittivity	[F/m]
δ	Skin depth	[mm]
R	Electrical resistance	[Ω]
X	Electrical reactance	[Ω]
α	Temperature coefficient of resistivity	[1/K]
I_c	Conductor current	[A]
I_s	Ground screen current	[A]
$\vec{E}$	Electrical field	[V/m]
P	Electrical power	[W]
λ	Thermal conductivity	[W/mK]
T	Temperature	°C
T_0	Reference temperature 20 °C	°C

1 Introduction

1.1 Background

In the Norwegian distribution grid, it is custom to ground the end of the cable ground screen in each end of the cable length. As a result, a ground screen current will flow due to the voltage induced in the cable ground screen by the current in the cable conductor and surrounding current carrying objects. At cable jointing points, the metallic screen of the cable, in addition to the conductor, must be jointed in a satisfactory way to assure a low resistance path for the ground screen current through the entirety of the cable length. In addition, modern power cables usually consist of several metallic components in the cable ground screen, extending the issues of good electrical contact between ground screen parts not only to be a case at the cable ends, but through the entirety of the cable length. Severe faults have occurred regarding the mentioned cable parts in Norway, and although the number of reported faults in conjunction with these areas are not alarming, hidden figures are suspected in regard to it.

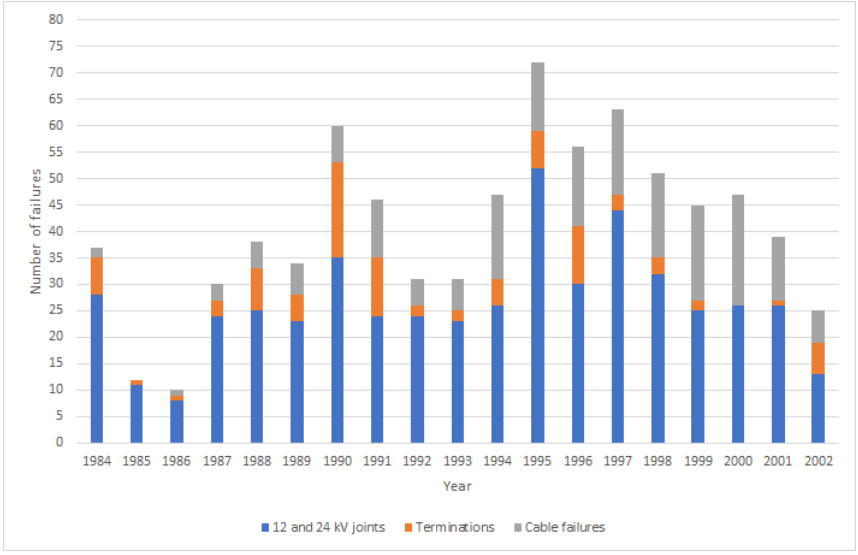

Figure 1.1: Figure showing the number of XLPE joint, cable and termination faults in the Norwegian distribution grid for the period 1984-2002 for 12 and 24 kV cables. The data is taken from SINTEF's report [2].

Because of the mentioned topics, a research program on power cable ground screen connections was initiated by REN AS in 2016, with SINTEF Energy Research, Norwegian utilities and cable and equipment manufacturers as partners [3]. The project will run to the end of 2019, with the intention of gaining a better understanding of the fault mechanisms causing the faults in metallic screens, and further use this knowledge to introduce standardization tests in this area of cable technology. The project is funded by the Norwegian Research Council [1].

1.2 Hypothesis

Prior to the project, SINTEF Energy Research acquired a failed cable joint for analysis. The cable joint was a cold shrink type, and upon delivery to SINTEF it consisted of both failed and non-failed joints. Upon dissection of the non-failed joint, it was seen that considerable heat had been present near the force springs in the jointing of the cable ground screen. Further dissection showed that the force spring which ensures mechanical connection between the copper wires and the joint ground screen was improperly installed, causing it to be in series between these two parts. The same improper installation was seen in the failed cable joint when opened. Analysis showed that the temperature in the non-failed joint had reached temperatures of 104-106 °C close to the outer semiconductor, causing sand to melt into the cable outer sheath. The differences between correct and incorrect force spring installation is shown with a cross section in figures 1.3 and 1.4, respectively. It is likely that the force spring made of stainless steel has led to an increased resistance when placed in series with the copper wires of the cable and the joint ground screen, as described by the flowchart in figure 1.2.

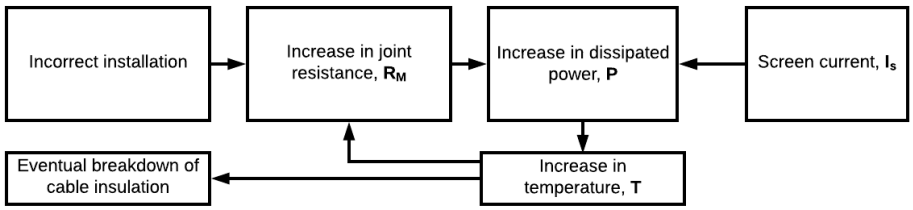

Figure 1.2: Flowchart showing the suspected mechanisms behind the known fault scenario, being the background for the master thesis.

The hypothesis of this master thesis is thus that the stainless steel layers of the force spring in series with the copper components in the ground screen connection leads to an increase in the resistance, further causing an increase in dissipated power leading to overheating of the outer sheath, semi-conductor and insulation, eventually causing a thermal breakdown of the joint and cable.

In this master thesis, two different ground screen connection designs have been studied, both used in cold shrink joint designs. The first design, type I, emphasize a design

were two force springs are used, while type II only use one. Type I is the type that was installed on the mentioned cable joint SINTEF Energy Reasearch acquired.

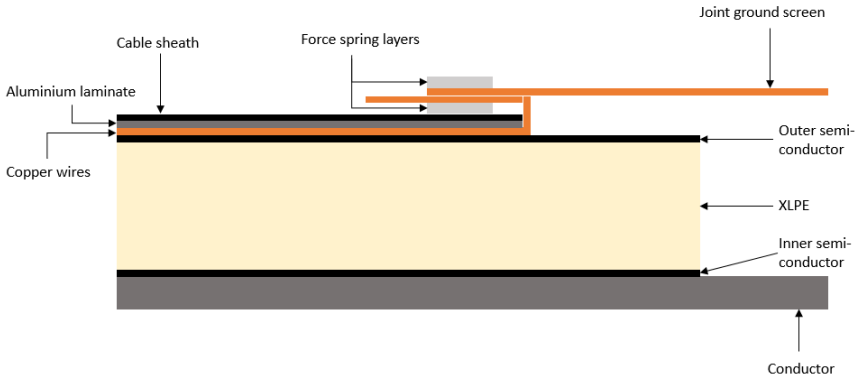

Figure 1.3: Figure showing a correct installation of the force spring in the ground screen connection arrangement. The copper wires and the joint ground screen are laid together in the force spring, with the force spring applying a mechanical load on them, ensuring a good electrical contact.

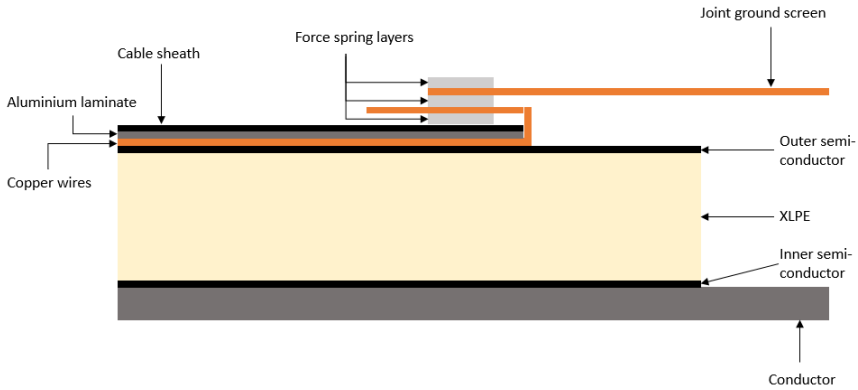

Figure 1.4: Figure showing an improper installation of the force spring in the screen joint arrangement. The force spring can be seen in series with the ground screen wires and joint ground screen, causing what is believed to be an increased resistance and reduced contact in the arrangement.

1.3 Objectives and approach

In order to investigate the above mentioned hypothesis, several tasks was performed:

- Design and building of a test setup to allow the installation of the two ground screen connection types.
- Decision of the best approach for measuring the voltage drop across the joint installation, to be able to calculate the ground screen connection resistances of each connection.
- Heat cycling with the ground screen connections installed as specified by the producers.
- Heat cycling with the ground screen connections installed in the known, improper way.
- Resistance measurement of the ground screen connections before and after the heat cycle series with a micro-ohm device.
- Resistance measurement of the test setup between each heat cycle of the two heat cycle series, to see if the same resistance values were obtained during load and no-load scenario.

1.4 Structure of the report

The structure of the report is as follows. Chapter two presents the relevant theory for the experimental work, ranging from cable design to contact theory. Chapter three gives a comprehensive explanation of the test setup made, measuring methods and cycling procedures used in the experiments. Chapter four gives a presentation of the results from the experiments and a discussion of these. In the two final chapters a conclusion is given, in addition to a suggestion of further work related to the work presented. The report also consist of several appendices with content ranging from heat cycle plots to data sheets, in order to complement the information given in the report.

2 Theory

2.1 Power cable structure

Figure 2.1 shows how a medium voltage power cable can be built. Although a lot of different designs exist, the figure gives a good impression of the main parts of the cable.

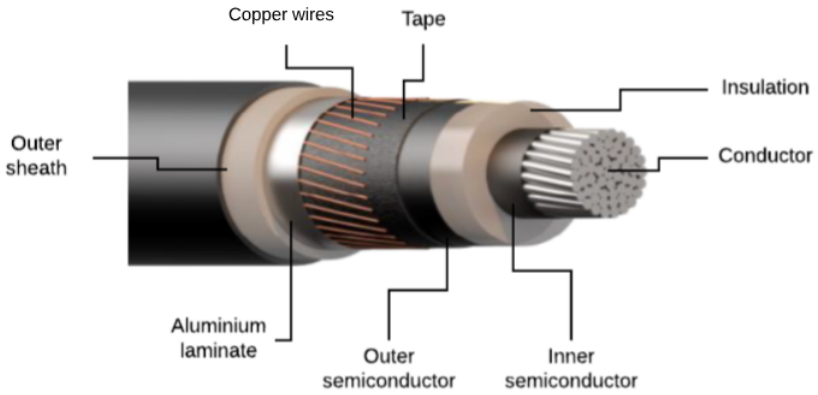

Figure 2.1: Picture showing the construction of a power cable typically used in the Norwegian distribution grid [4].

At the center of the power cable, the conductor is located. The purpose of the conductor is to carry the load current to the point of consummation. On the surface of the conductor, the inner semi-conductor is located. The purpose of the semi-conductor is to even out the electric field along the surface of the conductor. It is often extruded onto the conductor along with the main insulation. The main insulation is normally made of cross-linked polyethylene (XLPE), and must be applied in a sufficient thickness to be able to withstand the operational voltage as well as a certain over voltage. Outside the insulation another layer with semi-conductor follows with the same purpose as the inner semi-conductor. Then a layer of filler or tape may follow. These parts are often added with a swelling powder that will attract any water that could enter the cable axially. The copper wires (of the cable ground screen) is then laid either above or underneath the tape and fillers. Above the copper wires a laminate made by aluminium is added. The purpose of the copper wires and laminate is described in subsection 2.1.1. Above the aluminium laminate an outer sheath is added to provide mechanical strength and protection to the cable. In figure 2.1 the outer sheath consist of two parts, with the outer layer being semi-

conductive. This allows the sheath to be electrically tested after installation such that eventual faults to the sheath can be detected. Such a design is called TSLF.

It is important to keep in mind that many variations exist for which order the parts are added, and if they are added at all. To differentiate the different structures of the cable designs, a four-letter code system has been developed. This system is described in [5] and [6], and is summarized in the list below:

- 1st letter: Type of insulation
- 2nd letter: Sheathing
- 3rd letter: Armouring, screen
- 4th letter: Exterior sheathing, corrosion protection

Several configurations of the system letters above exist, but types of interest in this project are TSLE and TSLF, which both exploits a design with an aluminium laminate. The structure of these cables are summarized in table 2.1. Of the two types, TSLF is the type mainly in production today for use in onshore power grids.

Table 2.1: Design differences of TSLE and TSLF.

	1	2	3	4
TSLE	XLPE insulation	Filler/taping and concentric conductor	Aluminium laminate	Polyethylene
TSLF	XLPE insulation	Filler/taping and concentric conductor	Aluminium laminate	Semi-conducting polyethylene

2.1.1 Cable ground screen and aluminium laminate

The cable ground screen of the cable is usually made up of stranded copper wires, twisted helically around the cable arrangement. The cable ground screen has several purposes [7]:

- Protection for the surroundings in case of fault.
- Serve as a conductor for the charge and discharge currents in the cable.

The aluminium laminate is applied to prevent radial ingress of water that might cause water treeing and eventual breakdown of the cable. CENELEC HD620 [5] states that "provided there is electrical contact between the wire screen and the metallic tape its conductance may be regarded as part of the metallic screen." Hence, the aluminium laminate may effectively become a part of the cable ground screen. By exploiting this, the overall cross section of the copper wires can be reduced.

Several design concepts exists for the layout between the aluminium laminate and the copper wires. The copper wires and the aluminium laminate can either be laid in parallel with direct contact, or a semi conductive ribbon can be added between the two parts. The

use of different techniques with regards to this might lead to different degrees of contact between the copper wires and the aluminium screen.

Since cables usually are laid in groups of three, the current in each cable will act mutually on each other, causing a voltage to be induced in each of the cable ground screens due to the time dependent magnetic fields from the current carrying conductors. The induced voltage in the cable ground screen of a three phase cable system is dependent on the following factors [8]:

- The magnitude of the load current
- Laying configuration
- The spacing between each cable
- Resistance of the ground screen

When single core cables are used in distribution networks, two laying configurations are normally used: flat and trefoil configuration, as shown in figure 2.2. Flat configuration will provide additional spacing between the phases giving better thermal conditions, raising the current carrying capability of the system. The increased spacing will however lead to an increased reactance between the cables, giving higher induced ground screen voltages. Trefoil configuration will compared to flat have worse thermal conditions, but on the other hand less spacing, giving a reduction in the induced ground screen voltage. For the flat configuration the induced voltages will be largest and equal for the two outer phases, given equal spacing between the phases. For the trefoil configuration, the induced ground screen voltage will be equal in size for all three phases.

If additional groups of three phase cables are present in the same trench, the induced voltages will be further dependent on these cables.

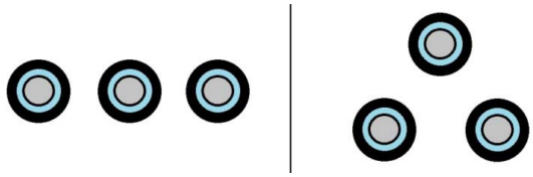

Figure 2.2: Figure showing the two laying configurations. Left: flat configuration. Right: trefoil configuration [9].

If the cable ground screen is grounded in one end only, it will act as an open circuit with a floating voltage on the open end. Depending on the operating voltage and length of the cable, this voltage might pose a threat to the cable insulation and surroundings if sufficient measures are not taken. To prevent this, the screen can be grounded in both ends. This will however lead to a current flow in the screen. In Norway, grounding of both cable ends is most common in the distribution grid which might be due to the recommendation given by the The Norwegian Directorate for Civil Protection (DSB) [10].

The mathematical background for the induced voltages and ground screen currents will be presented in section 2.3.

2.2 Cable jointing

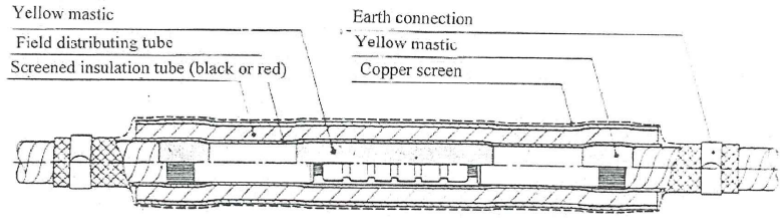

Figure 2.3: Picture showing the typical construction of a heat shrink cable joint. A constant force spring can be seen on each side with the label "Earth connection" [6].

Due to limitations during manufacturing, a cable is rarely manufactured in its full length to be used in the field. Hence, it is necessary to joint several cable lengths to provide the desired length. For medium voltage cables, jointing is usually performed on-site during installation which means that the execution and quality of the joint is much influenced by the installer. Combined with the difficulty of controlling the environment in which the jointing is performed, several faults might be introduced during the jointing.

Various types of cable joints exist, both heat shrink and cold shrink types. Heat shrink joints consists of several layers that are placed in a given order before being shrunk and fixed with the help of a blow torch. Cold shrink joint kits consists of one body which contains all the individual layers in a heat shrink joint. The joint body is then shrunk in place by removing a spiral from the inside of the joint body.

Just as for the main conductor, the cable ground screen must be connected and jointed in a satisfactory way across the joint. Several methods exist for this purpose, both soldering, the emplacement of contact plates and use of constant force springs.

Some jointing kits are delivered with an external joint ground screen (usually heat shrink joints) which is laid across the joint after the stress control tube has been placed, while the ground screen from each cable end are jointed with the use of a joint ferrule. Other cable joints emphasize a design where the joint ground screen is placed inside the joint body (usually cold shrink joints). Electrical contact is then ensured by using a clamping device in each end of the joint body, connecting the cable ground screens with the joint ground screen.

If the aluminium laminate and copper wires has sufficient contact across the cable length, or if sufficient contact is achieved at each side of the cable joint, it is important that the

copper wires has a big enough cross section area to conduct the current induced in the two conductive parts across the cable joint. This is because the aluminium laminate will not be present across the cable joint as it is removed along with the outer sheath. If the copper wires are not dimensioned for this, a bottle neck situation might occur, with a current density larger than what the copper wires can conduct. As a result, overheating of the cable ground screen might occur in the jointing because of cable design and not the design of the cable joint.

2.2.1 Constant force spring usage in cable joints

As mentioned in section 2.2, several methods exists for the jointing of the cable ground screen in cable joints. A common method is by using a component known as *spring roll* or *constant force spring* (hereinafter referred to as constant force spring or simply force spring). The constant force springs are used for several purposes, namely

- Attachment of joint ground screen to the conductive outer sheath in TSLF design, thus providing electrical contact across the joint for the outer conductive sheath.
- Attachment of aluminium plate to aluminium cable laminate in order to ground the aluminium laminate.
- Attachment between copper wires and joint ground screen.

The constant force spring is made up of a steel stripe of constant width which is rolled into a spiral. It can be applied where needed by unrolling it around the object on which it is meant to apply a pressure on. As seen in the list above, it is used for several purposes in cable joint designs as it allows easy connection between different parts without the need of heat (soldering) or any other tools. It is used in both medium and high voltage cable designs.

A disadvantage with constant force springs is directly connected to its advantage, the simple installation from the mechanical force it exerts. Easy application also mean that improper installation might occur. CIGRÉ B1.25 [11] states that it is important that the copper wires are spread out when cable ground screen jointing is performed, in order to avoid higher temperatures. In a constant force spring arrangement, bunching of the copper wires will cause the force spring to be lifted from parts of the arrangement it is meant to exert a pressure on. As a result, the force spring will exert less pressure on the copper wires in proximity to the bunched wires. The consequence is then that the degree of contact in the cable ground screen connection is reduced. In addition, the current density in the bunched wires will increase. The same paper also state that constant force springs should be avoided for cable designs were the designed screen current will exceed 200 A, as the use of force springs might lead to hot spots. Concerns regarding the installation of ground screen connections are also raised by CIGRÉ B1.22, in "Cable Accessory Workmanship on Extruded High Voltage Cables" [12] where to risks and required skills for this area are mentioned.

2.3 Electromagnetic background

2.3.1 Induced screen currents

Since the main purpose of the of the cable ground screen is to serve as a safety precaution in case of a fault, it must be grounded in either one or both ends of the cable length. Due to the alternating current in the cable conductor, as well as from the current in surrounding cables, a time dependent magnetic field will induce a voltage per length across the cable ground screen as given by equation 2.1, from [7]:

$$e_{ind} = I_c \cdot \omega \cdot M' = I_c \cdot 2\pi f \cdot \frac{\mu_0}{2\pi} ln \frac{2a_M}{d_M} = I_c \cdot f \cdot \mu_0 \cdot ln \frac{2a_M}{d_M} \qquad [\text{V/m}] \qquad (2.1)$$

Here, M' is the mutual inductance between conductor and ground screen per unit length and d_M is the mean diameter over the cable ground screen. a_M is the geometric mean distance of the flat configuration, while ω is the angular frequency given by $\omega = 2\pi f$.

Depending on whether single point or double point grounding is used, the induced voltage will give different issues, as explained in section 2.1.1. If grounding is performed at both ends of the cable screen, the screen ends will efficiently be shorted. Thus, an induced current will circulate in the ground screen given by equation 2.2 from [7].

$$I_S = \frac{e_{ind}}{\sqrt{{R'_M}^2 + {X'_M}^2}} \qquad [\text{A}] \qquad (2.2)$$

e_{ind} is the voltage induced in the ground screen as given by equation 2.1, while R'_M is the per length resistance of the ground screen. X'_M is the reactance per unit length of the ground screen, given by

$$X'_M = \omega M' \qquad [\Omega/\text{m}] \qquad (2.3)$$

Assuming the ground screen to be purely resistive, its resistance will be determined by equation 2.4

$$R = \rho \frac{l}{A} \qquad [\Omega] \qquad (2.4)$$

ρ is the materials resistivity. A low value means the material is a good conductor, while a high value is associated with the material being an insulator.

The induced current in the ground screen will be in the opposite direction of the load current in the cable conductor as a result of Lenz's law, and will give rise to ohmic losses in the screen as given by equation 2.5

$$P_{loss} = R_M \cdot {I_S}^2 \qquad [\mathrm{W}] \tag{2.5}$$

It is evident that a relatively small increase in the cable ground screen resistance can lead to large power dissipation due to this relation. An increased power dissipation will in addition lead to an increase in the temperature, increasing the resistivity and resistance of the cable ground screen, further increasing the power loss. This will be explained in section 2.4. Due to the increased temperature from this dissipated energy, the overall current rating of the cable system will be reduced.

2.3.2 Induced electromagnetic losses in power cables

Due to the alternating current in the conductors used in power cable networks, a magnetic field will be created which induce a current, opposing the current in the conductor. This will effectively push the current to the surface of the conductor, causing the current density through the cross section of the conductor to be non-uniform. This effect is called the *skin effect* [13].

Due to this effect, the resistance of a conductor will be greater when conducting an AC current compared to a DC current. However, the effect will not be prominent if the so called *penetration depth* is larger than the diameter of the conductor. The penetration depth is where the current density of the conductor is reduced by $1/e$, and is given by the following equation [13]

$$\delta = \sqrt{\frac{2}{\omega \mu \sigma}} \tag{2.6}$$

At a power frequency of 50 Hz, the penetration depth for copper with material properties as given by table F.1 in appendix F is approximately 5.4 mm. As is shown in appendix G and H, this is much larger than the diameter of the conductors of interest in this report. Hence, using DC instead of AC will not cause a source of error when it comes to skin effect.

The magnetic fields present in power cable networks might also cause closed circulating current loops to be induced in conductive parts, called *eddy currents*. For these eddy currents to occur, it is necessary for the conductive parts to have a certain magnetic permeability. The losses due to eddy current in force springs has previously been studied as a part of this project, and was found to be negligible [14].

2.4 Consequences of increased temperature

Figure 2.4 shows how the electrical resistivity and the thermal conductivity of metals change with an increasing temperature.

The resistivity of a metal is dependent on the metals temperature, and will change as given by equation 2.7

$$\rho = \rho_0(1 + \alpha(T - T_0)) \qquad [\Omega m] \tag{2.7}$$

Here, ρ_0 is the materials resistivity at temperature $T_0 = 20$ °C. α is temperature coefficient of resistivity, and gives the increase in resistivity per centigrade.

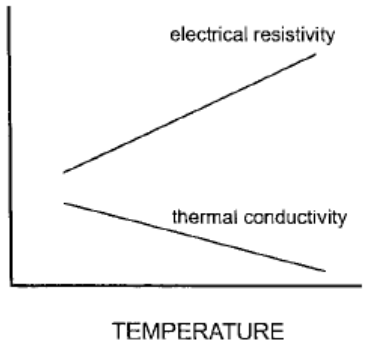

Figure 2.4: Schematic showing how the electrical resistivity and thermal conductivity is dependent on temperature in metals [15].

From figure 2.4, it can also be seen that the thermal conductivity λ decreases linearly with an increasing temperature.

Because of how these two properties in a metal change with temperature, an important observation can be done for current carrying metals. If the current I_s of equation 2.5 is of such a magnitude that sufficient heat is dissipated to increase the temperature of the conductor with resistance R_M, the resistivity of this metal will increase as given by equation 2.7, further increasing the overall resistance. Given a constant current I_s in equation 2.5, a further increase in the dissipated power will occur. The result might be a thermal runaway, with a closed loop of the above mentioned mechanisms.

As a result of the increasing temperature as explained above, the thermal conductivity of the metal(s) will decrease, causing the ability of heat transportation from the material to be reduced. This will then cause an accumulation of heat in the metal, further raising the temperatures.

Because of these mechanisms, a *hot spot* might be created in the cable system. If the hot spot temperature is larger than the maximum service temperature of the insulation mate-

rial, and the hot spot persists for a sufficient amount of time, the material might lose its mechanical and insulating properties.

Equation 2.8 gives the thermal breakdown strength of an insulation system with applied AC voltage [16]

$$U^2 = \frac{8}{\epsilon_0 \omega} \int_{T_0}^{T_{max}} \frac{\lambda}{\epsilon''} dT \qquad [\mathrm{V}^2] \tag{2.8}$$

Here, T_0 is the surrounding or surface temperature, while T_{max} is the maximum temperature in the insulation, which usually will be close to the conductor surface. It can be seen that an increase in the ambient temperature T_0 will reduce the voltage that can be applied on the cable. A reduction in the thermal conductivity λ will also give a reduced breakdown strength. Equation 2.8 is valid for AC voltage applications, but a much similar expression exists for DC applications.

2.5 Contact resistance background

2.5.1 Constriction resistance

The content of this chapter is mainly based on the works of Holm [17] and Ruppert [18].

When two electrodes in an electric contact are mated, the areas that seem to be in contact from a macroscopic view is called the *apparent contact area*, denoted A_a. However, since that the contact surfaces are not smooth in a microscopic point of view, only some parts of the electrodes will be in contact. This is known as the *load bearing area*, denoted A_b. The load bearing area of the contacts can be described by the mechanical load and the hardness of the electrodes, as shown in equation 2.9 [18].

$$A_b = \frac{P}{H} \qquad [\mathrm{m}^2] \tag{2.9}$$

Here, the hardness H [N/m^2] is a measure of a materials ability to oppose plastic deformation [19][20]. P is the mechanical load with unit [N].

From equation 2.9 it can be seen that the load bearing area is proportional to the applied force. Further, not all of the load bearing area will conduct the current through the contact. If oxide layers are present at the electrode surfaces, these will have to be pierced to make electric contact. This can either be done by mechanical force or by applying a sufficient voltage across the electrodes such that this oxide layer is ruptured. This area is then known as the *conductive area*, A_c. The three different contact areas are shown in figure 2.5.

Since the current has to travel from an electrode to another through a limited number of contact spots, an increased resistance will occur due to this reduction in cross section

area for the current. This resistance is known as the *constriction resistance*, R_c. This resistance depends on the resistivity of the material(s), radius and the shape of the contact spot [17], in addition to the total number of contact spots. The current lines through the these contacts spots causing the constriction resistance, is illustrated in figure 2.6.

If the cylinder in figure 2.5 did not consist of two members making up a contact but instead were a single solid cylinder with the same end-points a and b, its resistance could be calculated by either equation 2.4 or Ohm's law, denoted R^0_{ab}. By dividing the cylinder in two and mating the ends like a contact, a slightly increased resistance would be measured from Ohm's law (equation 2.4 can not be used with a contact) due to the constriction resistance, now denoted R_{ab}. By using equation 2.10 as proposed by Holm [17], the constriction resistance is found as

$$\boldsymbol{R} = R_{ab} - R^0_{ab} \qquad [\Omega] \tag{2.10}$$

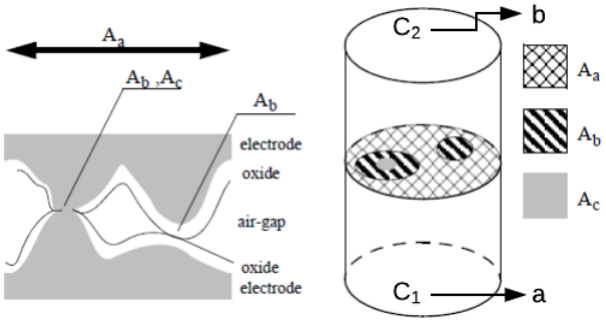

Figure 2.5: To the left: cross-section of surfaces between to conductors, showing the apparent contact area, A_a, the load bearing area, A_b and the conductive area A_c. The same areas are seen to the right, but in a cylindrical contact [18].

The resistance of a single constriction in a *monometallic* electrode is given by equation 2.11

$$R_c = \frac{\rho}{4a} \qquad [\Omega] \tag{2.11}$$

Here, a denotes the radius of the contact spot.

Since an electrical contact consist of two electrodes, the total constriction resistance of the so called *a-spot* will be twice that of equation 2.11.

$$R_c = \frac{\rho}{2a} \qquad [\Omega] \tag{2.12}$$

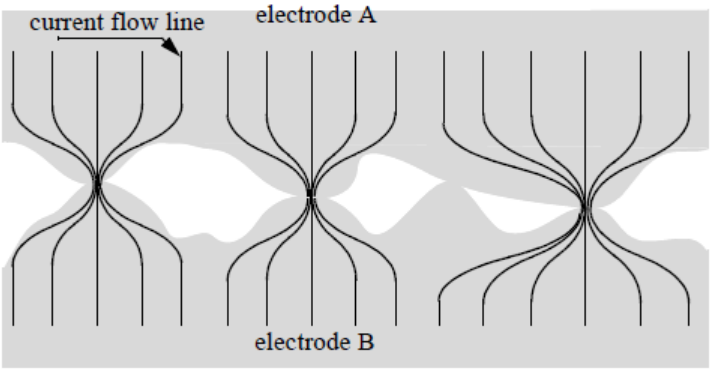

Figure 2.6: Figure showing how the current is forced through the points of contact [18].

Equation 2.12 is valid for circular contacts spots, with the contact spot radius much smaller than the radius of the cylindrical contact members [15], as seen in figure 2.5. It is also assumed that the contact members are of the same material, hence having the same resistivity.

If the contact members of the contact are made of two dissimilar metals, the contact is called *bimetallic* and a single constriction resistance is given by equation

$$R_c = \frac{\rho_1 + \rho_2}{4a} \qquad [\Omega] \tag{2.13}$$

The above equations give the constriction resistance for a contact with only one conducting contact spot. However, a contact usually consist of several contact spots between the contact members, as illustrated in figure 2.6. When several a-spots occur between the members in the contact, the total constriction resistance of these spots can be added as the sum of parallel connections, given that the spots are not to close too each other, such that they do not connect [18]

$$\frac{1}{R_{c,TOT}} = \sum_n \frac{1}{R_n} \qquad [1/\Omega] \tag{2.14}$$

Here, the subscript n denotes the constriction resistance number.

The constriction resistance and the internal material resistance of a contacts members are usually not the only contributions to the overall contact resistance. The contact members will often be covered by an oxide layer which have a lower conductivity than the internal material of the contact member(s), further increasing the overall resistance. This oxide layer may either be the result of the metals reaction to oxygen and other chemicals, or may have been added during manufacturing. The resistance due to these oxide layers are given by equation 2.15

$$R_f = \frac{\sigma_f}{\pi a^2} \qquad [\Omega] \tag{2.15}$$

Here, σ_f is the resistance per area of film, while a is the radius of the contact spots as previously used.

The total constriction resistance of a contact can now be found by combining equation 2.12 or 2.13 depending on equal or unequal materials, before adding the increased resistance due to the film with equation 2.15, and then calculating the total constriction resistance of the parallel resistances

$$R_n = R_c + R_f \implies \frac{1}{R_{c,TOT}} = \sum_n \frac{1}{(R_c + R_f)_n} \qquad [1/\Omega] \tag{2.16}$$

As illustrated in figure 2.5, the oxide layer of two contact members might cause two asperities that are in contact with each other to in fact be insulated from another. This is usually the case when contact members are mated, meaning that the oxide layer must be removed or ruptured in order to allow flow of current to occur. This can either be done by mechanical removal of the layer, or by a process known as *fritting* (not to be confused with fretting). Fritting further consist of two mechanisms, A-fritting and B-fritting [18]. A-fritting occurs when the electrical field $\vec{E}$ across two contact members reaches a sufficient level where the oxide layer of the contact members is ruptured, causing metal to metal contact between the members. B-fritting occurs when the current flow through an a-spot, originally initiated by A-fritting, is further widened.

2.5.2 Contact resistance as a function of pressure

By combining the equation for the load bearing area, equation 2.9, and the general expression for the resistance R equation 2.4, and further defining the area of equation 2.4 as A_b, the following equation can be derived.

$$R = \frac{\rho \cdot l \cdot H}{P} \qquad [\Omega] \tag{2.17}$$

Assuming a constant hardness and length of the contact resistance, R will be a function of pressure in the contact as well as the temperature in the contact area. Further, assuming the temperature to not be a governing contributor to the overall resistance, equation 2.17 can be written as [21]

$$R = kP^{-x} \qquad [\Omega] \tag{2.18}$$

Here, $x = 1$ for the transformation of equation 2.17 to equation 2.18. Kongsjorden [21] gives that x varies depending on whether elastic or plastic deformation occurs in the contact, with

$x = 1/3$ for elastic deformation
$x = 1/2$ for plastic deformation

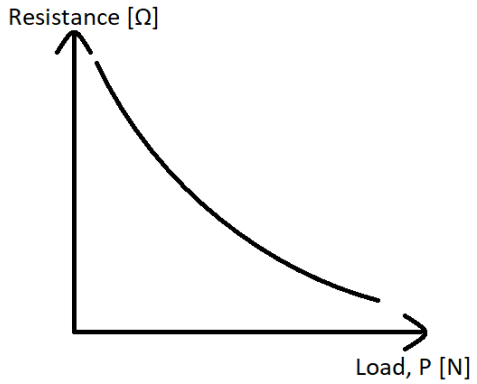

Figure 2.7: Figure showing the contact resistance varying as a result of changing load, based on a similar figure in [21].

For a contact consisting entirely of metal, the thermal expansion due to an increased temperature might not be prominent, due to metals having a relatively low coefficient of thermal expansion. However, if the arrangement is part of a greater system consisting of thermoplastic or thermosetting materials that might be exposed to heating and hence thermal expansion, these components can cause a pressure to be exerted on the contact arrangement as they have a much larger coefficient of thermal expansion than the metals used in current conduction (see table 2.2), and will thus expand much more than metals. This might lead to a reduction in the contact resistance, as proposed by equation 2.17 and 2.18. A power cable is such a system, consisting of much plastic material which will expand when heated.

Table 2.2: Table showing the coefficient of thermal expansions for relevant materials in this project. A larger coefficient in the table is associated with a greater thermal expansion when exposed to an increased temperature.

Material	**Coefficient of thermal expansion [$10^{-6}/K$]**
Stainless steel 1.4310	17.0 [22]
Cu	16.5 [23]
Sn	23.0 [23]
XLPE	320.0 [16]
HDPE	320.0 [16]
LDPE	150.0 [16]

3 Experimental method

The following chapter will give a description of the experimental work performed as a part of the project work, namely

- Test object preparation
- Ground screen connection types and installation method
- Resistivity measurement of joint ground screen and test objects
- Test setup configuration
- Heat cycling procedure
- Correction of ground screen connection resistances

3.1 Test object preparation

Both the test objects and the reference cables were made of the same cable type, a cable with TSLF design and parameters as given in table 3.1. The ground screen design of the cable consists of copper wires wound helical around the outer semiconductor, with a tape lying in between the two. The aluminium laminate is applied directly above and on the copper wires, and glued to the outer sheath. Information regarding the resistivity and cross section of the copper wires alone is given in appendix H.

The reason for choosing this cable design and the dimensions was that the TSLF/TSLE design was of particular interest of study in the main research project, mainly due to the interaction between the aluminium laminate and the copper wires. In addition, the mentioned dimensions would be more fitted for recreation of the known fault installation. A cable with either a larger conductor cross section area or insulation level would require more powerful equipment to be used, reducing the available space, as well as using more time before reaching temperatures of interest in the project. Choosing a cable type with smaller dimensions could have been done, but since the 24 kV cable was available as a part of the main project, this cable was chosen.

In the following subsections, a *test object* (T.O.) is defined as a cable piece of the mentioned design, customized in such a way that a ground screen connection could be installed on each end of the cable piece.

Table 3.1: Table showing the parameters of the cable type from which the test objects were made. The dimension of the metallic ground screen is the sum of the copper wires and the aluminium laminates cross section areas. For specific information regarding the copper wires, see appendix H.

Dimension	Unit	Size
Insulation level	[kV]	24.0
Outer diameter	[mm]	38.5
Diameter across insulation	[mm]	29.6
Minimum thickness insulation	[mm]	4.85
Conductor cross section	[mm^2]	240
Metallic screen cross section	[mm^2]	35.0

3.1.1 Test objects

For each ground screen connection type, three test objects were prepared to be connected in series, giving the opportunity of six ground screen connections to be tested. The dimensions that these objects were crafted to, can be seen in figure 3.1. A picture of a finalized test object (for type I) can be seen in figure 3.2.

By using three test objects, the total number of ground screen connections for each type would be six, increasing the statistical basis to be used in the results and the discussion. This was favorable, due to the reason that each connection would differ from one another because of stochastic variations during installation.

The dimensions as shown in figure 3.1 was chosen to maximize the available space in the laboratory, while also ensuring that there was sufficient spacing between adjacent ground screen connections such that they would not influence each other thermally.

The section for the voltage measurement was set to a width of 20 mm (seen as two white rectangles in figure 3.1), as this would be sufficient to get the voltage measuring point in form of a twisted copper wire in place, while maintaining as much as possible of the outer sheath. In these measuring areas, the fillers laying between the copper wires and the aluminium laminate was removed to allow a better connection of the voltage measuring points. The fillers below the copper wires was left in place.

The length of the outer sheath between the 20 mm section and the XLPE/OSC (**o**uter **s**emi-**c**onductor) was set to 65 mm. The reason for this was that when trying to reduce the length below this, the outer sheath would become more exposed to acting forces, both radially and axially on the piece, making it come lose and being able to move. Making this piece of the outer sheath longer would better these conditions, but would also increase the distance between the voltage measuring point on the copper wires and the actual ground screen connection.

Each test object was fitted with 240 mm^2 cable lugs in each end, with a bolt hole of 12 mm.

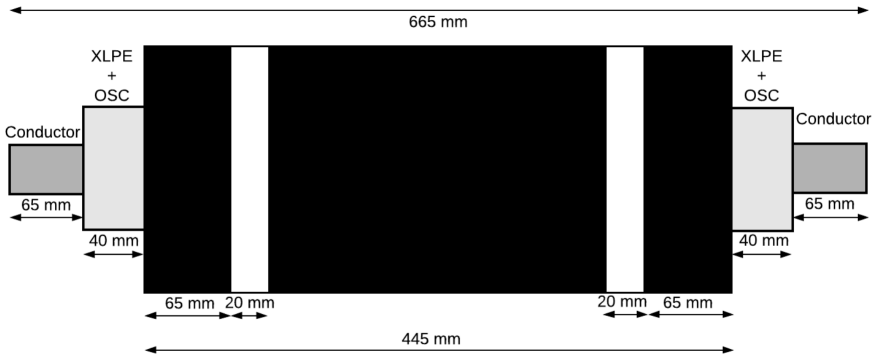

Figure 3.1: Figure showing the measures of each test object for type I and type II. The white area is where the outer sheath was removed to connect the voltage measuring points. The black areas are where the outer sheath was kept intact.

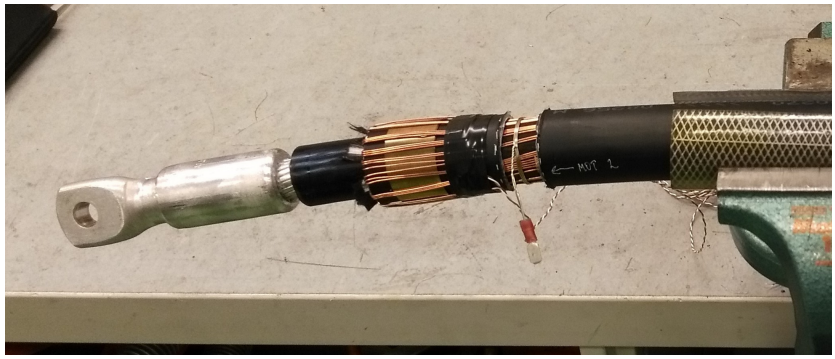

Figure 3.2: Picture showing one side of a finalized test object. From the left: cable lug, inner force spring (type I) with the copper wires bent across and above, thermocouple lying below the force spring and voltage measuring point attached at the copper wires where the outer sheath is removed. The picture is axisymmetric around the right edge of the picture.

3.1.2 Reference test objects

For each ground screen connection type, a reference test object was made to be connected in series with the test objects. The purpose of the reference objects was to monitor the reference temperatures of the conductor, cable ground screen and outer sheath of a similar cable where the ground screen connection was not installed. The measures of these reference cables are shown in figure 3.3, with a finalized reference test object in figure 3.4.

Each test object was fitted with 240 mm^2 cable lugs in each end, with a bolt hole of 12 mm.

The reason for making two reference cables in the setup, was to allow the possibility of testing with different cable ground screen current levels in the two designs at the same time. In such a case, the temperature development would be different in the two types, making two reference cables necessary.

IEC 61442 "Test methods for accessories for power cables with rated voltages from 6 kV up to 30 kV" [24], gives suggestions for the determination of the cable conductor temperature. Here, it is specified that a reference cable of this kind should have a minimum length of 2 m, with the thermocouples placed 0.5 m from the cable ends. However, having two reference cables of this length in the test setup would be impractical due to the available space in the laboratory, and the dimensions in figure 3.3 was chosen instead.

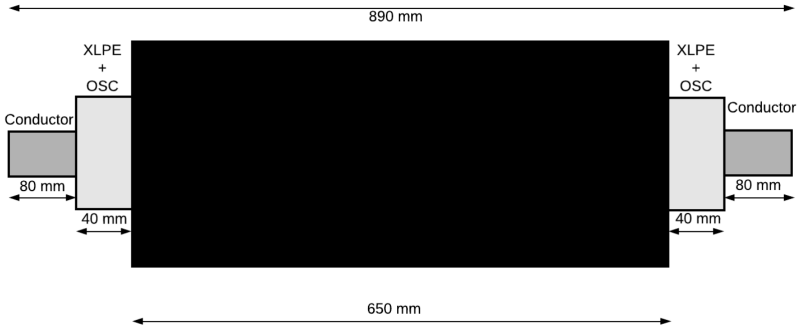

Figure 3.3: The measures of the reference test object for each type. The copper wires enter the reference cable where the outer sheath begins, after XLPE+OSC. Black colour indicates the outer sheath.

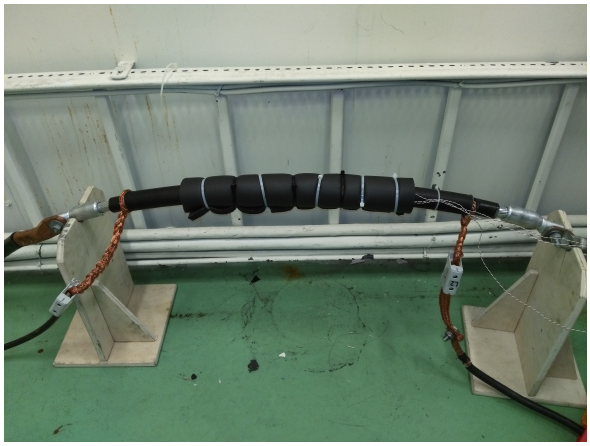

Figure 3.4: Picture of a finalized reference object, with thermal insulation applied. Screen and conductor connections can be seen on the cable ends. In addition the thermocouples are seen on the right side.

3.1.3 Voltage measuring points on test objects

To measure the voltage across the ground screen connection both during testing and between tests with the micro-ohm meter, it was necessary to access the screen of each test object for each ground screen connection. Since the test objects exploits a TSLF design where the aluminium laminate and the copper wires are laid in direct contact, it was possible to connect the voltage measuring point at both components. However, it was decided to measure directly at the copper wires and not the aluminium laminate, by removing the aluminium laminate and the outer sheath. The reasons for this was:

- Reproducibility. If the aluminium laminate had been chosen as the part to be measured on, the outer sheath would have to be removed. The outer sheath and the laminate is glued together, which means that a heat source would have to be used when removing the sheath. When this method was tested, it was seen that for some parts the laminate would be compressed into the copper wires increasing the degree of contact between the two, while for other places of the object the laminate would be lifted, causing a reduction in the contact between them as seen in figure 3.5a and 3.5b, respectively. Additionally, the aluminium laminate is made up of a aluminium sheath which is glued together axially, with a bit of overlap. If the solution with measurement on the laminate had been chosen, care should have been taken to ensure that the outer sheath was removed along the wrapping direction of the laminate such that the laminate was not unwrapped or damaged. A cross section where the sheath was removed would often consist of both of the mentioned cases around the circumference of the cable, when this method was tested. In addition, measures would have to be carried out to remove or reduce the impact that the aluminium oxide layer would cause during measuring, as well as remnants of glue. The mentioned factors above are also included in CIGRÉ B1.22 report [12], highlighting these difficulties and the training required to carry out the process in a satisfactorily way.

- The fact that the copper wires would be the component that would transfer the current from the cable ground screen into the joint ground screen, as seen in figure 1.3. Measuring on the laminate would thus lead to unnecessary increase in resistance, since the measuring would be performed on a component which would not conduct the current I_s through the ground screen connection.

The chosen solution with measuring carried out directly on the copper wires, can be seen in figure 3.20b.

The approach chosen, with measurement carried out on the copper wires would still leave the aluminium laminate in place for the part of the cable sheath between the measurement window and the ground screen connection. Thus, this aluminium laminate would lie in parallel with the copper wires for this part, which could lead to some of the current to travel through this conductive part. But since the laminate itself not was connected to a source, the effect of having this parallel element in the sheath with its associated voltage drop, was considered to be negligible.

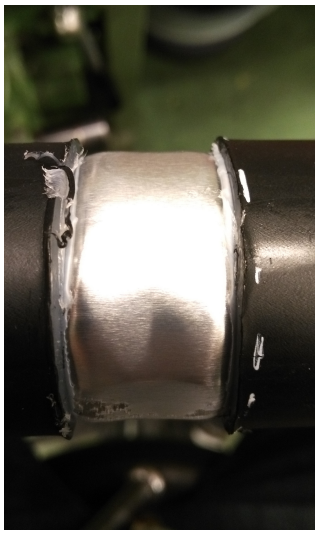

(a) Picture showing how the laminate was lifted when the outer sheath was removed.

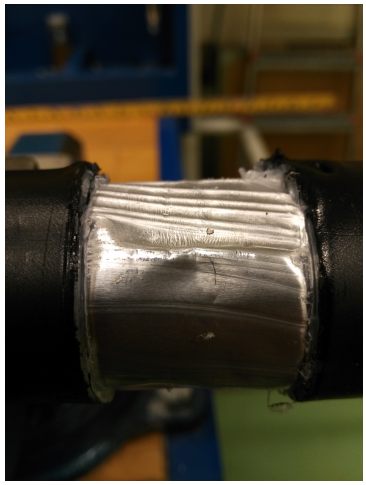

(b) Picture showing the laminate wrapped around the copper wires, when trying to remove the outer sheath of the cable. Remnants of glue can also be seen.

Figure 3.5: The two cases that was experienced when trying to remove the outer sheath with the use of heat.

3.2 Ground screen connection types

The ground screen connection solutions investigated in this project are both of the cold shrink design from two different manufacturers, called type I and type II. Both designs exploit a ground screen connection solution where the copper wires are jointed together across the cable joint by the help of a braided joint ground screen which is connected to the copper wires on each side of the joint by mechanical force exerted by force springs.

3.2.1 Force springs

Table 3.2 shows the parameters of the different force springs supplied with the two ground screen connection types, with a picture of the springs in figure 3.6. Type I uses a design with two force springs, one small and one large. Type II use only one spring, which replaces the two springs of type I.

Table 3.2: Comparison of the different force springs used in the experiments.

	Type I, small	Type I, large	Type II
Inner diameter [mm]	22	22	24
Outer diameter [mm]	23	27	29
Width [mm]	25	25	16
Thickness [mm]	0.3	0.3	0.44
Length [mm]	230	700	505
Min usage [mm]	NaN	30	31
Max usage [mm]	NaN	39	50

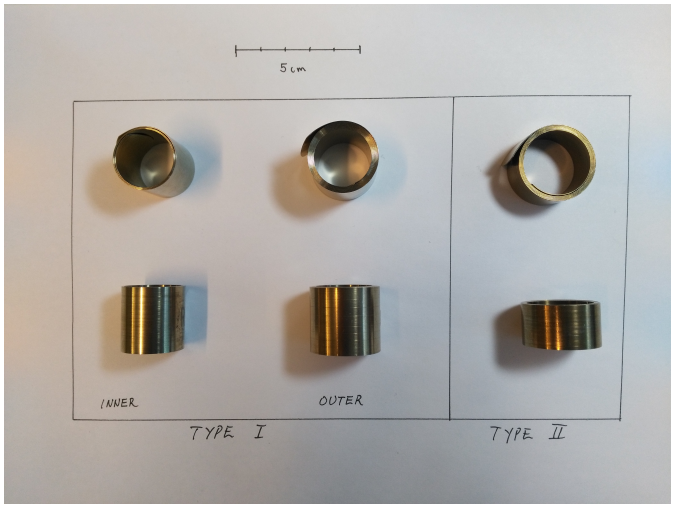

Figure 3.6: Picture showing the different force springs used in the experiment.

3.2.2 Installation of ground screen connections

Although the two types both are used in cold shrink cable joint design and comprise of the same basic elements, the way they are installed vary a bit.

Correct installation of ground screen connections

Type I

Type I uses two almost identical force springs, the only difference being the length of the two, as can be seen in table 3.2. The shortest (smallest) force spring is attached directly onto to the outer sheath of the cable in a range of 40 mm from where the sheath was removed. The copper wires are then laid back above the force spring, and cut in 40 mm length before being attached and held in place with PVC tape. Then, the braided joint

ground screen in the joint body is laid back above the copper wires, and the long (large) force spring is applied with two turns right above the small spring, copper wires and joint screen. The ends of the braided screen are then placed back inside the force spring, and the rest of the spring is applied. Three layers of PVC tape is then applied across the force spring arrangement.

Since the installation manual only specify that the force springs should be placed somewhere in an area of 40 mm from the end of the outer sheath, it was decided to place it 10 mm from the edge of the outer sheath.

Although not specified for the type, the remnants of the braided copper screen were laid back on top of the outer force spring after being cut. The reason for this was to have some margin that could be used when the improper installation was to be carried out.

If a complete joint kit were to be installed, the joint arrangement would also be covered by the joint kits outer sheath. As a replacement for this, thermal insulation was used, see section 3.4.3.

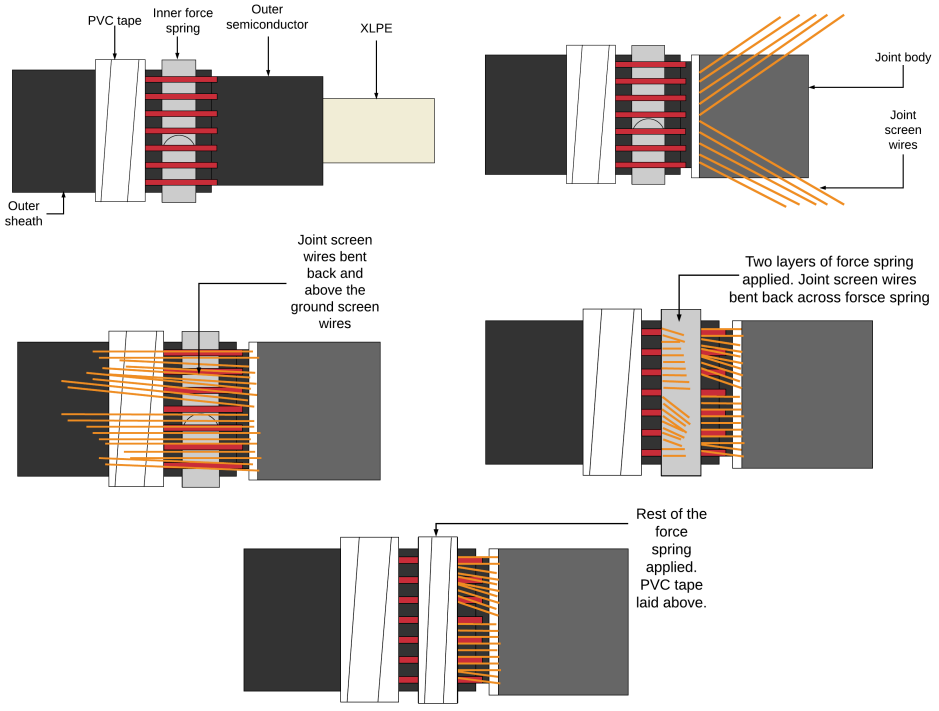

Figure 3.7: Installation procedure for type I. The red rectangles illustrates the copper wires of the cable.

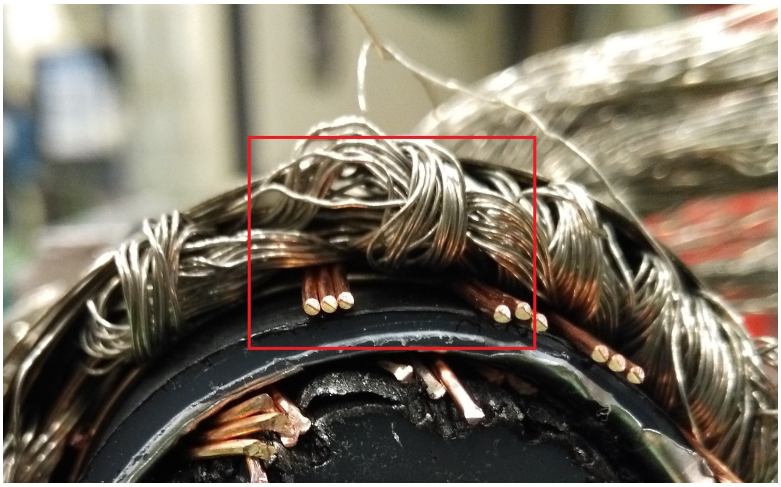

Figure 3.8: Picture showing the cross section of a correctly installed ground screen connection of type I. The cross section is taken from what would be the cable side of the joint in an installation. It can be seen that the copper wires and the joint ground screen is in direct contact (red box).

Type II

Type II only use one force spring, replacing the two used in type I. Here, the force spring is applied with one turn directly onto the outer sheath of the cable. Then, the copper wires are laid back onto the force spring layer together with the braided joint ground screen from the joint body above the copper wires, before the rest of the force spring is applied. What is left of the braided screen on the cable side of the joint is folded back over the force spring, and covered with one layer of PVC tape.

As for type I, the manual does not specify where the force spring should be placed in the 40 mm area from the edge of the outer sheath. Thus, as for type I, it was placed 10 mm from the end of the sheath.

Although the manual for type II specifies that the force spring should be covered by one layer of PVC tape, three was used instead. The reason for this was to make sure that the thermal conditions were close to identical for the two types, as well as being necessary to protect the Armaflex thermal insulation from scratches and damages that could be inflicted by the tips of the braided screen strands.

If the complete jointing kit were to be installed, a water barrier and the outer sheath would also be placed above the screen connection.

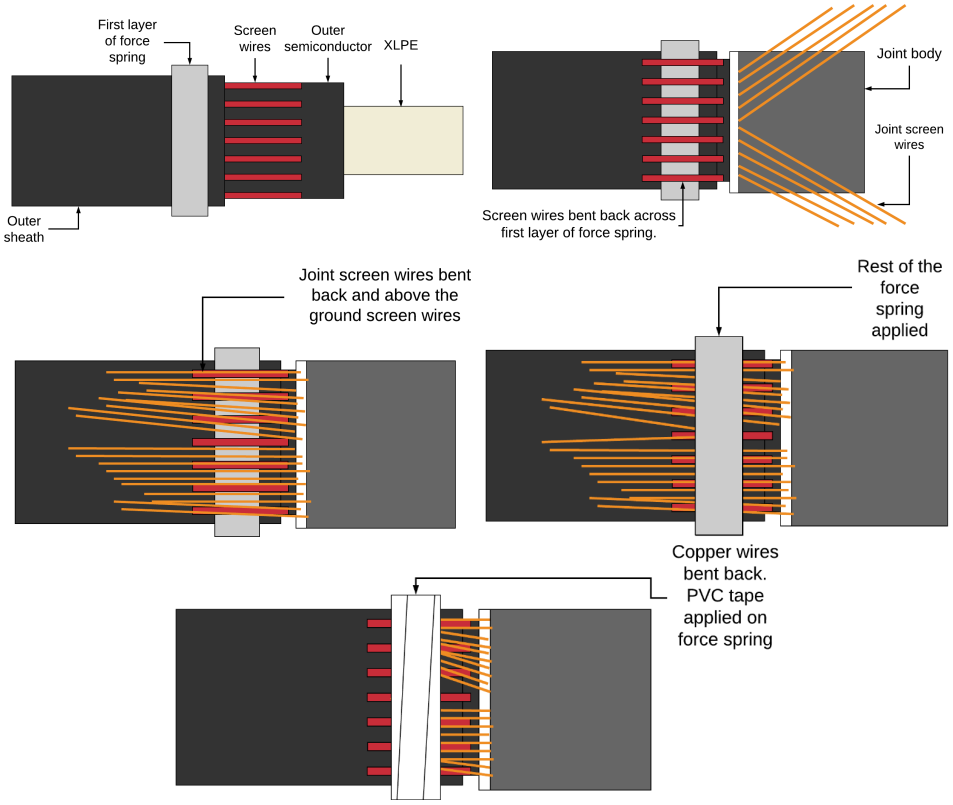

Figure 3.9: Installation procedure for type II.

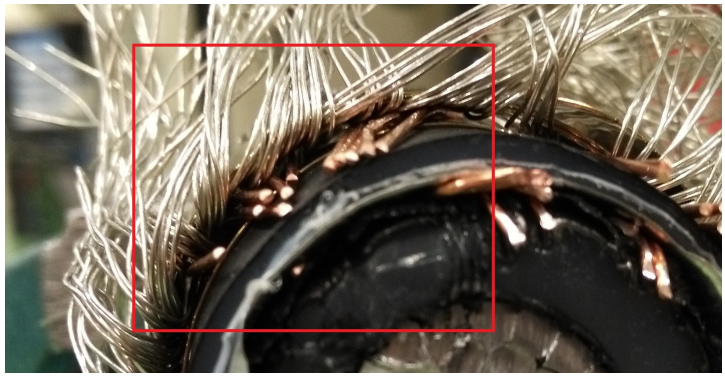

Figure 3.10: Picture showing the cross section of a correctly installed ground screen connection of type II. The cross section is taken from what would be the cable side of the joint in an installation. It can be seen that the copper wires and the joint ground screen is in direct contact (red box).

Incorrect installation of ground screen connections

In the following section, descriptions of how the incorrect installation was performed for the two types will be explained.

Although the fault experienced in the field had two layers of the force spring in series with the ground screen connection, it was chosen to only study the impact of one layer. The reason for doing so was to understand the main mechanisms behind the fault installation, the transition from copper wires to steel layer, current conduction through the layer, and transition from steel layer to joint ground screen.

Type I

- The arrangement with the small force spring was left untouched, with the copper wires still in place over it.
- One round of the outer force spring was applied above and onto the copper wires.
- Then the joint ground screen was applied above the force spring layer.
- The rest of the installation followed the installation manual. Two layers of the force spring was applied before the remnants of the braided screen was bent back into the force spring. The ends were then bent back on the top of the force spring, with three layers of PVC tape applied. Care was taken to make sure that these ends were placed at the force spring surface, such that they would not make contact that could improve the connection in such a direction that it would behave more like a correct installation.

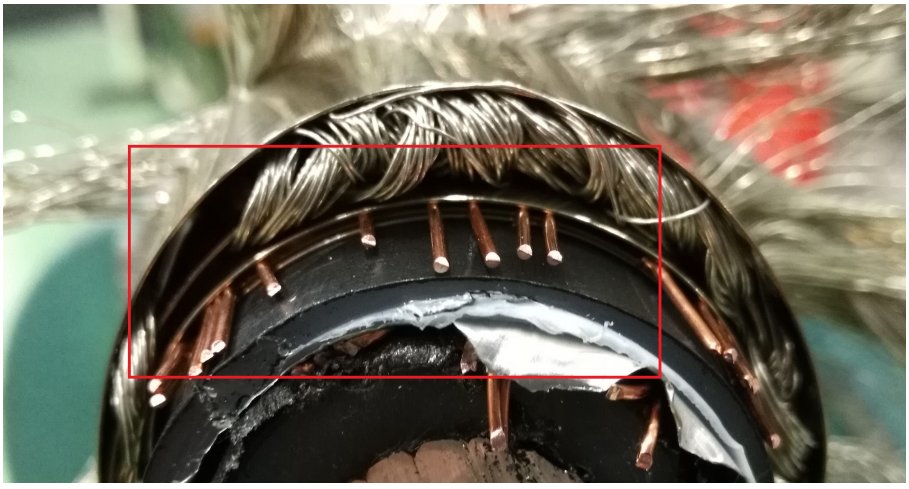

Figure 3.11: Picture showing the cross section of an incorrectly installed ground screen connection of type I. The cross section is taken from what would be the cable side of the joint in an installation. It can be seen that the copper wires and the joint ground screen is separated by a layer of the force spring (red box).

Type II

- One turn of the force spring was applied directly on the outer sheath of the cable.
- Then the copper wires were bent back across the force spring layer.
- Another layer of the force spring was then applied across the copper wires.
- The joint ground screen was applied.
- The rest of the force spring was applied as specified in the installation manual.
- The remnants of the joint ground screen was bent back across the force spring, and fastened with three layers of PVC tape. Care was taken to make sure that these ends were placed at the force spring surface, such that they would not make contact that could improve the connection in such a direction that it would behave more like a correct installation.

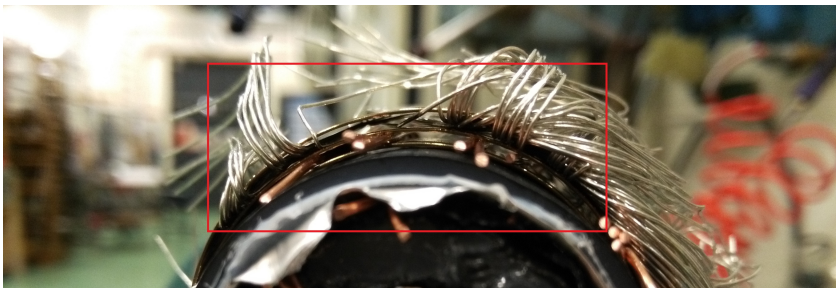

Figure 3.12: Picture showing the cross section of an incorrectly installed ground screen connection of type II. The cross section is taken from what would be the cable side of the joint in an installation. It can be seen that the copper wires and the joint ground screen is separated by a layer of the force spring (red box).

3.3 Determination of initial resistivities

3.3.1 Joint ground screen resistivities

To determine the resistivity of the braided joint ground screens, four-point resistance measurement was performed. The measurements were carried out using a micro-ohm meter.

The joint ground screen was applied on a plastic tube with outer diameter of 50 mm and length 500 mm. Tinned copper wire with a diameter of 0.68 mm was then applied in four different places by twisting as shown in figure 3.13 to accommodate connection for the current and for the voltage measuring as suggested by IEC 61284 [25]. Care was taken such that the twisted wires were not bunched.

The area of the joint ground screen was determined by measuring the diameter of the strands with a micrometer, and counting the total number of strands in the screen.

To gain sufficient accuracy when measuring the resistances, the micro-ohm meter device was set to a test current of 10 A with an accuracy of 0.1 μΩ. The "normal mode" on the instrument with current applied in both forward and backward direction was used, with the registered resistance being the mean value of these measurements. By doing so, the thermocouple effect, creating a voltage difference between dissimilar metals is cancelled. The current and voltage points were not moved after connection. Ten measurements were carried out for each joint ground screen.

The micro-ohm device does not correct the registered resistance with regards to a reference temperature. Thus, this had to be performed manually after testing by using equation 2.7. The ambient temperature therefore had to be registered during the measurements.

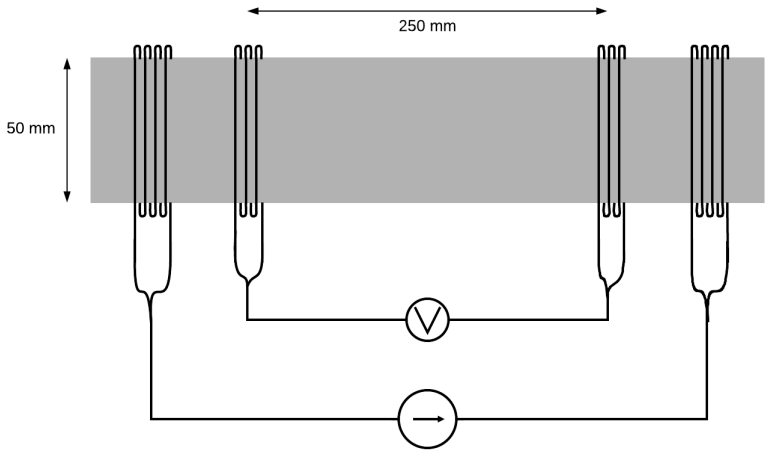

Figure 3.13: Schematic showing the four-point measurement of the joint ground screen resistivities.

Figure 3.14: Figure showing the joint ground screen supplied with each ground screen connection type. On the top: type I, on the bottom: type II. It can be seen that type I is rougher than type I. Type II is more compressed when delivered than type I.

3.3.2 Test object resistivities

After the cable pieces had been modified into the desired test objects, the resistivities of the copper wires of each T.O. was determined in the same way as for the joint ground screens in section 3.3.1. The only difference made was that the distance between the voltage connection points on the test objects was increased to 495 mm.

The total area of the copper wires was calculated by measuring the diameter of the individual strands with the use if a micrometer, and then counting the total number of strands.

3.4 Laboratory setup

3.4.1 Conductor jointing and thermocouple fitting

By having three test objects connected in series with cable lugs, a test object could be removed if it were to be damaged during testing.

For each ground screen connection, a thermocouple was placed on the outer sheath of the cable, underneath the force spring. The reason for this placement was that the heat development in the force spring and its impact on the outer sheath and further into the insulation was of interest (see figure 3.15). The end of the thermocouple was placed underneath the middle of the force spring width, meaning a distance of 23 mm from the end of the cable sheath for type I, and 18 mm for type II, due to the fact that the edge of both force springs was placed 10 mm from the end of the outer sheath. Each thermocouple was covered with two layers of PVC tape to make sure it would stay in place when installing the ground screen connection.

Thermocouples was also installed on the two reference cables. One thermocouple was placed at the surface of the conductor, by drilling a hole down through the cable insulation. Since the applied voltage to the cables would be low, this would not cause concern with regard to safety. The same method was applied to place a thermocouple beneath the outer sheath to monitor the temperature of the ground screen. A final thermocouple was placed at the surface of the outer sheath, as this would correspond to the placement of the thermocouple below each ground screen connection on the test objects.

A thermocouple was also placed between a bolt and nut, and laid inside the test cell to monitor the temperature of the ambient air.

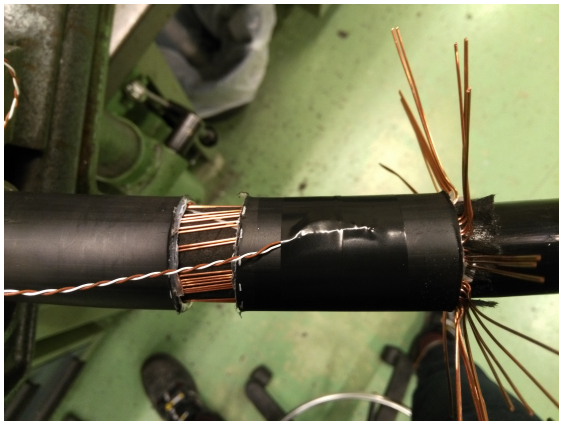

Figure 3.15: Installation of thermocouple on the cable sheath, with ground screen connection to be placed above. To the left, the cut through the outer sheath to access the copper wires can be seen. To the right of the spread copper wires, the XLPE insulation with outer semiconductive layer.

Each test object was jointed with fitting bolts, washers and nuts before a plastic tube with an inner diameter of 5.5 cm cut in two was placed around the joint and fixed with cable ties, as seen in the schematic of figure 3.16, with the finalized conductor joint shown in figure 3.17 and 3.18. The reason for this was to isolate the two current carrying components, the aluminium conductor and the cable ground screen consisting of the copper wires, joint ground screen and the ground screen connections. Since only low voltage was to be applied in test circuit during the experiments (U < 10 V), this would provide sufficient insulation.

As can be seen from figure 3.17, the cable lugs were placed with the opposite sides of how cable lugs normally should be installed. The reason for this was to prevent the jointing from becoming too wide. To compensate for this, the two sides of the lug that were to be jointed was brushed down with sand paper in opposite directions of each other to ensure good electrical contact.

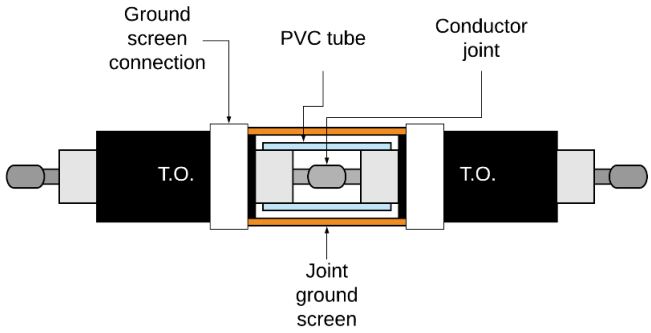

Figure 3.16: Figure showing the connection of each T.O. in the circuit schematic of figure 3.24.

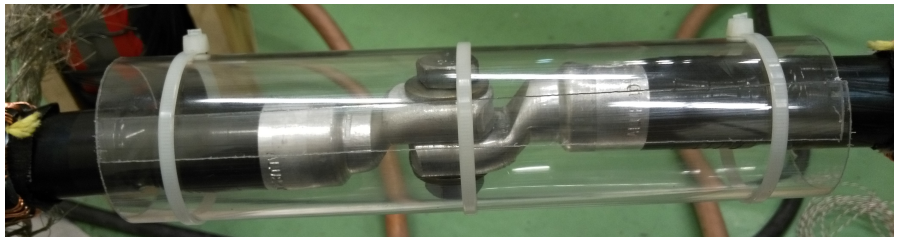

Figure 3.17: Picture showing the cable lug joint between two test objects, with the applied plastic tube outside it.

Figure 3.18: Figure showing the braided joint ground screen in place across the plastic tube covering the cable lug jointing. This picture shows the type I ground screen connection. The duct tape was applied to prevent the lead of the voltage measuring point to get metallic contact elsewhere on the screen.

3.4.2 Installation of voltage measuring points

To be able to measure the voltage drop across each ground screen connection, appropriate potential points had to be installed at the test objects. Since the current carrying parts of the ground screen connections consist of either stranded or braided parts, it was of importance to find a fitting *equalizer*. The purpose of these equalizers was to make sure that all of the ground screen parts which were to be measured at was at the same voltage potential before voltage measurements could be carried out. The chosen solution was to twist tinned copper wire around the copper wires of the cable ground screen and the ground joint screen, heavily based on the standard IEC 61284-1997 annex G [25], describing requirements and tests for fittings for overhead lines. The method has previously also been suggested by Dang and Braunovic [26].

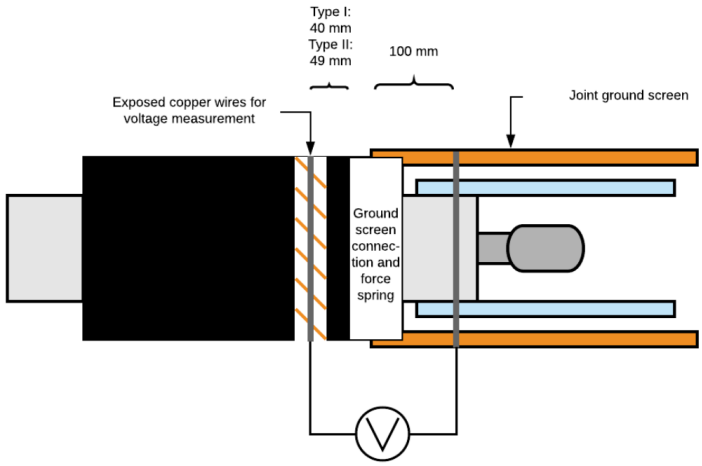

Figure 3.19: Schematic showing the connection of the voltage measurement across the ground screen connection. The ground screen parts are shown in orange, while the blue parts represent the plastic tubes used to isolate conductor and screen. Note that the distance between the voltage measurement on the copper wires and the edge of the force spring varies for the two types.

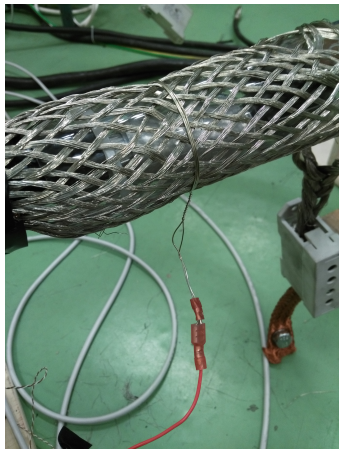

(a) Picture showing the connection of the voltage measurement on the joint ground screen. In the picture, the joint ground screen of type I is seen.

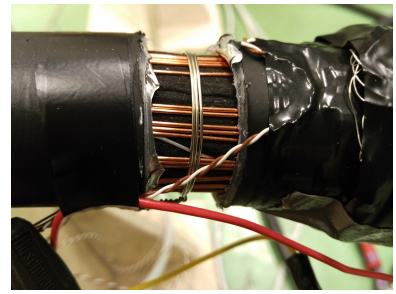

(b) Picture showing the connection of the voltage measurement on the copper wires.

Figure 3.20: Figures showing the connection of the voltage measuring points on the braided joint ground screen and the copper wires.

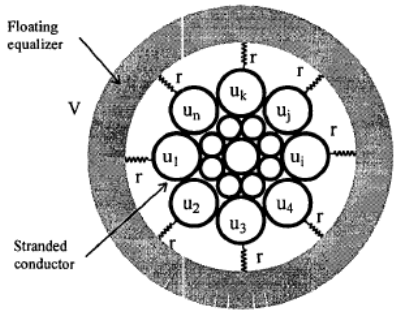

Figure 3.21: Figure showing the principal behind the equalizer used, here named *floating* equalizer [26]. The resistances *r*, is the resistances between each strand and the equalizer, and is neglected in the measurements and calculations in this project.

For the voltage measurements across the ground screen connections, tinned copper wire with a diameter of 0.68 mm for the reference tests and 0.50 mm for the main tests was applied with three turns on the each side of the ground screen connections, as shown in figure 3.19. This was also used in section 3.3.1 and 3.3.2. On the cable side of the ground screen connections, the voltage point was applied at the center of the window cut in the outer sheath as seen in figure 3.20b, while it was placed 100 mm from the middle of the force spring on the joint ground screen of the connection, as seen in figure 3.20a. This is shown schematically in figure 3.19. The end of each voltage point was then connected to a cable lug. To connect the voltage measurements to the data logger, Nexans PFSK 0.5 mm^2 cable was used. Since this cable consist of four conductors, the two conductors that was not used were connected with the cable screen of this signal cable and grounded in one end while isolated in the other, as seen in figure 3.22. The reason for doing this was to avoid distortions in the analog voltage measuring signals caused by EMI. The remaining conductors carrying the voltage measurements were connected to cable lugs to allow connection on the test objects potential points.

It would be preferable to connect the measuring points closer to the force spring than what is presented above to get a better measurement of the resistance. This was however troublesome due to several reasons. For the measuring points on the cable side, the cross section through the outer sheath into the copper wires could have been placed closer to the joint itself. But by doing this, the piece of the outer sheathing where the force spring is placed would become smaller, further making it less stiff and more susceptible to slide either way on the copper wires, as mentioned in section 3.1.1. This was experienced when trying to make test objects with a shorter outer sheath, and was not desirable. Some of this also applies to the placement of the measuring point on the joint ground screens. At the given distance where they were placed, the diameter of the screen was more constant than closer to the ground screen connection. Placing it closer to the ground screen connection where the diameter decreased could make the measuring points move during cycling and testing, which would not be acceptable.

After the measuring cables had been connected to the data logger, each voltage measure-

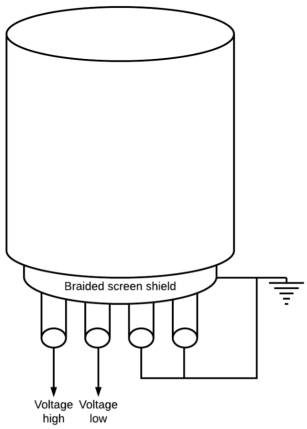

(a) Schematic showing the principle for the connection of the conductors in the voltage measuring cable connecting each ground screen connection and the data logger, and the grounding of the unused conductors.

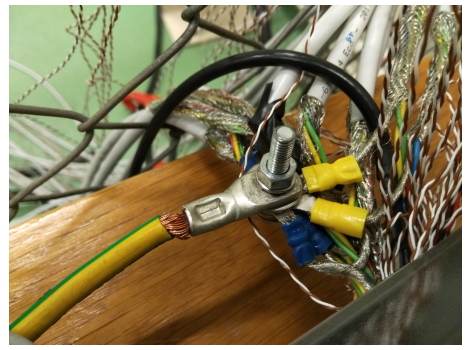

(b) Actual photo of the grounding. The unused conductors and screen of each cable is crimped together with yellow or blue cable lug and connected to ground through the green/yellow grounding cable.

Figure 3.22: Figures showing the connection and grounding of the voltage measurement cables for each ground screen connection.

ment pair was shorted together with a jumper, and the voltage was measured. By doing this, the measurement error could be found and subtracted from the results. The measurement errors can be found in table C.1 in appendix C.

3.4.3 Thermal insulation of test setup

After all the connections were made, the ground screen connections and the reference cables were insulated thermally. The reason for this was to increase the temperature stability and reduce the impact of the ambient air and surroundings, in addition to give a more realistic scenario that resemble a situation where the setup was placed in the ground.

For this purpose, Armaflex was used. Each ground screen connection as well as the reference measurements on the reference cables was covered with one layer of Armaflex having a thickness of 13 mm. The layer placed across each ground screen connection was cut as a square with sides of 250 mm, with the force spring placed in the middle. This can be seen in figure 3.23. Each layer of Armaflex was then fastened with cable ties to keep the layer in place, while also keeping the layer of insulation as tight as possible to prevent interaction with the ambient air and draft.

For the reference cables, the width of the layer was between 430 and 530 mm.

Fresh Armaflex insulation was applied before the reference tests, and replaced before the main tests with the improper installation when the connections had to be opened and changed. This was done because the cable ties used to fasten the insulation would leave imprints during cycling, which could influence the thermal conditions if they were used again.

(a) Ground screen connection being covered with Armaflex. The duct tape seen is used to keep the voltage measurements leads in place. The force spring is located at the middle, with both PVC and duct tape.

(b) Ground screen connection and measuring points wrapped in Armaflex, held in place by cable ties.

Figure 3.23

3.4.4 External circuits in the lab

The schematics for the laboratory setup used in the experiment can be seen in figure 3.24, with the actual setup seen in figure 3.25. The setup consisted of a DC-source (Farnell H30/100, a total of two available) connected to the cable ground screens of the test objects of each type, connected in series. A jointing cable was fed through a ring transformer and connected to the conductor of the test objects, with additional jumper cables completing the circuit. The connections of both cable ground screens and conductors was made such that the two types could be disconnected from each other, allowing individual DC-sources to be used on the two cable ground screen types such that different cable ground screen currents could be investigated for the two simultaneously, while still using a common AC source for the load current.

The choice of using a DC source to supply the cable ground screen current were due to several reasons:

- Previous experiments in the project with the force spring in series with the ground screen [14], showed that it was difficult to keep the induced voltage constant when using a ring transformer to supply the circuit through a variable voltage source. Using a DC-source would make regulation of the current easier and more stable.
- By using a DC source, the cable ground screen current could be adjusted as wanted, making it less dependent on the magnitude of the load current in the conductor.
- Using a DC source would ensure a DC-voltage drop across the ground screen connections, making voltage measurements easier than if AC had been used.
- Almost all theory regarding the topic contact resistance is based on DC-current.
- Using DC in the cable ground screen would not cause noticeable error regarding skin effect, as discussed in the theory of chapter 2.3.2.

To be able to imitate the actual cable ground screen currents that might occur in the grid, the largest DC source available in instrument archive was used, the previously mentioned Farnell H30/100 sources, able to output 100 A_{DC} and 30 V_{DC}.

The current outputs were monitored with ampere-meters. The DC current in the ground screens was measured with a Fluke i1010, while the AC load current was measured with a Fluke i1000s, both connected to the data logger.

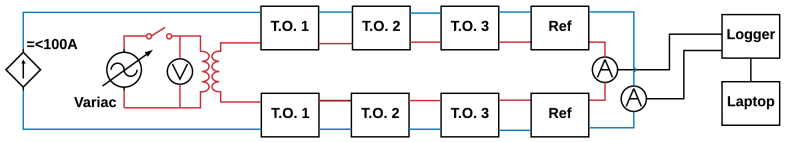

Figure 3.24: Schematic showing the circuit used for the experiment. Blue lines show the DC wiring connecting the cable ground screens, while the red lines show the AC wiring of the cable conductors.

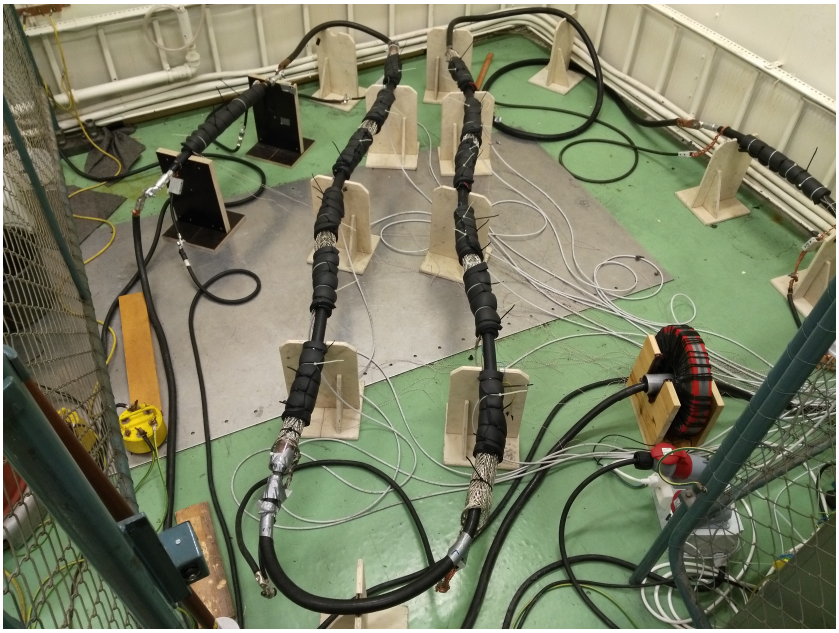

Figure 3.25: Figure showing the setup in the lab. To the left type I with its reference cable, on the right-side type II with its reference cable. In addition, the ring transformer and junction box with safety circuit can be seen at the bottom right of the picture.

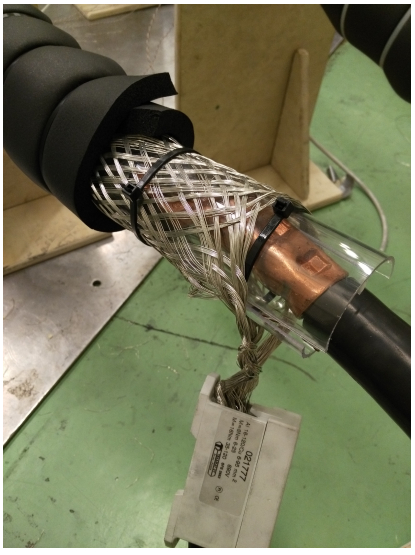

(a) Picture showing the connection of test object conductor to a jumper cable for interconnection, as well as interconnection of the cable ground screen arrangement.

(b) Picture showing the connection of the braided joint ground screen to a terminal for interconnection.

Figure 3.26

To allow safe use of the test setup, a safety circuit was installed to de-energize the test setup in the event of an over temperature and/or over current. The schematics and layout of this safety circuit is shown in appendix D.

3.5 Cycling procedure

A cable and joint system in the field will rarely be subject to steady state conditions. During a day, week and season the load of a cable will change depending on a number of factors. As a result, both the current (conductor and cable ground screen) and temperature of the cable system will change.

To see how the ground screen connections would behave during operation, it was decided to conduct heat cycling of the test arrangement. A heat cycle test is carried out by applying a constant current to a test arrangement while measuring the corresponding temperature development. The current is applied until a certain temperature criteria is fulfilled, and the current is switched off. This will allow the test arrangement to cool down, before additional heat cycles are performed. By following this procedure, it is possible to gain a better understanding of how the system will react to the changes mentioned in the previous paragraph.

During a heat cycle the test objects will not only be exposed to an increasing temperature due to resistive losses, but also change in dimensions and pressure [27]. The cycling will also lead to stresses and aging which is more equal to the actual processes the cable system will experience during service in the field.

3.5.1 Reference tests with correct installation

The cycling performed during the reference tests drew influence from the heat cycle test procedure for "Compression and mechanical connectors for power cables for rated voltages up to 30 kV (Um = 36 kV)" (IEC 61238-1) [28]. The standard provides a suggestion to heat cycle testing of connectors, and consist of two parts; first heat cycle and second heat cycle. The *first heat cycle* in the standard is used to determine the reference conductor temperature and the median connector temperature. The median connector temperature is defined as the connector which experiences the third highest temperature during the first heat cycle. This connection is then used as a stability criteria in the following heat cycles. The stability criteria of the first heat cycle depend on the type of connector being tested. In the *second heat cycle*, the heat cycle duration and temperature profile is determined to be used in further tests. Current is applied until the reference conductor reaches the reference value as found in the first heat cycle with a tolerance of [0, 6] K and the median connector temperature changes less than 2 K over a 10 minute period. The heat cycle duration can then be divided into two time periods, t_1 and t_2, the time needed to reach the stability criteria and the time to reach a certain cold temperature, respectively.

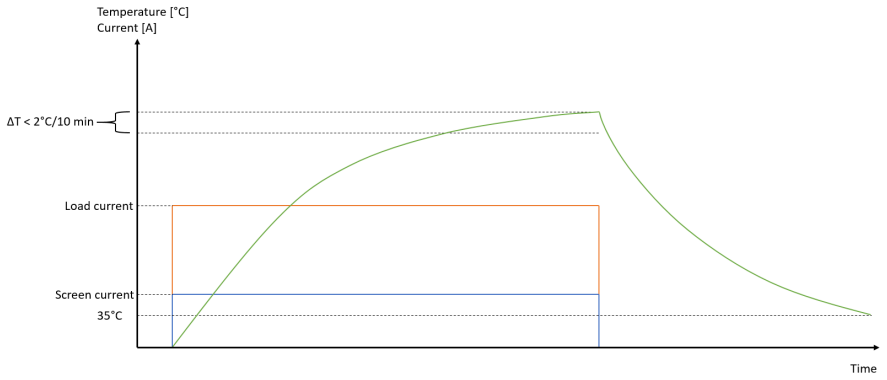

Figure 3.27: Figure showing a typical cycle from the reference (and main) tests. The orange line shows the load current through the conductor. The blue line shows the cable ground screen current. The green line shows the temperature rise, with the stability criteria shown on the y-axis. On the y-axis the 35 °C limit can be seen when the cycling was concluded. After this, a resistance measurement would be performed before a new, similar cycle was started.

The above procedure was customized into a heat cycling procedure to be used in the reference tests.

A first heat cycle was carried out with current flowing only in the conductor, with the cable ground screen left unconnected and grounded in one end such that I_s = 0 A. The purpose of this heat cycle was to determine the median ground screen connection temperature, which would be used as a stability criteria in the heat cycles to follow. In this cycle, steady state was considered reached when the temperature change in each thermocouple in the ground screen connections was less than 2 °C on a 15 minute basis, the same stability criteria as for one of the connector types in IEC 61238-1. The current used in this heat cycle was I_c = 440 A, which also would be used in the heat cycling series to come. From the steady state temperatures gained from this heat cycle, the median ground screen connection temperatures of type I and type II was determined, defined in the same way as the median connectors in IEC 61238-1. Emphasize was not given to the conductor reference temperature, as this was not the governing temperature in the investigation of the ground screen connections. The first heat cycle would also serve as a reference to see what the additional heat development by running a current in the ground screen connections would be, compared to a scenario with cable ground screen grounded in one end.

The median ground screen connections and the temperatures they where found from, are shown in appendix E.

The following heat cycles were carried out with current flowing both in the conductor and the cable ground screen. The same current was applied to the conductor loop, I_c = 440 A, while a screen current of I_s = 100 A_{DC} was applied from the DC-source.

The heat cycles were started either from ambient temperature at approximately 20 °C

or just below 35 °C, depending on if it was the first heat cycle of the test day or one of the following throughout the day, respectively. The sources were kept at the specified current levels until the temperature change in the median screen connections of *each* type was less than 2 °C during the last ten minute time interval. When this was achieved, the current sources were switched off and the cooling period of the heat cycle would begin. The cooling period was completed when each of the temperatures in the ground screen connections had reached a temperature below 35 °C.

The standard IEC 61238-1 [28] states that the total number of heat cycles to be performed is 1000. Naturally, this was a number that would not fit with the time frame of the project. Due to time limitations and the fact that a maximum of four tests could be carried out each day due to the duration of each heat cycle, the total number of heat cycles for the reference test were set to 25. Since the ground screen connections were installed correctly it was not predicted that the increase in resistance would be of such a magnitude which would need a great number of heat cycles to be carried out in order to see a development and formation of a trend.

Each heat cycle was carried out with the opposite polarity of the last cycle, meaning that cycles with odd numbers had one polarity, while cycles with even numbers had the opposite polarity. By doing so, it would be possible to see how the ground screen connections would act when exposed to a changing polarity in the cable ground screen current.

The reason for using the currents of I_c = 440 A and I_s = 100 A_{DC}, was mainly due to two reasons. Firstly, it was due to limitations what concerns the available equipment. The DC source used was the largest available, with a maximum output of 100 A. The load current was also close to the maximum value that the variable voltage source was able to induce when the test setup was finished. However, these values correspond well with field values. Simulations on ground screen currents have previously been performed in COMSOL as part of the project [14]. Here, the ground screen currents and its effects was investigated on a similar cable design as in this project, with varying load current and distance between the cables in a flat configuration. For a distance between the cables of 40 mm (approximately one cable diameter), the induced cable ground screen currents for varying load current is shown in figure 3.28. As can be seen, a load current of 440 A will induce a ground screen current of 90-100 A, which is closely matched to that available in the test setup.

Both the reference tests and the main test used a measuring interval during the heat cycles of one minute for the measuring of temperature and voltages.

Resistance measurement

The resistance of each ground screen connection was measured with the micro-ohm device both prior to and after the reference tests had been carried out. This was done as described in section 3.3.1 and 3.3.2, by measuring across the ground screen connection with the measuring points placed as explained in section 3.4.2. It was not possible to use the micro-ohm device to measure the resistance between each cycle, as this would demand the Armaflex to be removed each time. This would naturally affect the degree of

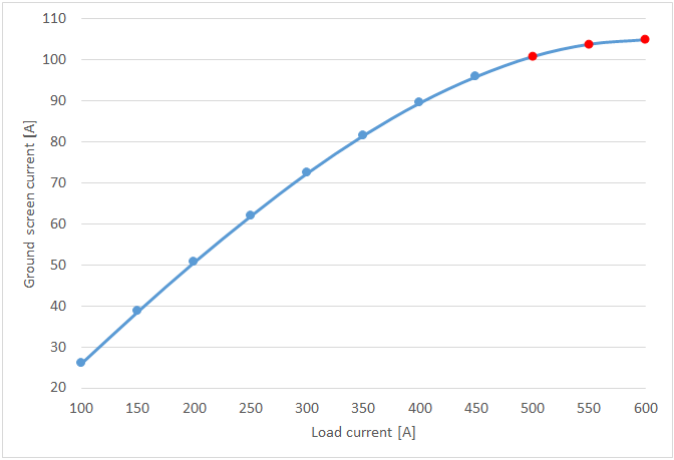

Figure 3.28: Figure showing the induced ground screen currents as a function of varying load current. Constant distance between cables in flat configuration of 40 mm, and buying depth of 70 cm. Red dots indicate simulations where the conductor temperature of the cable in the middle of the flat configuration reached a temperature above 90 °C. The temperature at the surface is 15 °C.

contact in the jointing, altering the results, and was thus not an acceptable approach.

Resistance measurement between the heat cycles was conducted by using the DC-source of the test setup as a current source. This was carried out immediately after every temperature measurement had fallen below 35 °C. It would be preferable to perform this measurement at a steady state temperature equal to ambient temperature. This would however demand a long cooling period, greatly increasing the time needed for the experiments. If the resistance measurements were to be carried out at steady state temperature in the ground screen connections equal to ambient temperature, the number of cycles would be restricted to one heat cycle per day. The resistance measurement took up to 15 minutes, which would allow the test objects to cool a further couple of degrees before a new heat cycle test was started. This would give a slight source of error, since the resistance is dependent on temperature.

Each resistance measurement consisted of two measuring periods of two minutes each, with opposite polarities in the two periods, much like the in-built method in the micro-ohm meter. The reason for switching the polarity was due to the risk of thermoelectric voltages arising across the ground screen connections [28]. The resistance measured was then the average of the two resistances of each polarity. The voltage drop across each ground screen connection was recorded at an applied current of 2 A_{DC}, with the voltage drop measured at a ten second interval during the two minute period. The resistance of each polarity was then calculated as the average of each of these ten second intervals. The reason for using a current of 2 A_{DC} in these resistance tests was to make sure that there would not be any heat dissipation that could cause the temperature to increase, thus channging the resistances.

3.5.2 Main tests with improper installation

The cycling procedure used in the cycling tests with improper ground screen connection installed, used many of the same elements as in the reference cycling, although some elements had to be adjusted.

The first heat cycle was carried out as for the reference tests with the cable ground screen grounded in one end, giving I_s = 0 A. However, the results from this cycle would only serve as a reference and not give the median ground screen connection temperatures from which the stability criteria would be deducted. The reason for this was that the initial measurements with the micro-ohm meter showed large differences in the resistance of ground screen connections from the same type. It was thus expected that the median ground screen connection temperatures found from the first heat cycle with I_s = 0 A would not be representative when ground screen current was be applied, as the temperature development would be very different among the ground screen connections. Instead, it was decided to select the screen connection for which the stability criteria of 2 °C would apply to from initial tests with $I_s \neq 0$ A and I_c = 440 A, as this was seen as more representative.

Initial tests were carried out with screen currents of I_s = 30, 40 and 45 A, as it was clear that a current of I_s = 100 A could not be used. These tests showed that it was particularly one connection of each type that experienced a quite larger temperature development than the remaining five. It was desirable to choose these two as the connections for which the 2 °C criteria should be applied to during cycling. However, the mentioned connection belonging to type I showed to be quite unstable in parts of the heat cycle, where it would decrease in temperature before increasing again. To avoid problems this might cause regarding reaching the stability criteria and the duration of the cycling, it was decided to instead use the connection with the second largest temperature recorded during these initial cycles for type I. For type II, the ground screen connection with the highest recorded temperature was chosen. The initial tests showed that a screen current of 30 A_{DC} would give sufficient room for the increase in temperature which was expected to occur during the cycling. These initial heat cycles can be seen in appendix M. The numbering of the ground screen connections which the stability criteria would be used on, are shown in appendix E.

Since it was expected that the improper installation would cause additional heating in the ground screen connections, another criteria was introduced to override the 2 °C criteria in the case of such an overheating. If any of the screen connections were to register a temperature above 90 °C during one minute (two measurements), the sources would be switched off, and the cooling period would begin. The reason for choosing this upper limit was to preserve the test objects for later use by not exposing them to unnecessary aging, damage and stress.

Resistance measurement

Resistance measurements were carried out between each heat cycle, similar to measurements performed during the reference heat cycles, described in section 3.5.1.

3.6 Correction of ground screen connection resistance

Since the voltage measuring points could not be attached directly beside the ground screen connections, parasitic voltage drop from the copper wires and joint ground screen would be included in the results when measuring the ground screen connection resistances. As a result, this influence on the resistance had to be removed after the conclusion of the experiments.

In this correction it was assumed that all physical measures of the two conducting parts, copper wires and joint ground screen, was kept constant through all of the experiments. The only quantity that was set to change during the course of the cycling and the measurements was the resistivity of the aforementioned parts, which would change as a result of the changing temperature as given by equation 2.7.

The length of the two parts to be subtracted was defined as *the conductive part from the voltage measuring point to where it entered the constant force spring arrangement*, as proposed by Holm in equation 2.10. In the following, the contribution from the copper wires are denoted with a lowercase *a*, while the joint ground screen is denoted with a *b*.

Table 3.3: Length definitions used in the calculation of parasitic resistances.

	l_a [mm]	l_b [mm]
Type I	85.0	87.5
Type II	85.0	92.0

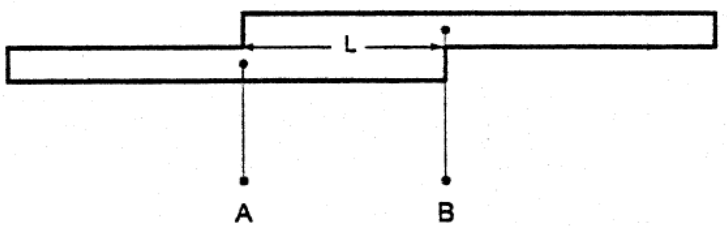

Figure 3.29: Figure showing the definition of the contact area, taken from [20]. The area to the left of *A* is the contribution from the copper wires. The area to the right of *B* is the contribution from the joint ground screen. Subtracting these two gives the actual ground screen connection length, here denoted *L*. *L* will be equal to the force spring width of the two types.

For each measuring point the contribution from the mentioned parts were calculated and adjusted with the measured temperatures by using equation 2.4 and 2.7. The copper wire resistances were adjusted by using the mean ground screen temperature measured with the two reference cables, while the joint ground screen resistances was adjusted by using the mean sheath temperature from the reference cables. The reason for using the sheath temperature for the latter was due to the fact that the joint ground screen in an actual joint would be placed on the outer sheath. However, the this would cause some error since the joint ground screen to a certain degree would be affected of the ambient temperature due to the part of the PVC tube and thus joint ground screen which would not be covered by thermal insulation. Alternatively, the force spring temperature of the joint could have been used, but this would most likely give a to large temperature for the joint ground screen as a whole since only the part of the joint screen placed inside the force spring would experience this temperature.

The actual joint resistance was then calculated by modifying equation 2.10 into the following equation for each screen joint

$$\boldsymbol{R} = \frac{U_{measured} - U_{error}}{I_{measured}} - R_a - R_b \tag{3.1}$$

Here, the subscript *measured* indicates the values measured at each ground screen connection in addition to the cable ground screen current measured for the whole screen assembly. U_{error} indicates the voltage measuring error at each connection, as given in table C.1 in appendix C. R_a and R_b is the resistance of copper wires and joint ground screen, respectively.

The above mentioned model was used to correct the resistance values acquired from cycling, resistance measurements between cycles and the measurements made with the micro-ohm device.

4 Results and discussion

In this chapter, the following will be presented and discussed:

- An explanation of the course of the heat cycles.
- Results from the reference heat cycles.
- Results from the main heat cycles.
- Results from the different methods used to assess the resistance of the cable ground screen connections, and a comparison of these.
- Observations made during the removal of the ground screen connections after the heat cycle series with the improper installation.

4.1 The course of a heat cycle

The following section will give an overall presentation of the course of the heat cycles, with the purpose of explaining the physical mechanisms occurring in a cycle. In addition, an explanation of what parts of the cycle duration that will be the main focus area in the discussion and comparison of the cycle results will be given.

Figure 4.1 shows a typical development of the resistance and temperature of the ground screen connections during a heat cycle (both correct and improper installation). As can be seen, the resistance starts from a higher value than the steady state value it reaches at the end of the heat cycle.

In this chapter a numbering system will be used on the ground screen connections, which can be seen graphically in figure I.1 in appendix I. The first number indicates the test object number, and the second number indicates the ground screen connection number on the test object.

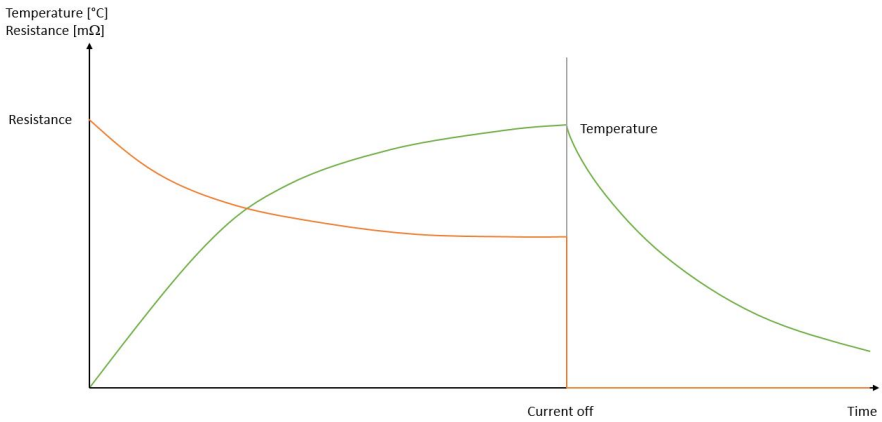

Figure 4.1: Figure showing a typical resistance-temperature development for a ground screen connection during a heat cycle.

4.1.1 Reference heat cycles

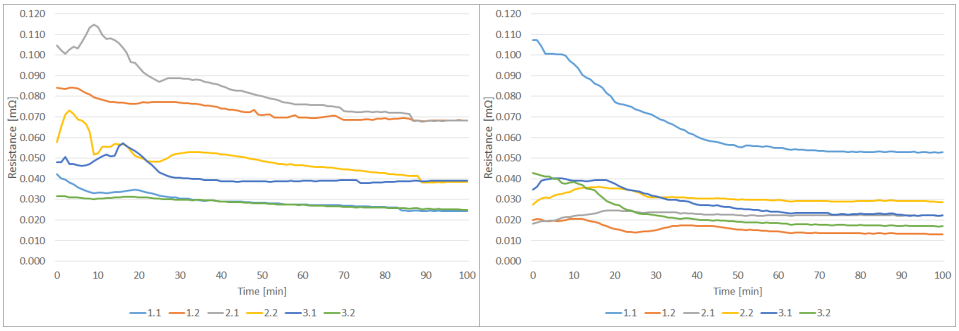

(a) Type I **(b)** Type II

Figure 4.2: Figures showing the resistance development of type I and type II during the first heat cycle, from the start of the cycle until the current sources were turned off.

Figure 4.2 shows the resistance development for the first heat cycle of the reference tests. It can be seen that the overall resistance follows a $1/P$ relation, similar to that proposed by equation 2.17 and 2.18, as well as figure 2.7. The increased pressure originates from the thermal expansion of the insulation, semiconductors and outer sheath, which is significantly greater than the expansion of the metals in the ground screen connections. The spiking seen at the start of the cycles is most likely due to the fritting mechanisms as explained in section 2.5.1. This is seen for both the first and the 25th cycle (figures 4.2 and 4.3).

In fact, this spiking can be seen in each of the heat cycles, from the first to the last. The

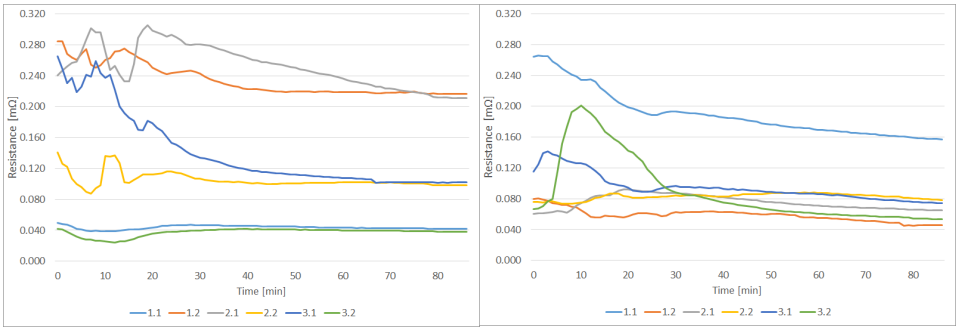

(a) Type I **(b)** Type II

Figure 4.3: Figures showing the resistance development of type I and type II during the 25th heat cycle, from the start of the cycle until the current sources were turned off.

reason is most likely that when the current sources are switched off, the test setup is allowed to cool down allowing contraction of the insulation, reducing the pressure exerted by it. This will reduce the number of contact spots in the ground screen connections, leaving air voids between the contact members. This will further initiate growth of oxide layers, effectively insulating the contact members from one another [29]. When a new heat cycle is started, these layers will have to be pierced by fritting to allow the ground screen current to flow.

By comparing the figures 4.2 and 4.3, several observations can be made regarding the development of the resistance during the heat cycle series.

Firstly, it can be seen from the resistance axis that the overall resistance values have increased (disregarding connections 1.1 and 3.2 of type I as well as 1.1 of type II, which will be explained later), both for the initial resistances at the start of the heat cycle, as well as the steady state value at the end of the cycle.

Secondly, the course of the resistance reduction during the cycle seems to have changed. The curves are no longer as smooth as at the start of the cycling series, with more spiking occurring along the resistance curves throughout the series, which can be seen in the heat cycle plots in appendix L.

It is thus reasonable to suggest that the growth of oxide layers and films is greater than what the fritting mechanisms are able to remove during a heat cycle. 25 heat cycles is however an insufficient number to conclude if this process of growth of insulating layers will reach a steady state at some point.

As can be seen from figures 4.2 (resistance) and 4.4 (temperature), there are two connections deviating for type I, and one deviating for type II. Connection 1.1 and 3.2 for type I shows both a lower recorded resistance and temperature than the rest of the connections of its type. For type II, connection 1.1 shows a significantly larger resistance value than the others while also having a much lower temperature. Comparing these figures with the corresponding figures from the 25th heat cycle, it is seen that these connections still devi-

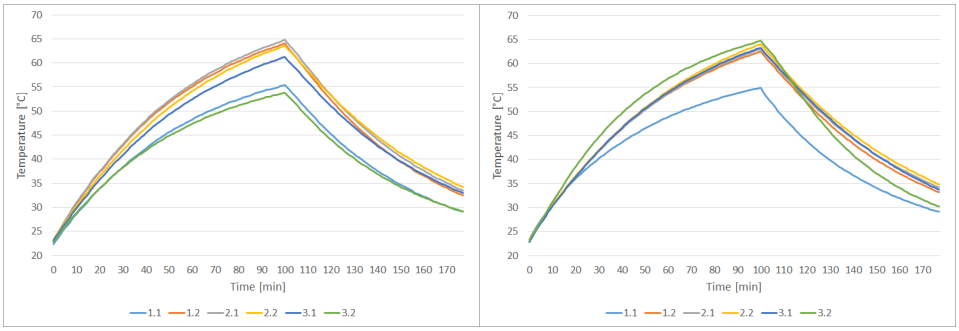

(a) Type I **(b)** Type II

Figure 4.4: Figures showing the temperature development of type I and type II during the first heat cycle. As can be seen from the temperature axis, the cycle was started from ambient conditions. The cycle ended when all temperatures had fallen below 35 °C.

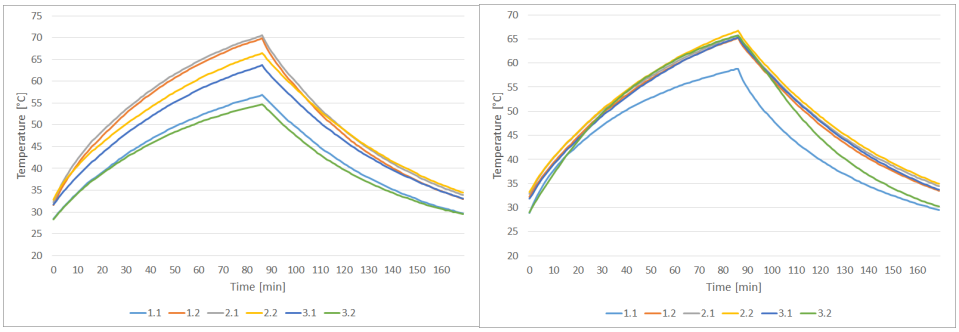

(a) Type I **(b)** Type II

Figure 4.5: Figures showing the temperature development of type I and type II during the 25th heat cycle.

ate. From the temperature figures it is also seen that the increase in temperature for these connections from heat cycle one to heat cycle 25 is low.

These observations are believed to be connected to edge effects occurring at the ends of the test setup for both type I and II. Connections 1.1 and 3.2 of both types are located at the ends of the test setup where jumper cables between the test objects, reference cables and current sources are located. It is believed that these connections offer better thermal conditions what cooling concerns, as the connections are not located close to a cable lug connection of adjacent test objects. It is however not clear why connection 3.2 of type II not deviates as for the other connections located at the ends.

On basis of the mentioned observations, it was concluded not to include the data for these three connections in the overall representation of the ground screen connections development, for the reference tests.

Further, to be able to compare the results from the different heat cycles, it was decided to use an average value for the resistance of the 10 last minutes of each heat cycle. This was based on the resistance plots as shown, where the resistance stabilizes towards the end of the heat cycle. Another advantage of using this period of the cycles for comparison was that while the resistance is quite stable, the temperature in the ground screen connections are still increasing. As a result, it may seem that the contact resistance is quite independent of the temperature in the ground screen connections. This is an advantage, as no theory was found with regards to how the contact resistance could be corrected to "cold" resistance, allowing a better comparison of the resistances through the course of the cycle series. Theory does exist with regards to this kind of temperature dependency, but is only valid for symmetric, monometallic contacts. Both contact problems in this project (correct and improper installation) is non-symmetric and bi- or trimetallic, which means that this theory cannot be applied.

A complete collection of the resistance and temperature plots from the reference heat cycles can be found in the appendices.

4.1.2 Main heat cycles

Figures 4.6 and 4.8 shows the resistance and temperature development of the first heat cycle of the main experiment, respectively. Figures 4.7 and 4.9 shows the development for the 25th heat cycle.

From the mentioned figures, it can be seen that the main and reference tests share much of the same characteristics. The resistance development at the beginning of the cycles still follows a $1/P$ curve as for the reference tests before reaching a steadier value, with connection 2.1 of type I and 2.2 of type II being more unstable than the rest. During the last ten minutes of the first cycle the resistance value is quite constant for all the ground screen connections except for connection 2.2 of type II which shows some spiking, and especially connection 2.1 of type I which during the period has a peak to peak value close to 2 mΩ. Both connection 2.1 of type I and 2.2 of type II has a significantly larger resistance than the other connections of its type.

The temperature development of the first heat cycle shows more spread between the measurements of each ground screen connection compared to the first heat cycle of the reference tests. Connection 2.1 of type I has a noticeably more unstable temperature increase than the other connections of its type, even decreasing at some points during the heat cycle. Connection 2.2 of type II shows a much greater temperature increase than the other connections of type II. From the observations above, it is seen that there is a clear coherence between the largest resistances and the highest temperature in the first heat cycle.

In the reference tests, three connections experienced lower resistance and temperature values than the others, due to what was believed to be edge effects. The same connections (1.1 and 3.2 of type I, 1.1 of type II) also experiences the lowest temperatures of the first heat cycle of the main experiment. However, they do not have a significantly different resistance value than the other connections.

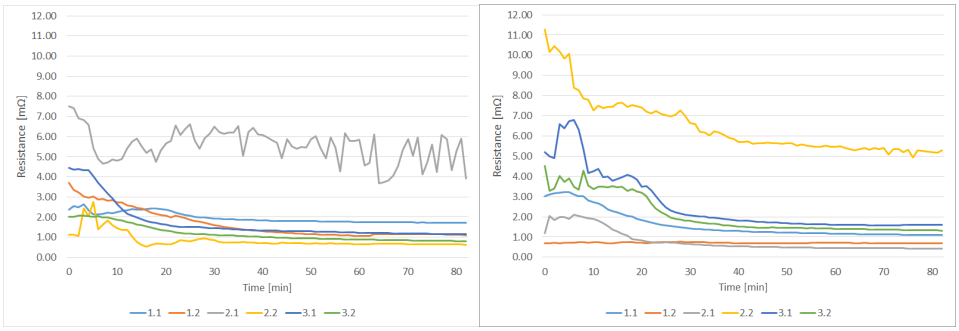

(a) Type I **(b)** Type II

Figure 4.6: Figures showing the resistance development of type I and type II during the first heat cycle for the improper installation, from the start of the cycle until the current sources were turned off.

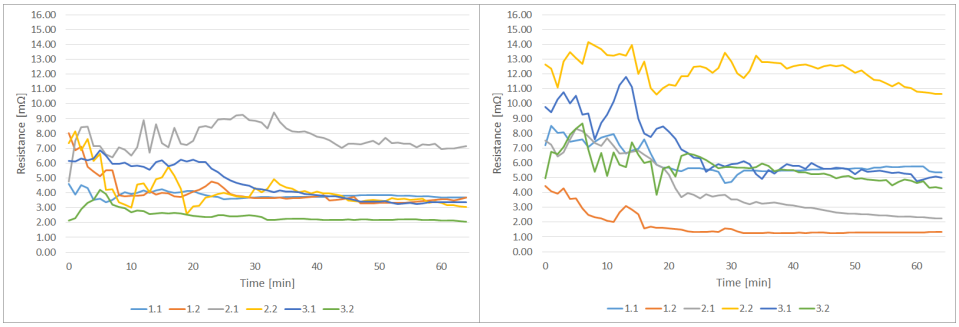

(a) Type I **(b)** Type II

Figure 4.7: Figures showing the resistance development of type I and type II during the 25th heat cycle, from the start of the cycle until the current sources were turned off.

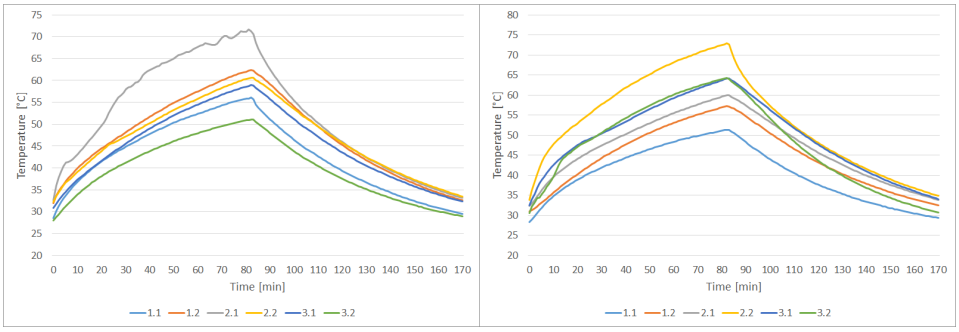

(a) Type I **(b)** Type II

Figure 4.8: Figures showing the temperature development of type I and type II during the first heat cycle.

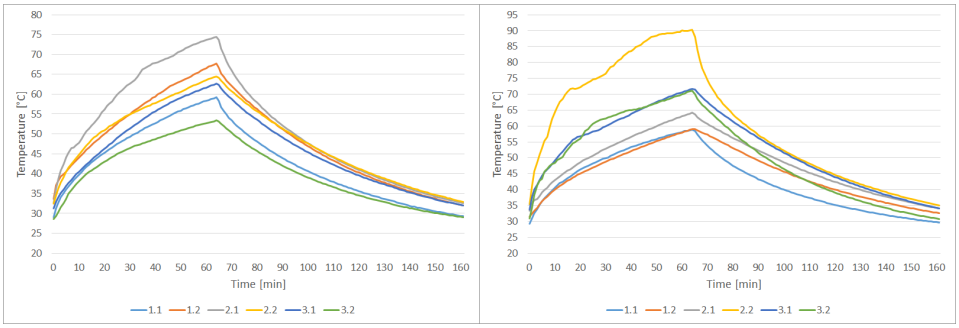

(a) Type I **(b)** Type II

Figure 4.9: Figures showing the temperature development of type I and type II during the 25th heat cycle.

Figures 4.7 shows the resistance development of the 25th and last heat cycle of the main heat cycles with improper installation. All of the connections have gained an increased resistance during the course of the heat cycles. It can also be seen that the resistances is less stable at the end of the cycle, with a much more unstable behavior throughout the heat cycling.

The temperature development of the 25th heat cycle is shown in figure 4.9. For type II, connection 2.2 has increased its difference to the other connections, reaching 90 °C. Its behavior has also become more unstable, with its growth rate increasing and decreasing during the heat cycle. Connection 2.1 of type I is more stable than at the beginning of the heat cycle series, and it seems that the other connections of type I has decreased their difference to the temperature of connection 2.1. A slight increase in the spread between the temperatures of type I can also be seen.

Although the resistances are much less stable during the last ten minutes of the heat cycle than what was experienced in the reference tests, it was however chosen to still use this period as a basis for comparison, as this part of the cycle is more stable than the rest of the cycle. From figure 4.7 it can be seen that the two largest resistances, 2.1 of type I and 2.2 of type II either has the largest ripple or change in value during the ten minute period. Based on this, the error included when using a mean resistance value as a representation would be most erroneous for these two ground screen connections. This might however not be crucial, as the resistance value of these two are significantly larger than the rest of their respective type, hence the representation of the size of these two connections will not be significantly impeded.

A complete collection of the resistance and temperature plots from the main heat cycles can be found in the appendices.

4.2 Heat cycling with correct installation

Before investigating the consequences of the improper installation it was of interest to see how the ground screen connections would behave during operation when installed correctly.

A total of 25 heat cycles were conducted. Because of the cycling procedure not being automated, a limited number of heat cycles could be performed each day. Because of this one of the heat cycles for each test day would be started from ambient temperature, while the following heat cycles from the rest of the test day would be started from an elevated temperature above ambient temperature. In the following it will be indicated whether a heat cycle was started with ambient temperature conditions in the ground screen connections or not.

The reference tests were conducted with a load current of 440 A_{AC} and a screen current of 100 A_{DC}.

4.2.1 Temperature and resistance development in the reference tests.

Figures 4.10 and 4.11 shows how the absolute resistance in the ground screen connections developed during the reference tests. Each point of the lines in the mentioned figures is the average resistance value of the last 10 minutes before the current sources were switched off. In each graph, the vertical dotted lines show heat cycles started with ambient temperature in the test setup, typically at the start of a test day.

From the figures, it can be seen that all of the ground screen connections for both type I and II experiences an overall increase in its resistance. In section 4.1, it was explained how connections 1.1 and 3.2 of type I and connection 1.1 of type II shows a different behavior compared to other ground screen connections of its type. This is also seen in the figures below, where the mentioned ground screen connections of type I shows a lower resistance and growth rate than the four other connections. Connection 1.1 of type II however, is significantly larger than other connections of type II. These connections thus seem to be non-representative for the overall behavior of the ground screen connection types.

Further, it seems that the resistance development is quite independent on whether the heat cycle is started with ambient temperature conditions or not. It does however seem that the development in some degree responds on the changing of the screen current polarity. The reason might be connected to reversal processes or measuring errors because of the changed current direction through the DC-ampermeters.

Further, it can be seen that the spread of the resistances of type II in figure 4.11 is much smaller than that of type I. The connections of type I is grouped in pairs, 1.1 and 3.2, 2.2 and 3.1, 1.2 and 2.1. Neglecting the first group of type I (the ones affected by edge effects), the grouping of the four others coincides with the localization of these connections

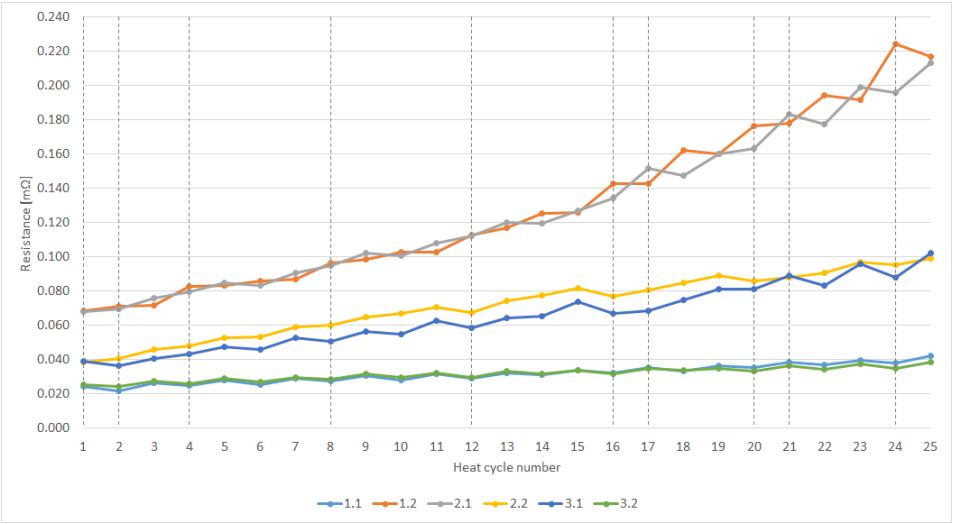

Figure 4.10: Figure showing the absolute resistance development during the reference tests for type I. Each point in the figure is based on the last ten minutes of the heat cycle. The dashed vertical lines indicates cycles that were started with the ground screen connections at ambient temperature conditions.

along the test setup, meaning that they are placed adjacent to the same cable lug joint of the conductor as shown in figure I.1 off appendix I.

Table 4.1 and 4.2 summarizes the most important developments for the resistance of type I and type II. Table 4.1 shows that the type I ground screen connections on average has increased with 0.105 mΩ during the 25 cycles conducted. Although this may not seem as much, it is an increase in the range of 150 to 220 % for the ground screen connections considered in this selection. In addition, 25 cycles is quite a low number of cycles if it is to be compared with actual connections in the field. As a more tangible way of comparison, the same values are included in per length units, where the width of the force springs are used in the calculations. The resistance limit for ground screens as given by HD620 is 0.524 Ω/km (for a cross section of 35 mm^2). It is clear that already at the start of the heat cycles and after 25 cycles, the ground screen connections are clearly above this limit. This is most likely due to two reasons:

- The presence of contact spots in the transition between the copper wires and the joint ground screen. The associated constriction resistance of these contact spots causes an increase in the resistance as compared to the bulk resistance of the materials alone, as explained in section 2.5.
- Growth of oxide layers in the ground screen connections and contact spots during the heat cycle series. This causes the resistance of R_f in equation 2.15 to increase, further increasing the total constriction resistance as given by equation 2.16.

For type II, table 4.2 shows that the ground screen connection resistance on average has

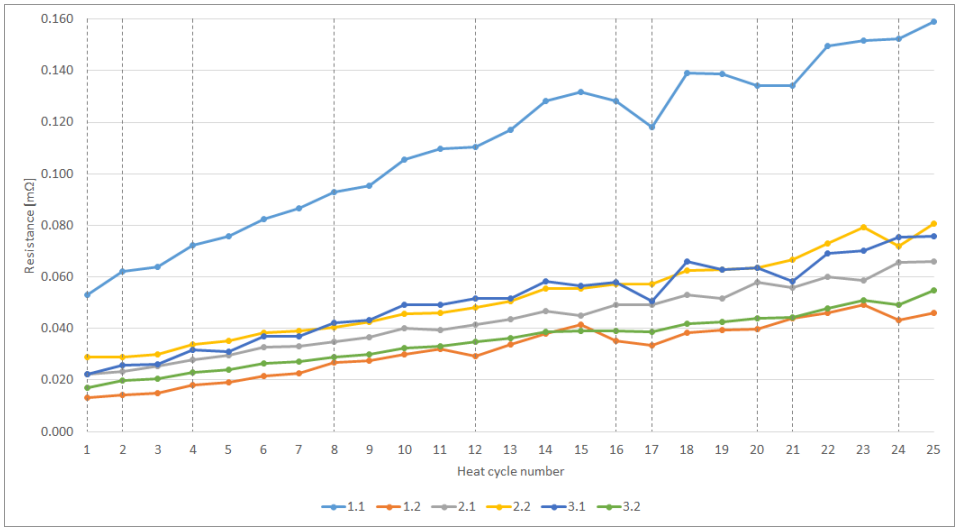

Figure 4.11: Figure showing the absolute resistance development during the reference tests for type II. Each point in the figure is based on the last ten minutes of the heat cycle. The dashed vertical lines indicates cycles that were started with the ground screen connections at ambient temperature conditions.

increased by approximately 0.044 mΩ, which corresponds to an increase between 175 and 250 % for the connections considered in that selection. As for type I, the connection type does not satisfy the 0.524 Ω/km limit of HD620 at the start of the heat cycles, nor at the end of the heat cycles.

Using the per length values of the types, a direct comparison can be made between the two. The initial difference between the two types starts at 0.841 Ω/km, and has increased to 2.264 Ω/km at the end of the cycling series on average, both in favour of type II. Thus, type I has a poorer performance which increases further through the course of the heat cycles.

This is interesting, as type II has a lower cross section area for the joint ground screen compared to type I as shown in table G.1 and G.2 of the appendices. The increased performance of type II compared to type I must therefore be related either to the force spring of the type, or the surface of the joint ground screen body. As described in section 3.3, the braiding of type II is more smooth than that of type I. Although a more rough surface normally would suggest more contact points being present as proposed by contact theory (see section 2.5), it might be that the smooth surface of the joint ground screen allows a greater area of the joint ground screen to be laid in between the copper wires causing an increased contact area. Also, the dimensions of the force spring might be such that a greater force acts on the arrangement, directly increasing the load bearing area as proposed by equation 2.9.

In figures 4.12 and 4.13, the temperature development of the two types during the heat

Table 4.1: Changes in resistance for type I during the reference heat cycles. The mean value is based on the four connections in the middle of the test setup, neglecting the ones effected by edge effects (connection 1.1 and 3.2).

	1.1	**1.2**	**2.1**	**2.2**	**3.1**	**3.2**
	Absolute resistance [mΩ]					
1st cycle	0.024	0.068	0.068	0.038	0.039	0.025
1st cycle mean		0.053				
Minimum during cycling R_{min}	0.022	0.068	0.068	0.038	0.037	0.024
Maximum during cycling, R_{max}	0.042	0.224	0.213	0.099	0.102	0.038
25th cycle	0.042	0.217	0.213	0.099	0.102	0.038
25th cycle mean		0.158				
$R_{max} - R_{min}$	0.020	0.156	0.145	0.061	0.065	0.014
	Per length resistance [Ω/km]					
1st cycle	0.975	2.731	2.727	1.536	1.562	1.009
1st cycle mean		2.139				
Minimum during cycling	0.878	2.731	2.727	1.536	1.461	0.964
Maximum during cycling	1.680	8.968	8.522	3.952	4.078	1.537
25th cycle	1.680	8.665	8.522	3.952	4.078	1.537
25th cycle mean		6.304				
$R_{max} - R_{min}$	0.802	6.237	5.795	2.416	2.617	0.573
Change in % from 1th to 25th cycle	72.25	217.2	212.5	157.2	161.1	52.35

Table 4.2: Changes in resistance for type II during the reference heat cycles. The mean value is all of the connections except 1.1, which was effected by edge effects.

	1.1	**1.2**	**2.1**	**2.2**	**3.1**	**3.2**
	Absolute resistance [mΩ]					
1st cycle	0.053	0.013	0.022	0.029	0.022	0.017
1st cycle mean		0.021				
Minimum during cycling	0.053	0.013	0.022	0.029	0.022	0.017
Maximum during cycling	0.159	0.049	0.066	0.081	0.076	0.055
25th cycle	0.159	0.046	0.066	0.081	0.076	0.055
25th cycle mean		0.065				
$R_{max} - R_{min}$	0.106	0.036	0.044	0.052	0.054	0.038
	Per length resistance [Ω/km]					
1st cycle	3.305	0.825	1.390	1.816	1.392	1.066
1st cycle mean		1.298				
Minimum during cycling	3.305	0.825	1.390	1.804	1.392	1.066
Maximum during cycling	9.940	3.071	4.114	5.032	4.746	3.427
25th cycle	9.940	2.880	4.114	5.032	4.746	3.427
25th cycle mean		4.040				
$R_{max} - R_{min}$	6.635	2.246	2.724	3.228	3.354	2.361
Change in % from 1th to 25th cycle	200.8	249.1	196.1	177.1	241.0	221.3

Table 4.3: Summarized temperature development of type I and II during the reference heat cycles. The mean values are based on the connections not effected by edge effects. The average values for $I_S = 0$ A was taken after 120 min of that heat cycle with cable ground screen grounded in one end.

	Type I	Type II
Mean temperature, $I_S = 0$ A [°C]	55.3	54.6
Mean temperature, 1st cycle [°C]	63.4	63.5
Mean temperature, 25th cycle [°C]	67.6	65.7
Mean difference, 1st and 25th cycle [°C]	4.2	2.2
% increase from 1st to 25th	6.6	3.5

cycles are shown. Each point of the graphs represents the maximum temperature recorded for each connection during a heat cycle. As for the resistance figures, the dotted lines indicate heat cycles started with ambient temperature conditions in the ground screen connections.

As for the resistance developments, the three connections previously mentioned that were affected by edge effects are seen here as well. Much of the same pattern as for the resistance developments is seen, with the temperatures of type I seemingly sorted in pairs, and the temperatures of type II more compact. The pairing as seen for type I might be related to the conductor joint being located between the two ground screen connections which makes up one of the mentioned pairs, which might dissipate heat causing these connections to have a more equal temperature (see figure I.1 in appendix I). The temperature of connection 1.1 of type II is seen to be much lower than the other connections of type II, despite having a much higher resistance as seen in figure 4.11. This is most likely because of the connection being located at the end of the test setup, where the cooling effect from the surroundings might be greater than for the rest of the ground screen connections of the same type.

Table 4.3 shows the mean temperature development of type I and II during the heat cycles. It can be seen that type I after 25 heat cycles has increased its maximum mean temperature by 2 °C more than type II.

Table 4.3 also shows the average temperature of the ground screen connections when grounded, such that $I_S = 0$ A. The average value is here taken after 120 minutes into that cycle, which on average is longer than the duration of the heating time in the heating cycles with a $I_S \neq 0$ A. Comparing these averages with the averages of the first heat cycle, it is seen that already at cycle number one of the main heat cycles, the temperature is larger when a screen current is applied, which is to be expected from equation 2.5. The differences for type I is 8.1 °C while it for type II is 8.9 °C.

As a comparison to the ground screen connection temperatures, the overall development of the maximum temperature of the reference cables can be seen in table 4.4. The values shown is the mean value of the measurements on the two reference cables. In this table, the column "Sheath" is the temperature measurements which corresponds to the placement of the ground screen connections. Comparing these values with the ones given in table 4.3, it is seen that the mean temperature of the ground screen connections is higher

Table 4.4: Summarized temperature development of the measurements conducted on the two reference test objects during the reference heat cycles.

	Cable ground screen	Conductor	Sheath
Mean temperature, $I_S = 0$ A [°C]	55.3	61.2	54.1
Mean temperature, 1st cycle [°C]	62.6	67.8	61.1
Mean temperature, 25th cycle [°C]	62.7	67.9	61.2
Mean difference, 1st and 25th cycle [°C]	0.1	0.1	0.1

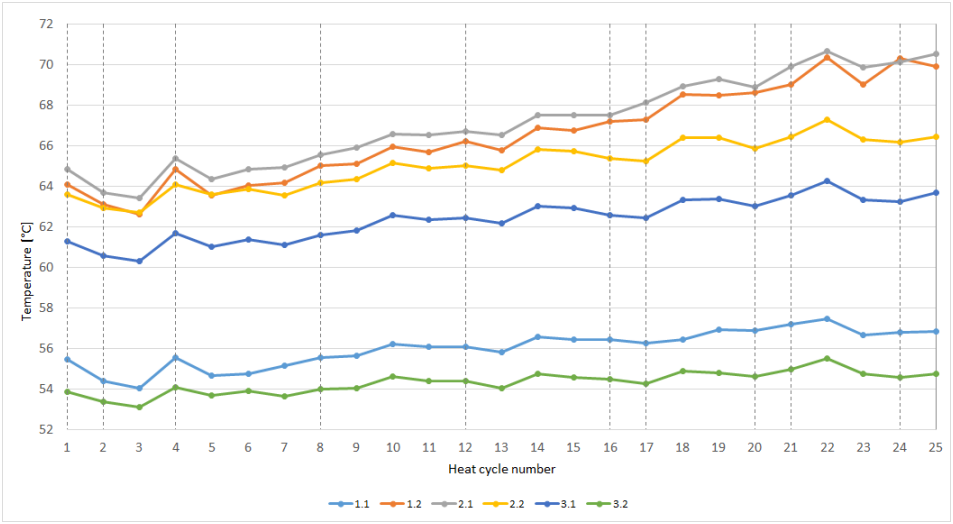

Figure 4.12: Figure showing the temperature development during the reference tests for type I. Each point shows the maximum temperature of the connection in that heat cycle. The dashed vertical lines indicates cycles that were started with the ground screen connections at ambient temperature conditions.

than the reference measurements at the sheath and in the cable ground screen, both at the start of the heat cycles and at its conclusion. The rest of the temperature development of the reference cables can be seen in figure K.1, in appendix K.

Figure 4.14 shows the heating time of each heat cycle, the time from the start of the heating cycle until the stability criteria was reached. It can be seen that the heat cycles started with ambient conditions takes more time to reach the stability criteria. This makes sense, as these cycles start with a lower temperature than the following cycles through the test day. From the figure, it seems that the heating time remains quite constant for the ambient times and the non-ambient times when isolated.

Table 4.5 shows the mean, maximum and minimum heating time registered as well as the overall change in heating time during the heat cycles. Further it seems that the non-ambient heating cycles with positive screen current has the largest heating time before reaching stability, compared with the ones with negative polarity of the same testing day.

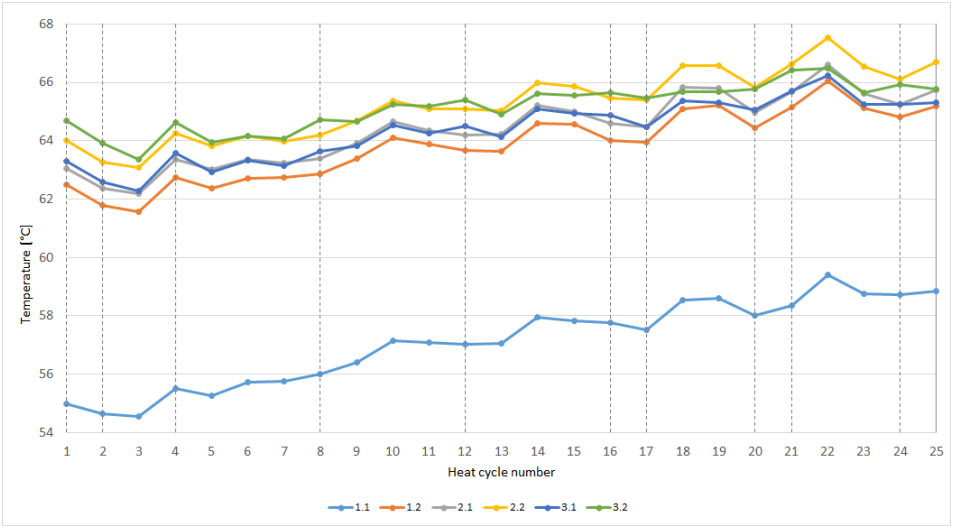

Figure 4.13: Figure showing the temperature development during the reference tests for type II. Each point shows the maximum temperature of the connection in that heat cycle. The dashed vertical lines indicates cycles that were started with the ground screen connections at ambient temperature conditions.

This can be seen for the cycles [5,7], [9,11], [13,15], [18,19] and [22,23] in figure 4.14. It is difficult to conclude from the collected data whether the heating time would change if further heating cycles had been carried out.

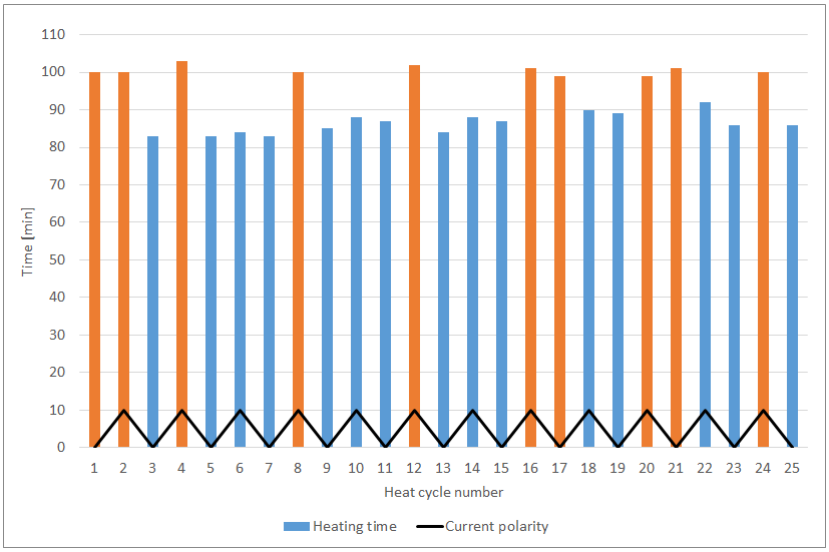

Figure 4.14: Figure showing the heating time development throughout the course of the heat cycles. Orange bars indicates heat cycles that were started from ambient temperature conditions. Black line indicates current polarity of the screen current, positive peak indicating positive screen current.

Table 4.5: Table showing the time from the start of a heating cycle until the stability criteria was reached. 3rd and 25th heat cycle was the first and last of the heat cycles started from non-ambient conditions, while the 1st and 24th heat cycles were the equivalent heat cycles for the ones started with ambient conditions.

	Heating time, overall [min]	**Heating time, non-ambient [min]**	**Heating time, ambient [min]**
Mean	92	86	101
Maximum	103	92	103
Minimum	83	83	99
1st heat cycle	100	-	100
3rd heat cycle	-	83	-
24th heat cycle	-	-	100
25th heat cycle	86	86	-
Overall change	-14	3	0

4.3 Heat cycling with improper installation

The heat cycles with the improper installation was conducted with the ground screen connections installed as explained in section 3.2.2. As for the reference tests, the main tests were conducted with a load current of 440 A_{AC} but the screen current used was instead 30 A_{DC}. 25 heat cycles were conducted.

4.3.1 Temperature and resistance development in the main tests.

In figures 4.15 and 4.16, the resistance development of the ground screen connections during the heat cycles of the main experiment can be seen. As for the reference cycles, each point is based on the mean resistance value of the connection during the last ten minutes of the heat cycle. Vertical dotted lines indicates heat cycles that were started with the ground screen connections having ambient temperature conditions.

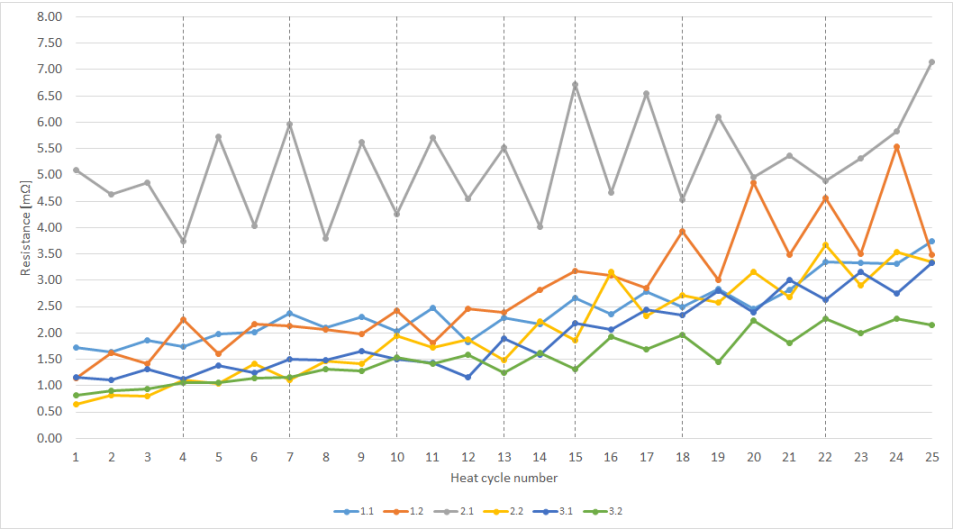

Figure 4.15: Figure showing the absolute resistance development during the main heat cycles with improper installation for type I. Each point in the figure is based on the last ten minutes of the heat cycle. The dashed vertical lines indicate cycles that were started with the ground screen connections having ambient temperature conditions.

The figures show that all of the ground screen connections experiences an increase in its resistance during the 25 heat cycles. Connection 2.1 of type I and 2.2 of type II both shows to have a larger resistance than the rest through the heat cycle series.

As for the reference tests, it does not seem that the resistance values are dependent on whether the heat cycle is started with ambient conditions or not. However, it seems again like the values obtained are somewhat dependent on the switching of screen current polarity, as can be seen from values going up and down, with an increasing trend. The im-

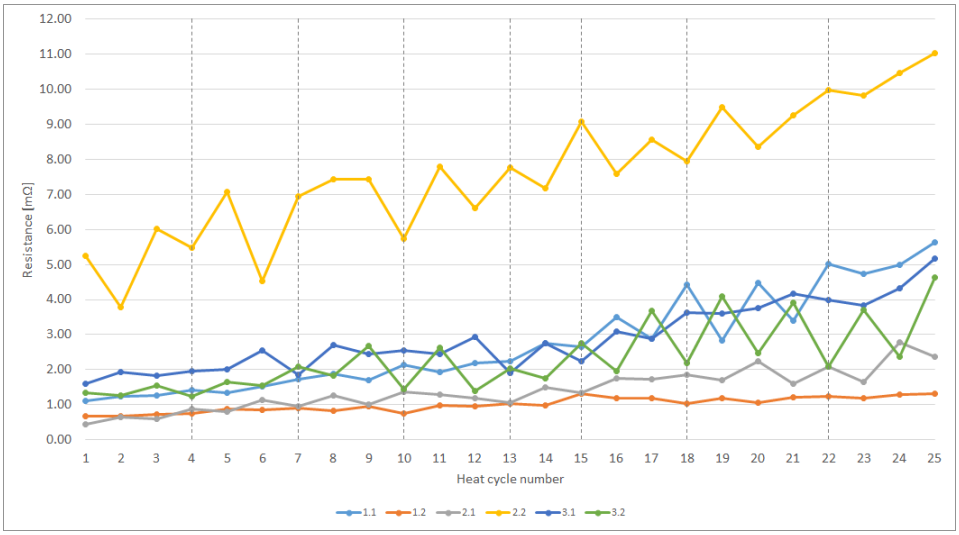

Figure 4.16: Figure showing the absolute resistance development during the main heat cycles with improper installation for type II. Each point in the figure is based on the last ten minutes of the heat cycle. The dashed vertical lines indicate cycles that were started with the ground screen connections having ambient temperature conditions.

proper installation seems to be more susceptible for this than the correct installation, as the peak values are larger and increasing with the number of heat cycles performed.

In figures 4.17 and 4.18 the corresponding temperature development is shown, with each point representing the maximum temperature recorded during each heat cycle. As for the resistance development, the temperatures seem to fluctuate some with the change in polarity, but not as much as the resistance does.

From the resistance and temperature figures, it seems that there is a good correlation between the development in resistance and the development in temperature. For both type I and II the order of the ground screen connection resistances can be found in the associated temperature figures. The exceptions are the previously mentioned ground screen connections with edge effects, showing less coherence between connection resistance and corresponding temperature.

In the reference tests, the mean values of the resistances and the temperatures were based on the ground screen connections which did not experience any edge effects. For the main tests with the improper installation, it was however chosen to include the resistances prone to edge effects in the mean resistance values. The reason for this was that from figures 4.15 and 4.16, no clear connection could be seen from the ground screen connections placement along the test setup (figure I.1 appendix I) and its recorded resistance, opposite of what was the case during the reference tests. It is likely that the stochastic parameters affecting these values from the installation are large, and all the ground screens should thus be included. For the temperatures however, it was still ev-

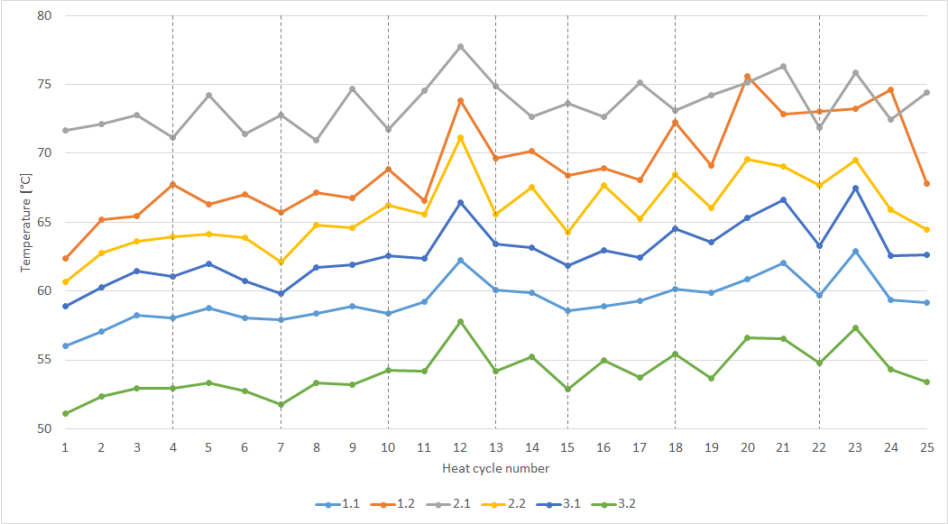

Figure 4.17: Figure showing the maximum temperature development during the main tests for type I. The dashed vertical lines indicate cycles that were started with the ground screen connections having ambient temperature conditions.

ident that the temperature development in the edge connections was affected by edge effects, causing them to be excluded from the selection giving the average values.

Tables 4.6 and 4.7 shows the most important changes in the resistance from the main heat cycles. The resistances of type I has on average increased by 2.105 mΩ. The percentage increase of each connection varies from 40 to 420 %, with connection 2.2 having the largest percentage increase while also having the lowest resistance value during the first heat cycle.

Type II has experienced an average increase of 3.286 mΩ, with the percentage increase ranging from 92 to 444 %. As for type I, it is the connection with the lowest resistance at the first heat cycle that has experienced the largest increase compared to the first heat cycle (connection 2.1).

Comparing the the two types by per length resistance, it can be seen that the mean value for type I after 25 heat cycles is 154.8 Ω/km, while it for type II is 313.7 Ω/km. Thus, the type II ground screen connection shows to have the largest resistance in both absolute value and per length.

Comparing the per length values at the first heat cycle to the values at the 25th heat cycle in table 4.8, it is also seen that type II not only has the highest resistance values overall, but also shows the greatest percentage increase. It thus seems that the degradation mechanisms in type II are worse than in type I. This is believed to be caused by the following:

- The thickness of the force spring of type II is greater than the force springs for type I. As a result, the travel path for the current through the force spring layer in series

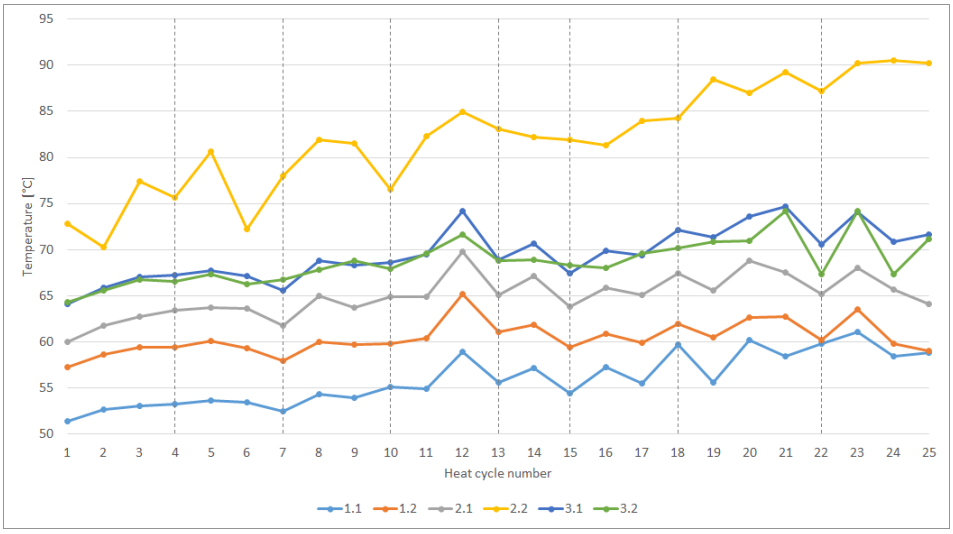

Figure 4.18: Figure showing the maximum temperature development during the main tests for type II. The dashed vertical lines indicate cycles that were started with the ground screen connections having ambient temperature conditions.

Table 4.6: Changes in resistance for type I during the main heat cycles.

	1.1	**1.2**	**2.1**	**2.2**	**3.1**	**3.2**
	Absolute resistance [mΩ]					
1st cycle	1.723	1.136	5.091	0.645	1.168	0.821
1st cycle mean	1.764					
Minimum during cycling	1.645	1.136	3.745	0.645	1.106	0.821
Maximum during cycling	3.740	5.536	7.145	3.680	3.334	2.277
25th cycle	3.740	3.493	7.145	3.351	3.334	2.149
25th cycle mean	3.869					
$R_{max} - R_{min}$	2.095	4.400	3.400	3.035	2.228	1.456
	Per length resistance [Ω/km]					
1st cycle	68.91	45.43	203.64	25.79	46.71	32.86
1st cycle mean	70.56					
Minimum during cycling	65.81	45.43	149.8	25.79	44.25	32.86
Maximum during cycling	149.6	221.4	285.8	147.2	133.4	91.08
25th cycle	149.6	139.7	285.8	134.0	133.4	85.96
25th cycle mean	154.8					
$R_{max} - R_{min}$	83.79	176.0	136.0	121.4	89.15	58.22
Change in % from 1th to 25th cycle	117.1	207.6	40.35	419.7	185.6	161.6

Table 4.7: Changes in resistance for type II during the main heat cycles.

	1.1	**1.2**	**2.1**	**2.2**	**3.1**	**3.2**
	Absolute resistance [mΩ]					
1st cycle	1.104	0.681	0.433	5.239	1.602	1.336
1st cycle mean	1.733					
Minimum during cycling	1.104	0.671	0.433	3.780	1.602	1.245
Maximum during cycling	5.634	1.310	2.777	11.03	5.165	4.625
25th cycle	5.634	1.308	2.357	11.03	5.165	4.625
25th cycle mean	5.019					
$R_{max} - R_{min}$	4.530	0.639	2.344	7.25	3.563	3.380
	Per length resistance [Ω/km]					
1st cycle	68.98	42.58	27.07	327.4	100.1	83.51
1st cycle mean	108.3					
Minimum during cycling	68.98	41.92	27.07	236.3	100.1	77.83
Maximum during cycling	352.1	81.90	173.6	689.1	322.8	289.0
25th cycle	352.1	81.76	147.3	689.1	322.8	289.0
25th cycle mean	313.7					
$R_{max} - R_{min}$	283.1	39.98	146.5	452.8	222.7	211.2
Change in % from 1th to 25th cycle	410.5	92.00	444.1	110.5	222.3	246.1

Table 4.8: Table comparing the mean resistance values of type I and II at the first and 25th heat cycle in per length values.

	Type I	Type II
1st [Ω/km]	70.56	108.3
25th [Ω/km]	154.8	313.7
Increase [%]	119.4	189.7

with the copper wires and the joint ground screen is larger for type II than type I. This causes l in equation 2.4 to increase, further increasing the resistance.

- As previously mentioned, the braided joint ground screen of type II is less rough than type I. For the correct installation, this was seen as an advantage. For the improper installation however, this seems to be a disadvantage. The reason for this is that the smoother surface will create less contact spots as seen in figure 2.5. This will increase the total constriction resistance given by equation 2.16. The resistance will be further increased by the heating caused by this restricted number of contact spots, causing an increased heating to occur.

Table 4.9 shows the summarized development in the temperature for type I and II. It can be seen that type II overall shows the largest increase in mean temperature, but this is much influenced by connection 2.2 of type II which had a significantly larger temperature than all the other connections. This can be seen in figure 4.18.

Table 4.9 also shows the average temperature of the ground screen connections when grounded such that $I_S = 0$ A. The average value here also taken after 120 minutes into

Table 4.9: Summarized development of the mean value of the maximum temperatures of type I and II during the main heat cycles. The mean values are based on the connections not effected by edge effects. The average values for $I_S = 0$ A was taken after 120 min of that heat cycle with grounded screen.

	Type I	Type II
Mean temperature, $I_S = 0$ A [°C]	57.3	57.4
Mean temperature, 1st cycle [°C]	63.4	63.7
Mean temperature, 25th cycle [°C]	67.3	71.2
Mean difference, 1st and 25th cycle [°C]	3.9	7.5
% increase from 1st to 25th	6.2	11.8

Table 4.10: Summarized development of the mean value of the maximum temperatures of the reference cables during the main heat cycles. The mean values are based on the connections not effected by edge effects. The average values for $I_S = 0$ A was taken after 120 min of that heat cycle with grounded screen. The 22nd heat cycle was the last heat cycle where the 90 °C was not reached.

	Ground screen	Conductor	Sheath
Mean temperature, $I_S = 0$ A [°C]	57.1	63.2	55.9
Mean temperature, 1st cycle [°C]	55.3	61.0	54.3
Mean temperature, 22nd cycle [°C]	55.3	61.0	54.4
Mean temperature, 25th cycle [°C]	53.1	58.6	52.3
Mean difference, 1st and 25th cycle [°C]	-2.2	-2.4	-2.0

that cycle, which on average is longer than the duration of the heating time in the heating cycles with $I_S \neq 0$ A. Comparing these averages with the averages of the first heat cycle, it is seen that already at cycle number one of the main heat cycles, the temperature is larger when a screen current is applied. The differences for type I is 6.1 °C while it for type II is 6.3 °C. It can be seen that the average temperature for the heat cycle with grounded screen has increased compared to what was the case during the reference tests. This might be because of the test setup already being exposed to a whole heat cycle series, which might have altered the properties of the test setup.

The corresponding temperature development of the reference cables are given in table 4.10. As for the reference heat cycles, the sheath temperature lies below that of the corresponding mean ground screen connection temperatures. The complete temperature development can be seen in figure K.2 in appendix K.

Table 4.11: Table showing the maximum and minimum temperature of each ground screen connection, as well as the difference between these two, from the main heat cycles.

	Type I						Type II					
Min [°C]	56.0	62.4	70.9	60.7	58.9	51.1	51.3	57.2	59.9	70.3	64.1	64.3
Max [°C]	62.9	75.6	77.8	71.2	67.5	57.8	61.0	65.2	69.7	90.5	74.6	74.2
Diff [°C]	6.9	13.2	6.9	10.5	8.6	6.7	9.7	8.0	9.8	20.2	10.5	9.9

Table 4.12: Table showing the time from the start of a heating cycle until the stability criteria was reached. The 22nd heat cycle was the last one conducted were 90 °C was not reached. Overall change indicate the change from the first cycle (either overall, ambient or non-ambient) to the last one. Numbers in parenthesis indicates times or changes not including the heat cycles reaching 90 °C.

	Heating time, overall [min]	**Heating time, non-ambient [min]**	**Heating time, ambient [min]**
Mean	88	86	95
Maximum	129	129	106
Minimum	64	64 (74)	82
1st heat cycle	82	82	106
22nd heat cycle	82	-	82
25th heat cycle	64	64	-
Overall change, first - last cycle	-18	-18	-24
T_{max}-T_{min}	65	65 (55)	24

Figure 4.19 shows the development in the heating time for the main heat cycles. The legend is the same here as for the reference tests but in addition, the heat cycles where the 90 °C criteria was reached (explained in section 3.5) for one of the ground screen connections are marked in yellow .

It seems that there is a slightly decreasing trend in this figure, both for the heat cycles started with ambient conditions and for the non-ambient ones. This is most likely caused by the degradation of the ground screen connections, causing the resistance to increase, further increasing the dissipated power in the connection. This again causes the temperature criteria to be reached in a shorter amount of time.

Table 4.12 shows the most important aspects from figure 4.19. Here, the 22nd heat cycle indicates the last heat cycle where the 90 °C criteria was not reached.

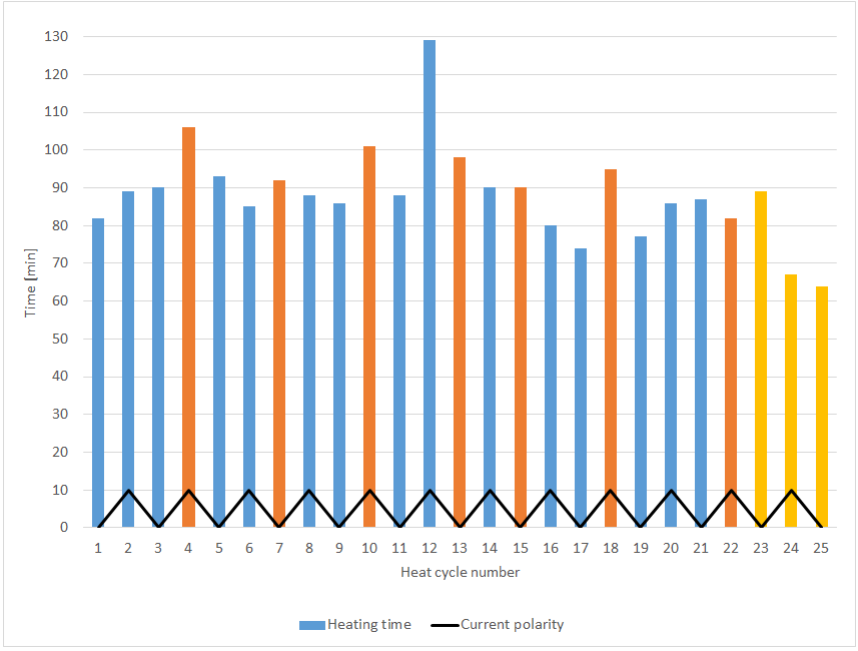

Figure 4.19: Figure showing the heating time development throughout the course of the heat cycles for the main test. Orange bars indicates heat cycles that were started from ambient temperature conditions. Yellow bars indicate heat cycles were the 90 °C criteria was reached, and the heat cycle terminated. Black line indicates current polarity of the screen current, positive peak indicating positive screen current polarity.

4.4 Comparison of heat cycle results

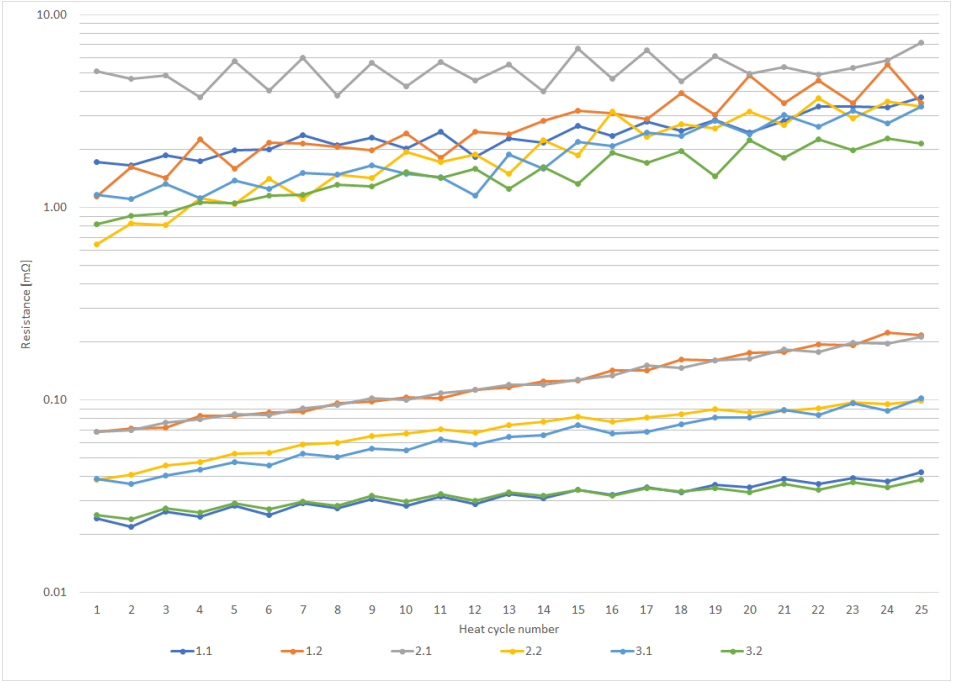

Figure 4.20: Logarithmic plot showing the resistance development of the type I ground screen connections for the reference and main heat cycles.

Figures 4.20 and 4.21 shows the resistance development of both the reference and main test for type I and type II respectively, as previously showed separately in section 4.2 and 4.3.

Figure 4.22 compares the development in average resistance for the two ground screen connection types in the reference and main tests, both in absolute and per length value. The selection of ground screen connections that these values are based on is given in section 4.2 and 4.3.

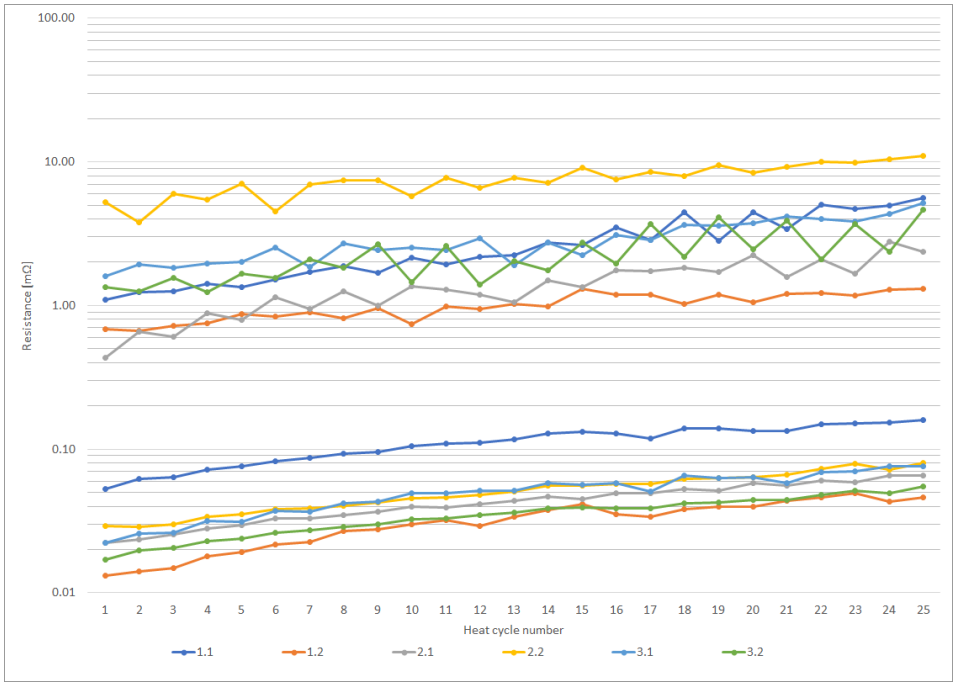

Figure 4.21: Logarithmic plot showing the resistance development of the type II ground screen connections for the reference and main heat cycles.

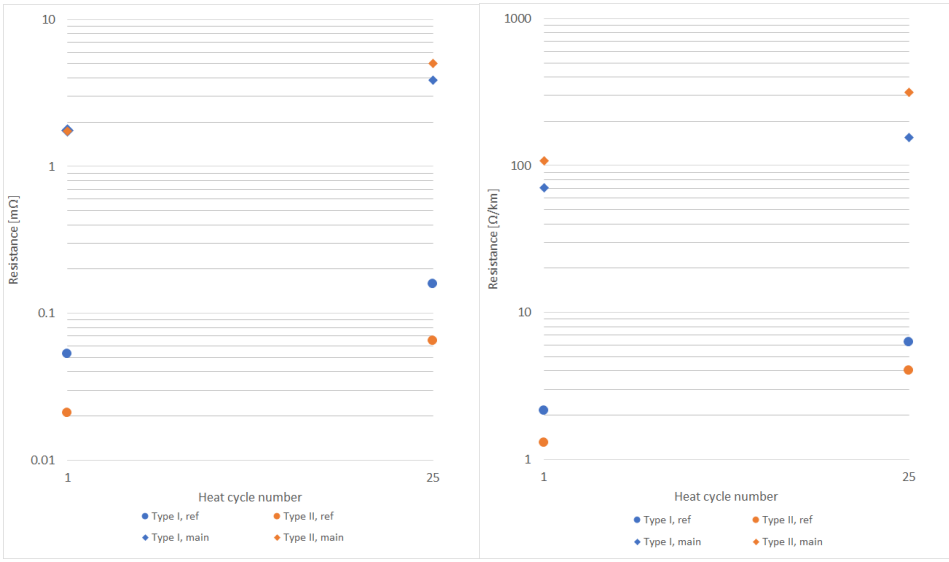

(a) Absolute resistance development.

(b) Per length resistance development.

Figure 4.22: Plots showing the average resistance development from the first to the 25th heat cycle of both reference and main tests. Circle indicates reference tests, diamond indicates main tests.

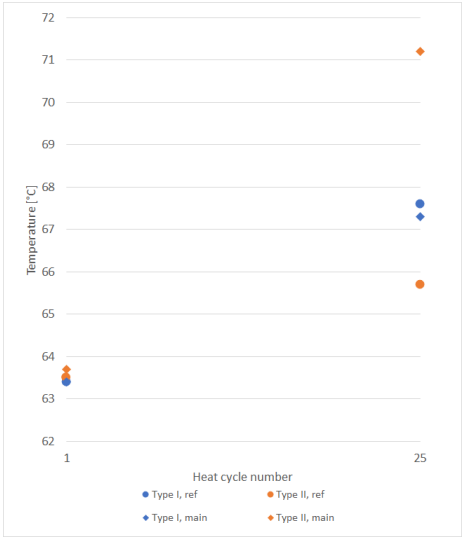

Figure 4.23: Plot showing the temperature development of for the reference and main heat cycles. Circle indicates reference tests, diamond indicates main tests.

From these figures it is seen that type II has the lowest resistance values of the two types when installed as intended, both in absolute value and in per length. The opposite is however seen with the improper installation. Type II now has the highest resistance value on average of the two, both in absolute value and in per length value.

As a consequence of having the highest average resistance for the improper installation, type II also shows to have the largest increase in average temperature, as shown in figure 4.23. From having the lowest average temperature at the end of the reference tests, the improper installation causes type II to gain the undoubtedly highest average temperature at the end of the main heat cycles. Type I on the other hand seems to have close to the same temperature development during the reference test and the main tests.

The temperature development for type I is almost identical for the two heat cycles performed, as seen in figure 4.23. Type II shows an increase in temperature compared to the reference tests. It is thus evident that the improper installation causes the temperature development to increase significantly compared to the correct installation, as one type shows almost identical temperature increase for a *reduced* ground screen current, while the other shows an increased temperature for a *reduced* screen current, as the screen current during the main tests only were 30 % of that used in the reference tests.

It is expected that the temperature increase would be higher, had a larger ground screen current been used in the main tests, as 30 A is a fairly low screen current for an actual three phase cable arrangement in flat configuration, as shown by the screen current simulations performed in section 3.5. It is thus reasonable to believe that the dissipated power will be greater in a real-life scenario. This is further supported by the formulas regarding screen currents and power dissipation.

Although only the temperature increase of connection 2.2 of type II may be considered as destructive over time, the temperature increase of the other connections may as well cause trouble, by causing an increased sheath temperature reducing the maximum service temperature as given by equation 2.8. An increase in the ground screen connections temperature will also reduce its thermal conductivity, further increasing the heat accumulated, as explained in section 2.4.

4.5 Measuring methods

An important part of the project, as explained in the preparation of the test objects in chapter 3, was to find an approach to measure the voltage drop across the ground screen connections.

In the sections above, all of the resistance values presented are based on the last ten minute period of each heat cycle, where the resistance value stabilized. In addition to these resistance values, condition assessment of the ground screen connections was performed with two additional methods throughout the course of the experiments

- Four-point resistance measurement with micro-ohm meter.
- Four-point resistance measurement with the DC-sources used in the heat cycles.

In the following sections, these methods will be compared with the values obtained from the previously presented heat cycle resistances, to see if these resistance measurements are fitted to be used as condition assessment of the ground screen connections.

4.5.1 Resistance measurement with the DC source

As explained in section 3.5, a four-point measurement was performed between each heat cycle after each ground screen connection temperature had fallen below 35 °C.

Reference tests

Figures 4.24 and 4.25 shows the development of the resistances from the measurements between the heat cycles, for type I and type II respectively. The resistance value is found by using the same approach as in the resistance values from the heat cycles, as explained in section 3.6.

When correcting the resistance values (removing the contribution from copper wires and joint ground screen), a problem occurred. Due to the low current of 2 A used in the measurements and the low resistance due to the correct installation, the corresponding voltage drop became low. As a result, the calculated resistances in the negative current direction for the assessment gave *negative* ground screen connection resistances. As a result, only the calculated resistances from the positive current direction is shown in figures 4.24

and 4.25. This was however only a problem for the reference test, and not for the equivalent measurements for the main test.

The reason for this negative resistance value might be connected to measuring errors from the ampere-meter.

By comparing the resistance development in these resistance measurements with the corresponding values from the heat cycles, it can be seen that there are some differences. For type I, the overall measured resistances tend to be larger than what was measured during the ten minute period in the heat cycles. The pattern and grouping that the resistances had in the heat cycles is also changed. Connections 1.2 and 2.1 do no longer clearly tend to have the largest resistance values. In the last heat cycles, both connection 2.1 and 2.2 gives large resistance values before dropping again.

For type II, the difference in resistance value is not as prominent as for type I. Connection 1.1 with edge effects is still measured to be the largest of these resistances, with an increasing trend. For the other connections, the spread in resistance value increases until midway in the heat cycle series, before being reduced at the end of the series.

Both type I and II shows a less smooth increase during these resistance measurements than during the heat cycles, with more and larger spiking occurring, reducing the reliability of the assessment.

The reason for the unsteady behavior of the resistance development during the condition assessment is believed to be the following:

After the reference heat cycle series, the thermal insulation was removed order to measure the resistance of the ground screen connections with the micro-ohm meter. It was then discovered that the voltage measuring points on the copper wires had become much looser than what it initially had been tightened to before the heat cycles. It is likely that the measuring point becoming lose is a direct result of the thermal cycles and the expansion and following contraction of the XLPE insulation. The degree of loosening varied from connection to connection, with some being worse than others. This was not seen at the equivalent measuring point on the joint ground screen above the conductor joint and the PVC tube. The reason for this is most likely that the amount of material which can expand during heat cycling is much less here, than on the cable side.

This loosening would cause a reduced contact between the measuring point and the copper wires of the test object, increasing the resistance r in figure 3.21 and causing some uncertainty in the voltage measurements which the resistance calculations were based on. Since the resistance measurements from the heat cycles were based on the last ten minutes of the cycle where it stabilizes, it seems that the insulation expands enough to tighten the voltage measuring point, allowing a reliable measuring to be made.

Due to the experiences mentioned above, other types of voltage measurement points should be considered. However, the problem with thermal expansion of the insulation and the requirement of the point being a voltage equalizer for the copper wires complicates this. Some type of hose clamp with a uniform inside could be considered, as this might be strong enough to withstand the expansion of the insulation. However, the

clamps force and width might cause a threat to the integrity of the cable insulation system, if parts of the cable were to squeeze up and past the edges of the clamp. This could cause field enhancement, further causing degradation of the insulation. Another possibility might to solder a measuring point onto the copper wires. This might however be difficult to realize while acting as a voltage equalizer along the circumference of the cable ground screen. A so called *welded* equalizer could also be considered, mentioned both by [26] and [28]. This might however be troublesome, as this method would require all the copper wires to be welded together with a common metal piece which then would be in series with the ground screen connection assembly.

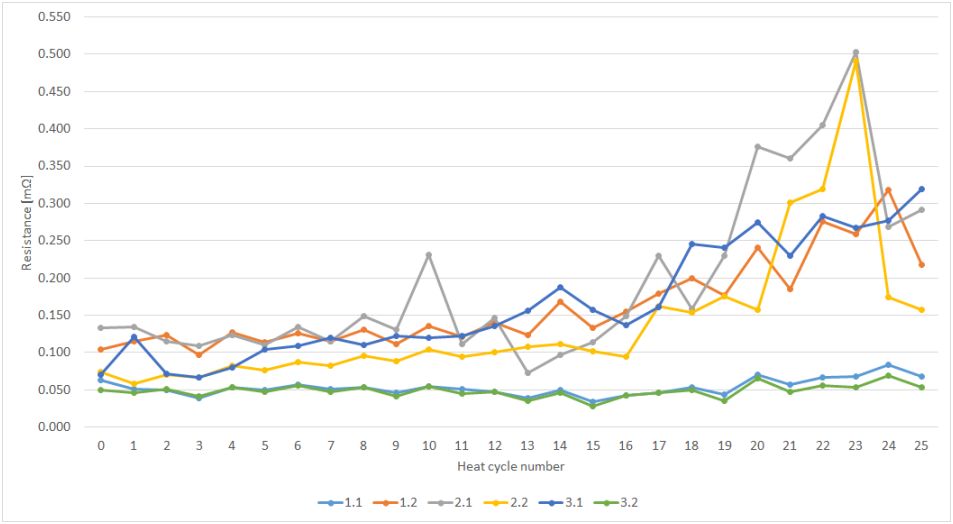

Figure 4.24: Condition assessment by resistance measurement of type I during the reference tests, between each heat cycle. Heat cycle zero corresponds to the measurement before the first heat cycle. Number one is then the measurement after the first heat cycle, and so on.

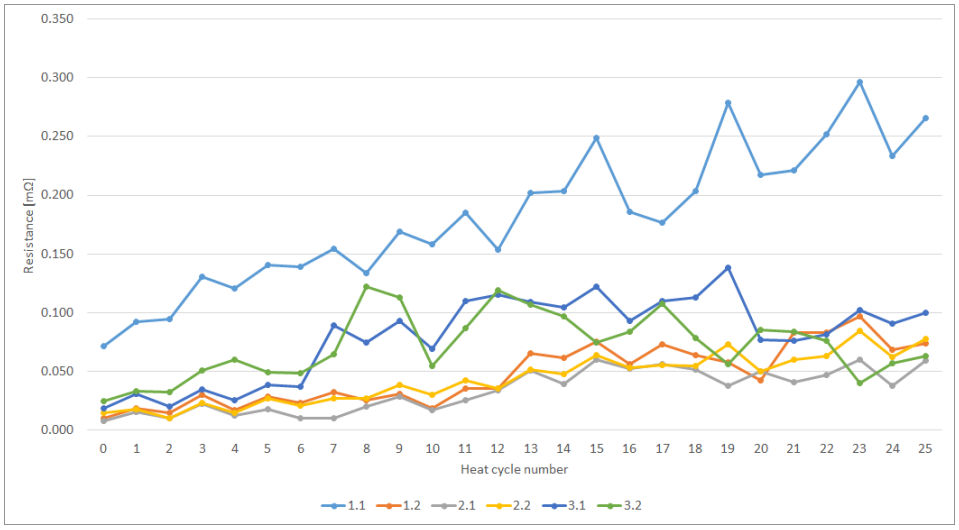

Figure 4.25: Condition assessment by resistance measurement of type II during the reference tests, between each heat cycle. Heat cycle zero corresponds to the measurement before the first heat cycle. Number one is then the measurement after the first heat cycle, and so on.

Main tests

Figures 4.26 and 4.27 shows the results of the resistance measurements between each heat cycle for type I and type II respectively, through the course of the main tests. For both type I and II a quite large development can be seen between measurement (heat cycle) zero and one. The reason for this is the following: measurement zero was conducted on the test setup after thermal insulation was applied. Then the three heat cycles of 30, 40 and 45 A was conducted to determine the ground screen current to be used on the improper installation. Condition assessment was not performed between these heat cycles, meaning that there are four heat cycles conducted between condition assessment zero and one (30, 40, 45 and then 30 A of the actual heat cycles).

As for the same resistance measurements of the reference tests, the resistance development deviates from that of the resistances from the heat cycles. For type I, the same spiking can be seen for connection 2.1 as in the resistance development in the heat cycles. Connection 2.2 of type I shows large deviations, tending towards zero in the middle of the heat cycles series before increasing again.

The resistances obtained for type II shows even less coherence than for type I, with the only connection showing similarities with the cycling results being connection 2.2.

The resistances measured with the measurements between each heat cycle is generally much larger than the corresponding values during the heat cycles.

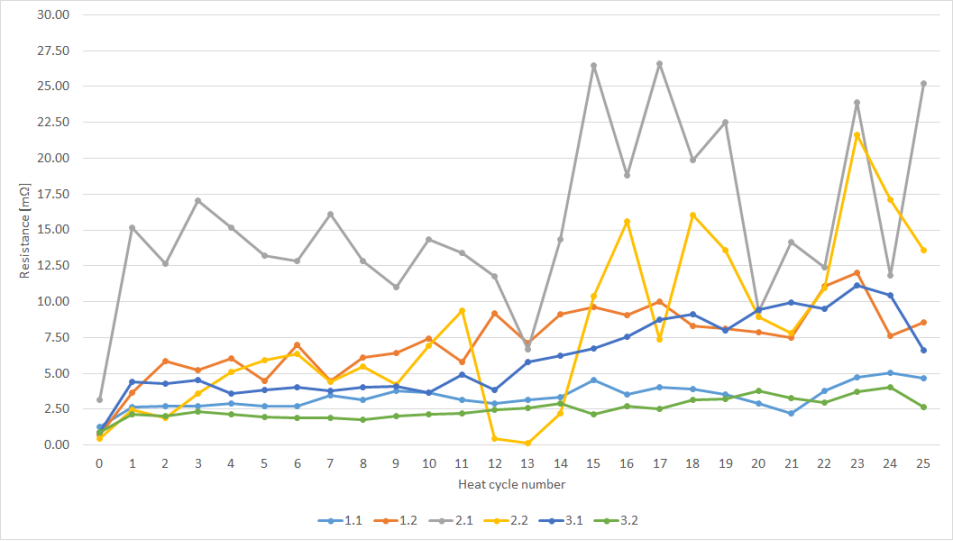

Figure 4.26: Condition assessment by resistance measurement of type I during the main tests, between each heat cycle. Heat cycle zero corresponds to the measurement before the first heat cycle. Number one is then the measurement after the first heat cycle, and so on.

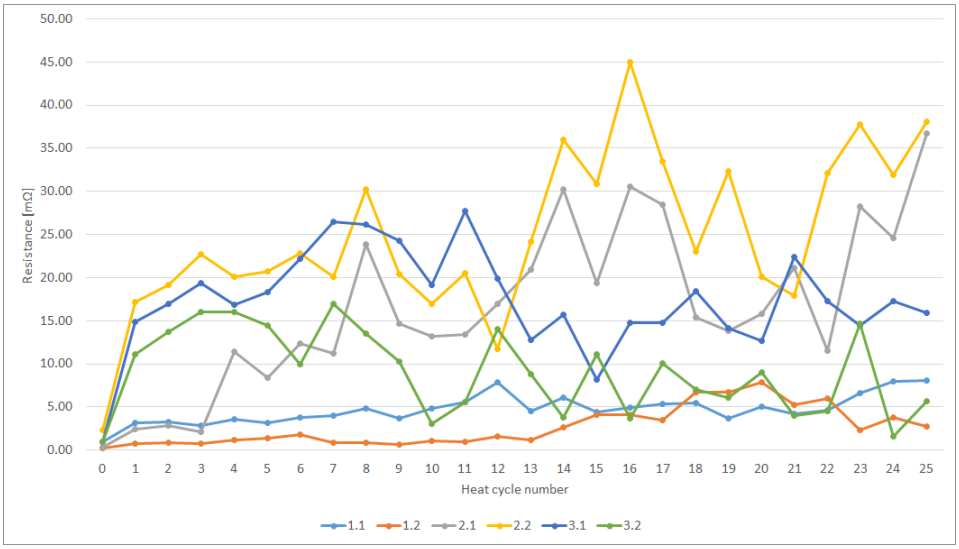

Figure 4.27: Condition assessment by resistance measurement of type II during the main tests, between each heat cycle. Heat cycle zero corresponds to the measurement before the first heat cycle. Number one is then the measurement after the first heat cycle, and so on.

4.5.2 Resistance measurement with micro-ohm meter

Both before thermal insulation was applied to the test setup and after the heat cycles were done, the resistances of the ground screen connections were measured with the micro-ohm meter, in the same way as it was used when measuring on the copper wires of the cable ground screen and the joint ground screen alone.

More details from these measurements are given in appendix J.

Measurements before the heat cycles

Figures 4.28 and 4.29 shows the resistance of the ground screen connections before thermal insulation was applied, in absolute value and in per length value respectively for both the reference and the main tests.

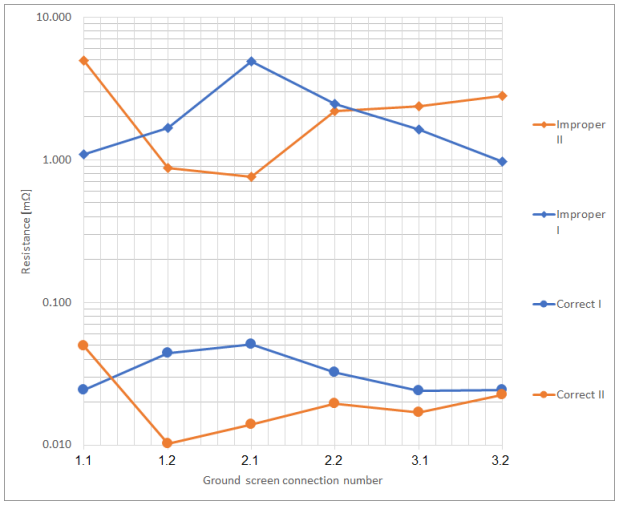

Figure 4.28: Figure showing the resistance of each ground screen connection with correct installation and improper installation with units mΩ. Correct installation is indicated with dot, while improper installation is shown with diamond shape.

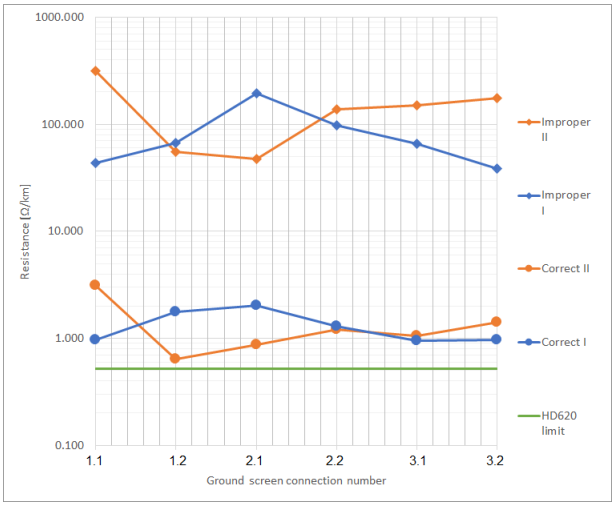

Figure 4.29: Figure showing the resistance of each ground screen connection with correct installation and improper installation with units Ω/km. Correct installation is indicated with dot, while improper installation is shown with diamond shape.

Measurements after the heat cycles

In this section the resistance measurements performed with the micro-ohm device after the heat cycles was completed, are shown.

As can be seen, the measurements were performed both with the old and new voltage connection points due to the loosening of the measuring point as explained in section 4.5.1.

For the measuring after the main heat cycles, new measuring points was only applied to type II. However, as can be seen from figure 4.32 and 4.33, values are shown for type I although this was not measured. These values for type I are based on the mean difference between the measurements with new measuring point on type II and the values obtained from the 25th heat cycle for type II, as these showed good coherence. The plotted value for type I in figures 4.32 and 4.33 is the value the 25th heat cycle of the main series for type I, with the mentioned difference subtracted. More information about these measurements can be found in appendix J.

Old measuring points

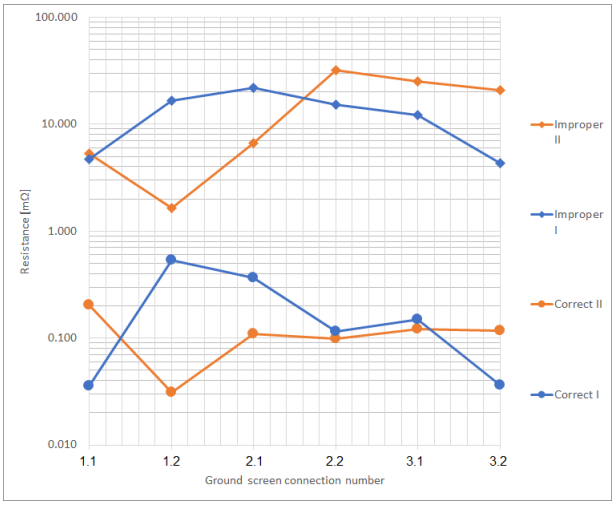

Figure 4.30: Figure showing the resistance of each ground screen connection with correct installation and improper installation after heat cycling, with units mΩ. Correct installation is indicated with dot, while improper installation is shown with diamond shape. The values are the ones measured with the partially loose voltage measuring points.

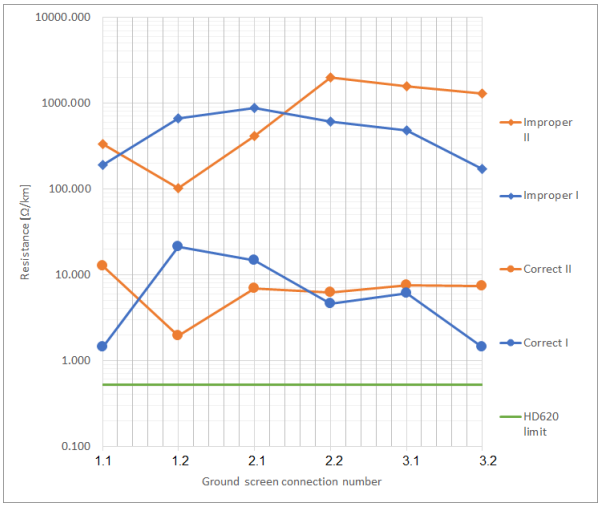

Figure 4.31: Figure showing the resistance of each ground screen connection with correct installation and improper installation after heat cycling, with units Ω/km. Correct installation is indicated with dot, while improper installation is shown with diamond shape.The values are the ones measured with the partially loose voltage measuring points.

New measuring points

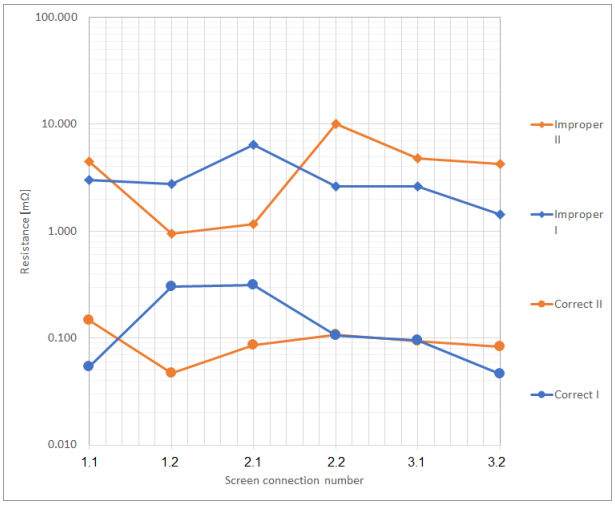

Figure 4.32: Figure showing the resistance of each ground screen connection with correct installation and improper installation after heat cycling, with units mΩ. Correct installation is indicated with dot, while improper installation is shown with diamond shape. The values are the ones measured with new measuring points.

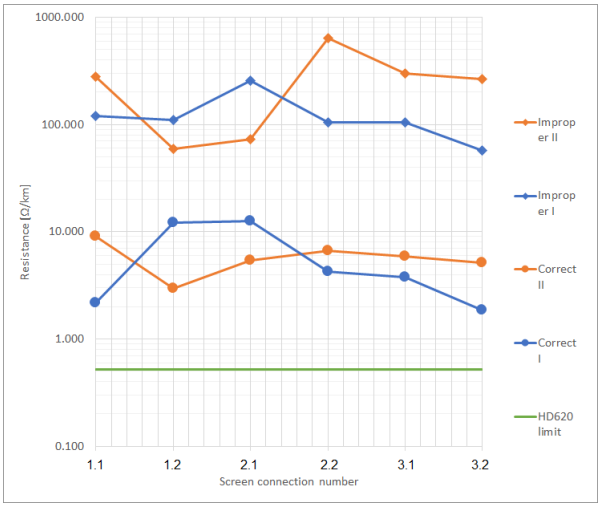

Figure 4.33: Figure showing the resistance of each ground screen connection with correct installation and improper installation after heat cycling, with units Ω/km. Correct installation is indicated with dot, while improper installation is shown with diamond shape. The values for the improper installation are explained previously in this section. The values are the ones measured with new measuring points.

4.6 Comparison of resistance measuring methods

4.6.1 Comparison at the beginning of the heat cycles

Reference heat cycles

For type I it seems that the overall ground screen connection resistance *increases* due to the additional tightening with the thermal insulation, with the micro-ohm meter giving the lowest resistance values, followed by the first cycling resistances and the condition assessment performed between these two giving the greatest resistance overall for all the connections.

For type II, the spread between the results from the different methods is smaller than what was is for type I. However, no method consistently gives the largest or lowest resistances. For some of the ground screen connections, resistance measurement between the heat cycles gives the greatest resistance value, while for others the first cycling of the experiments gives the greatest values.

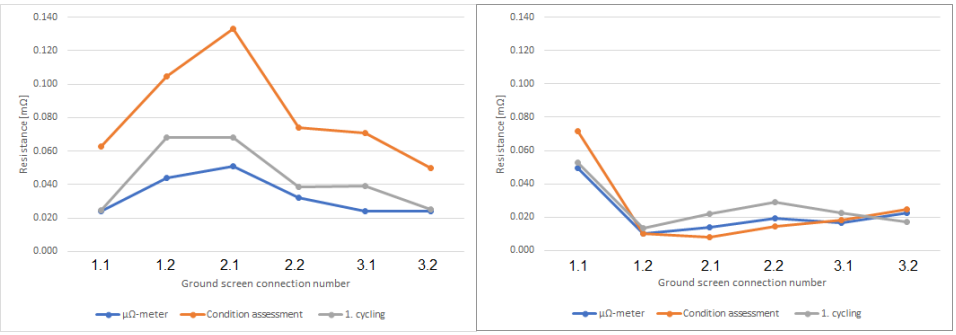

(a) Type I **(b)** Type II

Figure 4.34: Graphs showing the difference in measured resistance values for the different methods at the beginning of the cycling series, for the reference tests. Condition assessment here corresponds to resistance measurement number zero from the measurements with the DC-source.

Main heat cycles

For type I, a quite clear pattern is seen, with the values obtained with the micro-ohm meter being the largest apart from connection 1.1 and 3.2, which are close to the conditions assessment (resistance measurement between heat cycles) and the first cycling. This is most likely due to the edge effects experienced at both ends for this type.

The same trend, although less prominent, can be seen for type II. Less spread is here seen between the different methods for the connections 1.2, 2.1 and 2.2, while for connection

1.1, 3.1 and 3.2 it increases. The latter might be due to edge effects, as mentioned for type I.

For both type I and II it is clearly seen that the addition of thermal insulation with the associated tightening reduced the contact resistance in a quite different manner compared to what was seen for the reference tests. It seems that the additional pressure has reduced the resistance significantly since the measurement with the micro-ohm meter. This is believed to be caused by two main factors:

- Increased pressure in the contact between the copper wires and joint ground screen at the conductor joint side of the ground screen connection (in the 10 mm area between force spring and the edge of the outer sheath).
- Increased pressure inside the force spring arrangement, causing the load bearing area to increase as stated by equation 2.9.

For both type I and II, the resistances obtained from the first cycling is seen to be slightly lower than the first condition assessment. This is most likely due to the thermal expansion experienced by the cycling measurement, which increases the load bearing area and thus reduced the contact resistance.

From the above discussion, it thus seems that the condition assessment by the use of low current and the resistance measurement during the beginning of the heat cycle series are somewhat matched.

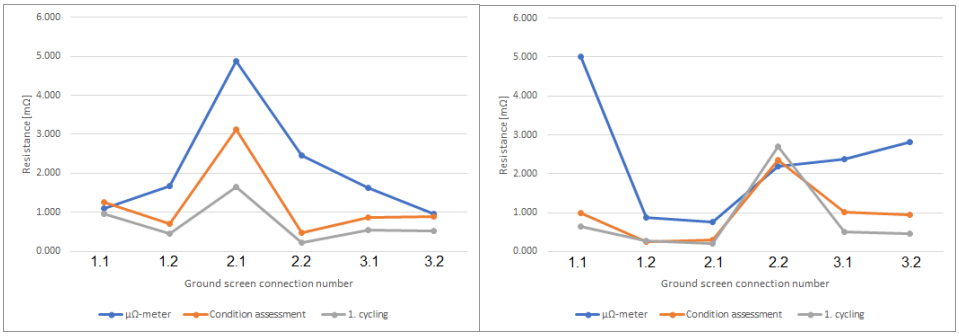

(a) Type I **(b)** Type II

Figure 4.35: Figures showing the difference in measured resistance values for the different methods at the beginning of the cycling series, for the main tests. Condition assessment here corresponds to resistance measurement number zero from the measurements with the DC-source.

4.6.2 Comparison at the end of the heat cycles

Reference heat cycles

Figure 4.36 shows the measured resistance for the different methods at the end of the heat cycle series for the reference experiment.

As pointed out in section 4.5.1, the voltage measuring points on the cable side of the ground screen connections were found to have become loose after the end of the heat cycles, causing the measured resistance to increase. For type I it is seen that the resistance measurement with the micro-ohm meter shows an even larger resistance than the last condition assessment. This is however strongly reduced when the measuring point is replaced by a new one.

For type II the spread between the measuring methods is much smaller than for type I, as also was the case at the beginning of the heat cycles.

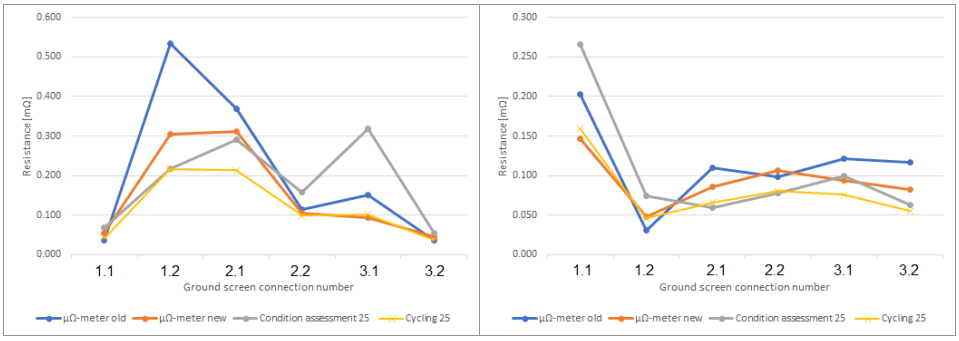

(a) Type I **(b)** Type II

Figure 4.36: Figures showing the difference in measured resistance values for the different methods at the end of the cycling series, for the reference tests. Condition assessment here corresponds to resistance measurement number 25 from the measurements with the DC-source.

Main heat cycles

Figure 4.37 shows the measured resistances for the different methods at the end of the heat cycle series for the main tests.

The measurement with the old voltage measuring points and the last condition assessment deviates greatly from that of the resistance from the 25th heat cycle. By replacing the old voltage measuring point with a new, it is seen that the measurement with the micro-ohm meter closely corresponds that of the last heat cycle. The orange line in 4.37a is based on the measurement with new voltage probes on type II, as explained in section 4.5.2 and appendix J.2.

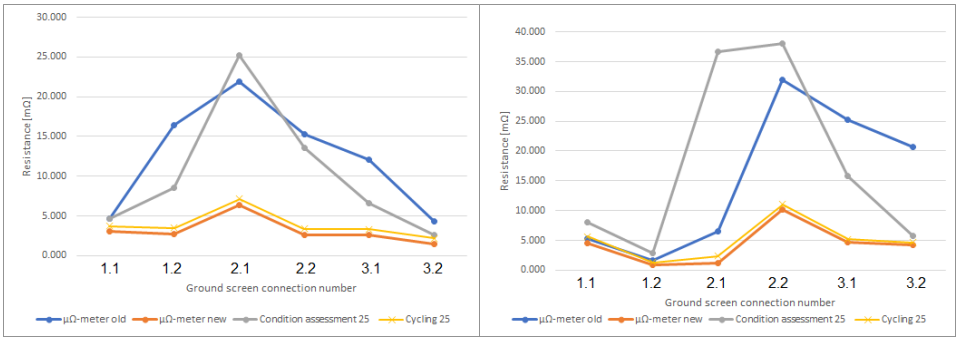

(a) Type I **(b)** Type II

Figure 4.37: Graphs showing the difference in measured resistance values for the different methods at the end of the cycling series, for the main tests. Condition assessment here corresponds to resistance measurement number 25 from the measurements with the DC-source.

4.6.3 Conclusion

From the results above it is seen that the resistance measurements method between the heat cycles at first seems to show good results and close resembles with the results from the heat cycles. However, through the course of the heat cycling this gets worse. At the end of each cycling series the voltage measuring points have become so loose that the resistance measurements done with them are unreliable. However, by changing the voltage measuring points the measurements closely resemble the values gained in the 25th heat cycle, implying that the thermal expansion during the heat cycle is sufficient to tighten the voltage measuring points around the copper wires during cycling. Thus, the sources of error which were present when the test setup had cooled down and condition assessment with low current from the DC source was performed, are removed during the end of the heat cycles.

It is evident that the method of condition assessment with the resistance measurement between the heat cycles used in the project should be reassessed, and a new, more reliable method should be found.

4.7 Investigation of ground screen connections after heat cycling

After the 25 heat cycles with the improper installation had been conducted, the thermal insulation of each ground screen connection was removed, allowing each connection to be investigated.

Some observations were common for both type I and type II. In almost all of the ground screen connections, the tip of the thermoucouples had left an imprint on the outer sheath, underneath the constant force spring and the PVC tape used to keep the thermocouple in place. This is a natural consequence of the thermal expansion of the sheath made from PE and the point shaped end of the thermocouple, which will be covered in the PE when this expands. In addition, the outer sheath made of PE has a thermal stability limit of 70-80°C [16] depending on its density. This might also have contributed, by making the PE of the outer sheath softer in the area where the ground screen connections was installed.

It was also seen that a layer of oxide had developed on the outside of the copper wires in the area between the force spring and the PVC tape which kept the copper wires ends in place. The oxide made the appearance of the copper more gray/black. This might be due to the heat development and direct contact with the thermal insulation.

(a) Oxide layer on copper wires.

(b) Imprint from thermocouple on the outer sheath, where the force spring was placed.

Figure 4.38

4.7.1 Type I

Type I showed to have the lowest temperatures of the two types during the main tests. It was thus expected that this type would show less sign of thermal aging and degradation than type II. This proved to be correct. Even the ground screen connection with the highest recorded temperature of the type during cycling, connection number 2.1, showed only signs of degradation similar to the general observations made in the previous section, as seen in figure 4.38.

4.7.2 Type II

Type II included the ground screen connection with the highest temperature measured independent of type during the cycles with improper installation, connection 2.2. It was expected that this connection would show more evident signs of aging and degradation than the other connections.

Upon removal of the thermal insulation of the mentioned screen connection, a piece of Armaflex was observed to have melted onto the PVC and force spring, leaving a cavity in the thermal insulation sheet.

When the first layer of the PVC tape with the melted insulation was removed, it was seen that a part on the edge of the PVC's circumference towards the test object was melted, leaving a bit of discolored tape around it. The shape of the melted area followed the curvature of one of the strands of the joint ground screen. The strand was heavily discolored, with remnants of the thermal insulation left on it.

What seems to have happened is that the mentioned strand has come in contact with the innermost layer of the force spring, laid onto the copper wires when the thermal insulation was applied and tightened. This would effectively act as a short circuit, and let the ground screen current pass from the spring layer in contact with the copper wires and directly into the joint ground screen without passing through the force spring layer which has a larger resistivity than the joint ground screen.

The measurements performed during the cycling showed that the maximum temperature recorded at this ground screen connection was 90.5 °C, as given in table 4.11. The data sheet for the PVC tape in figure B.2 in appendix B states that the temperature rating of the tape used is 90 °C, while for the thermal insulation the upper limit is 110 °C, as seen if figure B.1 in the same appendix. It is thus likely that the local temperature has been much higher than the recorded 90.5 °C, even though the thermocouple was located only 90° apart from this location. It is evident that the temperature is not uniform around and across the force spring, raising the question of using additional thermocouples in future investigations.

The rest of the ground screen connections of type II only showed the general signs of aging.

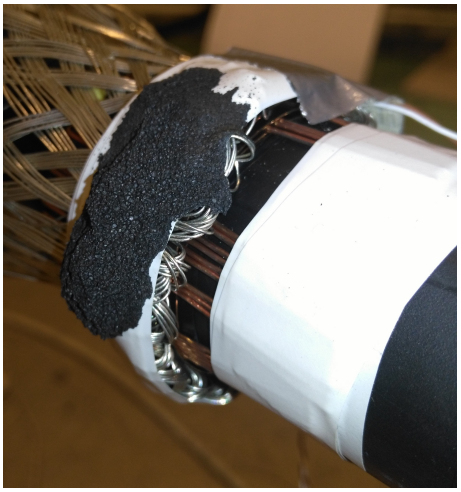

(a) The ground screen connection as seen when the thermal insulation was removed.

(b) The same arrangement as seen when the outermost layer of PVC tape with melted Armaflex was removed. The melted PVC with the strand short circuiting the arrangement can be seen in the middle of the picture.

Figure 4.39: Pictures taken during opening of the ground screen connection of type II with overall highest recorded temperature (connection 2.2).

5 Conclusion

In this project, a test setup was made to investigate the properties of ground screen connections of the "spring roll" method, with emphasis on a known improper installation with stainless steel in series with the electrical jointed parts. The ground screen connections were investigated by exposing them to heat cycles.

The conclusions of the work are:

- The resistance of the ground screen connections increases drastically when an improper installation of the force spring is performed, with a layer of stainless steel placed in series with the intended conductive parts.
- As a result, the temperature of the jointing arrangement increase. For type I investigated, the mean temperature after 25 heat cycles with a correct installation was 67.6 °C with 100 A applied compared to 67.3 °C with an improper installation and 30 A applied. For type II the corresponding averages was 65.7 °C and 71.2 °C.
- The method of using twisted copper wires as a voltage measuring point on the cable side of the test arrangement was shown to be unfitted, as it loosened during the heat cycle series, causing the resistance measurement results between each heat cycle to be unreliable. On the joint side of the screen connection, the method did however prove to have good reliability. A different method should be considered to replace the twisted copper wires on the cable side.

6 Further work

Suggestions to further work:

- Automation of the experimental setup, to allow cycling to continue constantly.
- Find a better type of voltage measuring point (equalizer) on the cable side of the ground screen connections.
- Diagnostic methods for the ground screen connections, both online and offline methods.
- Use tape (self-vulcanizing tape or duct-tape) instead of cable ties to fasten the thermal insulation around test objects, as this will exert a more uniform pressure around the test objects.
- Place the force spring arrangement close to the edge of the outer sheath. In other words, removing the 10 mm area between the edge of the outer sheath and the force springs used in this project.
- Investigate the heat development by using a ground screen current alone, without any heating from a current in the cable conductor.
- Investigate the ground screen connections with only one ground screen current polarity.
- Investigate the ground screen connections with AC current.
- Increase the number of thermocouples for measuring of the temperature in each ground screen connection.

Bibliography

[1] The Norwegian Research Council. *Reliable Power Cable Screen Connections*. 2018. URL https://www.forskningsradet.no/prosjektbanken/#/project/NFR/256261.

[2] Hallvard Faremo and Jan Tore Benjaminsen. *Feil på PEX-kabel og kabelustyr for 2001 og 2002 (12 og 24 kV)*. SINTEF Energy Research, 2006.

[3] Hans L. Halvorson, Sverre Hvidsten, Jens Kristian Lervik, and Harald Kulbotten. Experiences With Cable Faults Located at Metallic Screen Connections. *Cired 2017*.

[4] Draka Norsk Kabel. *TSLF 12/20(24)kV Data sheet*. 2017. URL http://draka.no/documents/tslf-122024kv.pdf.

[5] CENELEC. HD 620, 2010.

[6] Erling Ildstad. *High Voltage Equipment*. Department of Electric Power Engineering, 2017.

[7] Lothar Heinhold. *Power Cables and their Application - Part 1*. Siemens Aktiengesellschaft, 1990.

[8] Draka Norsk Kabel. *Teknisk håndbok - Kraftkabel*. Draka, 4th edition, 2017. URL http://media.draka.no/2016/07/Teknisk-Handbok-2010_final-til-web.pdf.

[9] Paul Taklaja, Ivar Kiitam, Petri Hyvonen, and Joni Kluss. Test setup for measuring medium voltage power cable and joint temperature in high current tests using thermocouples. *34th Electrical Insulation Conference, EIC 2016*, pages 480–483, 2016. doi: 10.1109/EIC.2016.7548642.

[10] Direktoratet for samfunnsikkerhet og beredskap. *Veiledning til forskrift om elektriske forsyningsanlegg*. https://www.dsb.no/lover/elektriske-anlegg-og-elektrisk-utstyr/veiledning-til-forskrift/veiledning-til-forskrift-om-elektriske-forsyningsanlegg/.

[11] CIGRÉ Working Group B1.25. Advanced Design of Metal Laminated Coverings: Recommendation for Tests, Guide to Use, Operational Feed Back. (February), 2011.

[12] CIGRÉ Working Group B1.22. Cable Accessory Workmanship on Extruded High Voltage Cables. (October), 2011.

[13] Robert Kristoffer Nilsen. Electromagnetics in Power Engineering. 2010.

[14] Peder Severin Søndenå. *Reliable Ground Screen Connections - Spring Rolls*. Norwegian University of Science and Technology, 2017.

[15] Roland S. Timsit. *Electrical Contact Resistance: Properties of Stationary Interfaces*. IEEE Transactions on Components and Packaging Technology, Vol. 22, No. 1, March 1999.

[16] Erling Ildstad. *Materials for High Voltage Applications*. Department of Electric Power Engineering, 2012.

[17] Ragnar Holm. *Electric Contacts*. Springer-Verlag, 1967.

[18] Christopher Ruppert. *Thermal Fatigue in Stationary Aluminium Contacts*. PhD thesis, Norwegian University of Science and Technology, 2001.

[19] Næss, Almar. *Metalliske materialer*. Tapir forlag, 1983.

[20] Milenko Braunovic. Effect of connection design on the contact resistance of high power overlapping bolted joints. 2002.

[21] Kongsjorden, Helge. *Electric Contacts Between Aluminium Conductors - A study of factors influencing their formation and degradation*. 1977.

[22] European Committee for Standardization. 10088-1: Stainelss steels, Part 1: List of stainless steels. 2014.

[23] Milenko Braunovic, Valery V. Konchits, and Nikolai K. Myshkin. *Electrical Contacts: Fundamentals, Applications and Technology*. CRC Press, 2007.

[24] IEC. 61442 - Test methods for accessories for power cables with rated voltages from 6 kV up to 30 kV, .

[25] IEC. 61284-1997 - Overhead lines, Requirements and tests for fittings, .

[26] Chinh Dang and Milenko Braunovic. An effective-resistance measurement technique for improving the current-cycling test of power connectors. 1999.

[27] Ali Naderian Jahromi, Ziqin Li, John Kuffel, Mark Fenger, and Jody Levine. Load-Cycling Test of High-Voltage Cables and Accessories. 2011.

[28] IEC. 61238-1 - Compression and mechanical connectors for power cables for rated voltages up to 30 kV (Um = 36 kV). Part 1: Test methods and requirements., .

[29] Magne Runde. *Material Transport and Related Interfacial Phenomena in Stationary Aluminium Contacts*. 1987.

[30] Ness Engineering. Metal Alloy Resistivity. URL `http://www.nessengr.com/techdata/metalresis.html`.

A Equipment used in laboratory

Table A.1: Equipment used in the laboratory

Equipment	Registration number NTNU/SINTEF
Control desk	B01-0144
Computer	P07-2246
Agilent Data Logger	G05-0169
Agilent Data Data Log Card	G05-0127-01
Hewlett Packard Data Log Card	G05-0096-01
Ring transformer	-
Farnell DC Power Supply H30/100	B02-0225
Farnell DC Power Supply H30/100	B02-0340
RS232 to USB adapter	P08-0570
Fluke i1000s AC Current Probe	I04-0492
Fluke i1010 AC/DC Current Probe	I04-0467
Fluke i1010 AC/DC Current Probe	I04-0469
Fluke 336 True RMS Clamp Meter	I04-0487
Relay Coupling Box	R04-0229
Thermocouple T-type, Farnell	Farnell part no: 16633499
Tinned copper wire, Ø = 0.68 mm	-
Tinned copper wire, Ø = 0.50 mm	-
Megger DLRO10HD - 10 A Digital Low Resistance Ohmmeter	H01-0116
Tektronix TDS2014C Oscilloscope	G04-0357
Mintoyo 0 - 25 mm (0.001 mm) Micrometre, C/N 293-230-30	-

B Datasheets

Technical Data - AF/Armaflex

Brief description	Highly-flexible, closed-cell insulation material with high water vapour diffusion resistance, low thermal conductivity and built-in Microban® antimicrobial protection.
Material type	Elastomeric foam based on synthetic rubber. Factory made flexible elastomeric foam (FEF) according to EN 14304.
Colour	black
Material Special Information	Self-adhesive coating: pressure-sensitive adhesive coating on modified acrylate basis with mesh structure, covered with polyethylene foil. Traces of silicon can be found on the protection paper/foil used to protect self-adhesive closures.
Applications	Insulation / protection for pipes, air ducts, vessels (incl. elbows, fittings, flanges etc.) of air-conditioning / refrigeration and process equipment to prevent condensation and save energy. Structure-borne noise reduction in service-water and waste-water installations.
Special Features	Increasing insulation wall thicknesses for tubes ensures that the surface temperature is maintained as the pipe diameter is increased.
Safety and Environment	Type III Environmental Product Declaration (EPD): Declaration number "EPD-ARM-20150060-IBB1-DE", Institut Bauen und Umwelt e.V. (IBU)
Remarks	Certificate of Constancy of Performance, Güteschutzgemeinschaft Hartschaum e.V. , Celle

Property	Value/Assessment				Test*3	Super-vision*4	Special Remark
Temperature Range							
Temperature Range	max. service temperature		+ 110 °C	(+ 85 °C if sheet or tape is glued to the object with its whole surface.)	EU 5654	○/●	Tested acc. to EN 14706, EN 14707 and EN 14304
	min. service temperature[1]		-50 °C				
Thermal Conductivity							
Thermal Conductivity		ϑ_m +/-0 °C	.	λ=	EU 5654	○/●	Declared acc. to EN ISO 13787 Tested acc. to EN 12667 EN ISO 8497
	Tubes (AF-1 to AF-4)	λ ≤ 0,033	W/(m • K)	[33 + 0,1• ϑ_m + 0,0008 • ϑ_m^2]/1000			
	Tubes (AF-5 to AF-6)	λ ≤ 0,036	W/(m • K)	[36 + 0,1• ϑ_m + 0,0008 • ϑ_m^2]/1000			
	Sheets, strips, tape (AF-03MM to AF-32MM)	λ ≤ 0,033	W/(m • K)	[33 + 0,1• ϑ_m + 0,0008 • ϑ_m^2]/1000			
	Sheets (AF-50MM	λ ≤ 0,036	W/(m • K)	[36 + 0,1• ϑ_m + 0,0008 • ϑ_m^2]/1000			
Water vapour diffusion resistance							
Water vapour diffusion resistance	Sheets (AF-10MM to AF-32MM) and tubes (AF-1 to AF-4)	μ	≥	10.000	D 4981 EU 5654	○/●	Tested acc. to EN 12086 and EN 13469
	Sheets (AF-50MM) and tubes (AF-5 to AF-6)	μ	≥	7.000			
Fire performance							
Reaction to fire[2]	tubes		B_L-s3, d0		EU 5654	○/●	Classified acc. to EN 13501-1 Tested acc. to EN 13823 EN ISO 11925-2
	sheets		B_L-s3, d0 (Z-56.269.3530)				
	tape		B / B_L-s3, d0 (Z-56.269.768)				
			B-s3,d0 (Z-56.269.768)				
Other Fire Class	UL - approved				UL: D 4613 D 3763 FM: D 4592 Railway: D 5391, D 5392, D 5402, D 5493 Ship Building: D2406, D 5555, EU 5474	○/●	UL: Tested according to UL94, IEC 60695 and Can/CSA-C.22.2 No0.17,, UL 746C FM: Tested according to UBC26-3, Class No.4924 Railway: Classified acc. to DIN 5510-2 Tested acc. to DIN 54837 Ship Building: Classified acc. to MED 96/98/EC MODULE D
	FM - approved						
	Railway (3-19 mm)		SR2, ST2, S4, FED < 1				
	Ship Building		low-flammable				
Practical Fire Behaviour	Self-extinguishing, does not drip, does not spread flames						
Acoustic Performance							
Reduction of structure-borne sound transmission	Insulation effect		≤ 28 dB(A)		D 3660		Tested acc. to DIN 52219 and EN ISO 3822-1

Figure B.1: Datasheet for the Armaflex thermal insulation used during the reference and main heat cycles.

Data Sheet

3M

RoHS
2002/95/EC
REACH
1907/2006/E

Temflex™ 1500
PVC Electrical Tape

1. Product Description

Temflex™ 1500 Electrical Tape is a good quality and general purpose PVC insulating tape.
Available colors are: black, blue, brown, yellow, yellow/green, gray, orange, red, white, purple and green.

It has good resistance to: abrasion, moisture, alkalis, acid and varying weather conditions (including sunlight). It is a polyvinyl chloride (PVC) tape that has a high electric strength, is conformable and provides good mechanical protection with minimum bulk. Temflex™ 1500 is classified as IEC 60454-3-1-5/F-PVCP/90 and has VDE Marks License.

2. Applications

- Primary electrical insulation for all wire and cable splices and repairs.
- Harnessing of wires and cables.
- For indoor and outdoor applications

3. Typical Properties*

Thickness[1]	0.15 mm
Elongation[1]	170 %
Tensile Strength[1]	20 N/10 mm
Adhesion to Steel[1]	1.8 N/10 mm
Adhesion to Backing[1]	1.8 N/10 mm
Temperature Rating[2]	0-90°C
Resistance to Flame Propagation[1]	self-extinguishing (acc IEC 60454-2 19.5 part b)
Electric Strength[1]	40 kV/mm
Electrolytic Corrosion[3]	A/B 1.8
Insulation Resistance[3]	$10^{11}\Omega$/25 mm

*These are typical values and should not be used for specification purposes.

[1] IEC 60454-2
[2] IEC 60085, IEC 60216
[3] IEC 60426

4. Installation Technique

The tape shall be applied in half-lapped layers with sufficient tension to conform and produce a uniform covering. In most applications, this tension will reduce the tape's width to 5/8 of its original width.
Apply the tape with no tension on the last wrap to prevent flagging.

5. Maintenance

Temflex™ 1500 Electrical Tape is stable under normal storage conditions.

6. Availability

Temflex™ 1500 Tape is available from 3M and your local 3M authorised electrical distributor.

Page 1 of 2 Issue 1

Figure B.2: Datasheet for the PVC tape used to cover the constant force springs during the heat cycles.

C Voltage measuring error for the ground screen connections

Table C.1: Measurement errors from the voltage measurement of the ground screen connections.

Ground screen connection number and type	Voltage [mV DC]
1.1, Type I	0.11
1.2, Type I	0.11
2.1, Type I	0.11
2.2, Type I	0.11
3.1, Type I	0.11
3.2, Type I	0.11
1.1, Type II	0.11
1.2, Type II	0.11
2.1, Type II	0.11
2.2, Type II	0.11
3.1, Type II	0.10
3.2, Type II	0.10

D Safety circuit

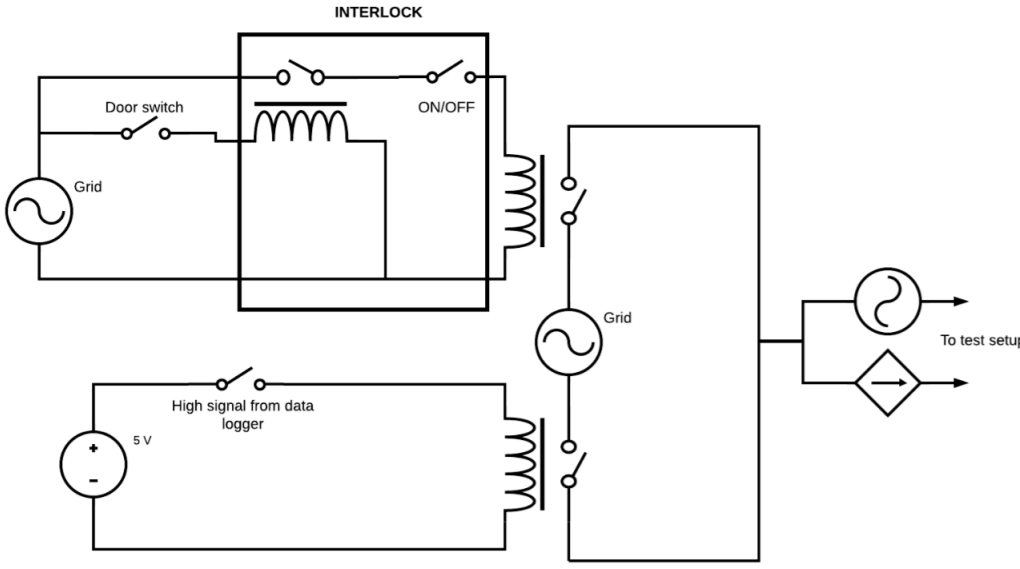

Figure D.1: Figure showing the schematics of the safety circuit.

(a) On top: output for the DC sources. Bottom: Outlet to the control desk and variable voltage source (Schuko) with its circuit breaker to the right.

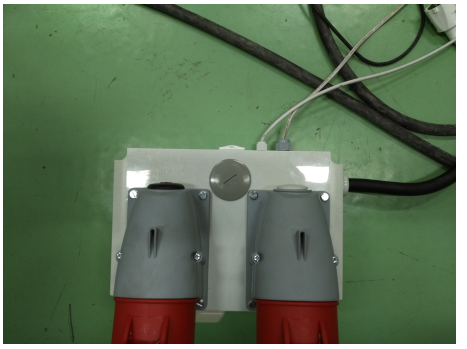

(b) On the top, from the left: high/low input to one relay from the data logger (white) and high-/low signal from interlock (gray). On the right side: mains input (black).

Figure D.2: Pictures showing the junction box made, which house the power outlets and safety relays.

E Temperature stability criteria

This section shows which ground screen connections that the stability criteria of 2 °C during the last ten minutes was to be applied on. For the reference tests, the method with median connection temperature from IEC 61238-1 [28] was used. For the main tests, the ground screen connection with the second largest temperature was chosen for type I, while for type II the ground screen connection with the largest temperature was chosen.

E.1 Reference heat cycles

Table E.1: Table showing the temperatures achieved from the first heat cycle with the cable ground screen grounded in one end, determining the median ground screen connection of each type. The temperatures are sorted from high to low, with type I to the left and type II to the right. Median ground screen connections are shown in bold.

Type I, connection number	Temperature	Type II, connection number	Temperature
2.1	56.4	3.2	57.0
2.2	55.8	2.2	54.7
1.2	**55.3**	**3.1**	**54.4**
3.1	53.5	2.1	53.9
1.1	47.9	1.2	52.8
3.2	46.7	1.1	45.7

E.2 Main heat cycles

Type I: 1.2

Type II: 2.2

F Material properties

Table F.1: Table showing some of the material properties of the relevant materials in the report. Tinned copper, used in the ground joint screens, are assigned with the material data of copper, as this is the main material of this part.

	ρ_0 [Ωm]	μ_r [H/m]	α [1/°C]	λ [W/mK]	H [10^2/mm^2]	Thermal expansion [10^{-6}/K]
Steel 1.4310	7.30E-7 [22]	6-19 [14]	0.00094 [30]	15 [22]	16 [23]	16 (at 100 °C) [22]
Tinned joint screen type I	2.09E-8	1	0.004	393 [16]	4-9 [23]	16.5 [23]
Tinned joint screen type II	2.04E-8	1	0.004	393	4-9	16.5
T.O. type I	1.82E-8	1	0.004	393	4-9	16.5
T.O. type II	1.84E-8	1	0.004	393	4-9	16.5

G Joint ground screen resistivities

In this chapter, the resistivity of the joint ground screens is presented. These results were used to remove the impact of the joint ground screen in the resistance measurements of the ground screen connections.

For the measuring of the joint ground screen resistances, the micro-ohm meter was set to the "10 A, 2.5 mΩ" range setting, giving an accuracy of 0.1 μΩ. For each joint ground screen, ten measurements were made and the value given is the mean of these. For the sake of comparability, the values are given in mΩ.

Although only four joint screens were to be used, it was chosen to measure on a total of five such that the fifth screen could be kept as a reserve.

G.1 Type I

The mean resistivity of the joint ground screens for the type I ground screen connection was found to be 2.09E-8 Ωm, with the area of the screen measured to a value of 50.56 mm^2 and each strand of the screen having a diameter if 0.30 mm. The resistivities was found by the use of equation 2.4 before correcting for the temperature with the use of equation 2.7. The value further used for the resistivity of the screens is the average of these values.

Table G.1: Resistivity of the ground joint screens for type I, calculated from the measured resistances. The parameter T describes the temperature in the laboratory at the time of measuring. l is the distance between the voltage measuring points. Each resistance value for the joint ground screens is the average value of ten measurements.

Joint screen	R [mΩ]	l [mm]	A [mm^2]	T [°C]	T_0 [°C]	α [1/°C]	ρ [Ωm]	ρ_0 [Ωm]	$\rho_{0,\text{average}}$ [Ωm]	R_0 [Ω/km]
1	0.100						2.02E-8	2.04E-8		
2	0.093						1.89E-8	1.91E-8		
3	0.106	250.0	50.56	17.50	20.00	0.004	2.15E-8	2.17E-8	2.09E-8	0.414
4	0.104						2.11E-8	2.13E-8		
5	0.108						2.19E-8	2.22E-8		

G.2 Type II

The mean resistivity of the joint ground screens for the type II ground screen connection was found to be 2.04E-8 Ωm, with the area of the screen measured to a value of 35.72 mm^2 each strand of the screen having a diameter if 0.40 mm. The calculation of the resistivities was carried out in the same way as for type I.

Table G.2: Resistivity of the test objects for type II, calculated from the measured resistances.

Joint screen	R [mΩ]	l [mm]	A [mm^2]	T [°C]	T_0 [°C]	α [1/°C]	ρ [Ωm]	ρ_0 [Ωm]	$\rho_{0,average}$ [Ωm]	R_0 [Ω/km]
1	0.150						2.14E-8	2.13E-8		
2	0.132						1.88E-8	1.88E-8		
3	0.147	250.0	35.72	20.80	20.00	0.004	2.10E-8	2.10E-8	2.04E-8	0.572
4	0.145						2.07E-8	2.07E-8		
5	0.144						2.05E-8	2.05E-8		

G.3 Comparison

As can be seen from table G.1 and G.2, the average value for the two resistivities are close to equal. The resistances of the two types differ by some tens of μΩ, which is due to the difference in cross section area of the types. While type I has a cross section area close to 50 mm^2, the cross section of type II is close to 35 mm^2. CENELEC HD620 [5] states that the minimum cross section area of the metallic screen is 35 mm^2 for a 240 mm^2/24 kV cable, while it for a 630 mm^2/24 kV cable should be 50 mm^2. 50 mm^2 is also the minimum cross section area of the largest cable dimension that the standard includes. It is thus likely that the producer of type I use the same joint ground screen for all cross sections of 24 kV joints and perhaps 36 kV joints, while the producer of type II uses a specified joint ground screen for each joint size, according to the criteria in HD620.

A better parameter for comparison is the resistance as a per kilometer value. For a screen with a cross section of 35 mm^2, the resistance requirement at a temperature of T = 20 °C is 0.524 Ω/km, while it for a cross section of 50 mm^2 is 0.387 Ω/km, as stated in HD620. From the tables, it can be seen that the joint screen of type I is thus within the resistance criteria if it is to be used as a replacement of a 35 mm^2 cable screen. However, its resistance is too large to replace a cable ground screen of 50 mm^2. Type II does neither fulfill the requirement for 35 or 50 mm^2.

The reason for using an average value for the resistivity of the joint ground screens was due to the variance in resistance of in each one of them, caused by different numbers of broken strands and the joint ground screens overall condition.

H Copper wire resistivities

In this chapter, the resistivity of the copper wires in the test objects are presented. These results were used to remove the impact of the copper wires in the resistance measurements of the ground screen connections.

For the measuring of the copper wire resistances, the micro-ohmmeter was set to the "10 A, 2.5 mΩ" range setting, giving a measuring accuracy of 0.1 μΩ.

The value for the resistivity of each cable test object was found in a similar way as for the joint ground screens, with ten measurements done on each test object. The average resistivity value is then the average of the three test objects of each type.

H.1 Type I

Table H.1: Resistivity of the copper wires in the test objects for type I, calculated from the measured resistances. The parameter T describes the temperature in the laboratory at the time of measuring. l is the distance between the voltage measuring points. Each resistance value for the test objects is the average value of ten measurements.

T.O.	$R_{measured}$ [mΩ]	l [mm]	A [mm^2]	T [°C]	T_0 [°C]	α [1/°C]	ρ [Ωm]	ρ_0 [Ωm]	$\rho_{0,\text{average}}$ [Ωm]	R [Ω/km]
1	0.420			21.00			1.83E-8	1.82E-8		
2	0.421	495.0	21.52	20.00	20.00	0.004	1.83E-8	1.83E-8	1.82E-8	0.845
3	0.415			20.00			1.81E-8	1.81E-8		

H.2 Type II

Table H.2: Resistivity of the copper wires in the test objects for type II, calculated from the measured resistances. The parameter T describes the temperature in the laboratory at the time of measuring. l is the distance between the voltage measuring points. Each resistance value for the test objects is the average value of ten measurements.

T.O.	$R_{measured}$ [mΩ]	l [mm]	A [mm^2]	T [°C]	T_0 [°C]	α [1/°C]	ρ [Ωm]	ρ_0 [Ωm]	$\rho_{0,\text{average}}$ [Ωm]	R [Ω/km]
1	0.420			20.50			1.83E-8	1.82E-8		
2	0.424	495	21.52	20.50	20.00	0.004	1.84E-8	1.84E-8	1.84E-8	0.854
3	0.427			20.50			1.86E-8	1.85E-8		

H.3 Comparison

Comparing the copper wires in the cable test objects made for both types, it can be seen that they are close to each other in their resistivity values, which was to be expected. The resistance requirement in HD620 for the cable ground screen of a 240 mm^2 24 kV cable is 0.524 Ω/km, given a cross section area of 35 mm^2 of the screen. Comparing the copper wires resistance value per kilometer with the mentioned requirement, it is seen that the average value of the two both lie above this. These values do however not show the whole picture, due to the fact that the aluminium laminate is removed on parts of the test objects, with the remaining parts floating on the cable copper wires. Since the manufacturers actively exploits the aluminium laminate as part of the metallic screen, the total resistance of the screen will decrease when this element in parallel is removed. This is also seen from the cross section areas in table H.1 and H.2 which is quite lower than the requirement of 35 mm^2, stated in HD620. The datasheet of the cable supplied by the manufacturer states that the screen resistance is 0.524 Ω/km and consists of the contributions of both copper screen wires and the aluminium laminate.

However, for the ground screen connection designs investigated in this project, the copper wires of the cable screen will be to only component which transfers the screen current from the cable ground screen to the joint ground screen. This means that the reduced cable ground screen section, consisting of only the copper wires, will have to be able to transmit a significantly larger current for this short distance than what it might be capable of.

I Ground screen connection numbering

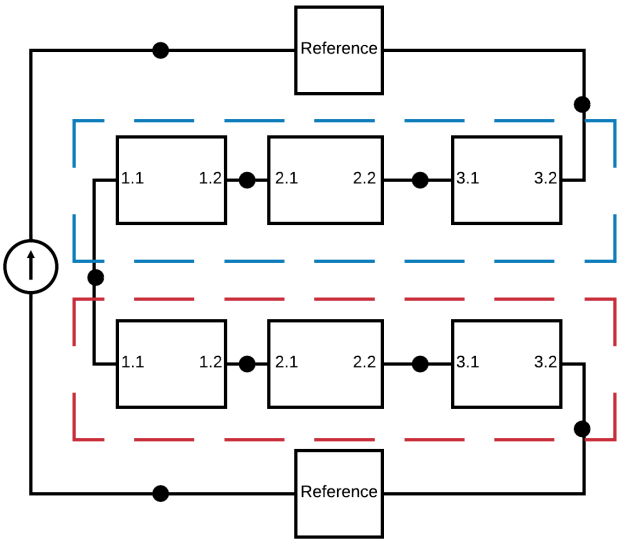

Figure I.1: Figure showing the numeration of the ground screen connections. Black dot indicates jointing point for both cable ground screen and cable conductor. The connections inside the dotted blue lines belong to type I, while the ones in inside the dotted red lines belong to type II.

J Measurements with micro-ohm meter

Both before thermal insulation was applied to the test setup and after the heat cycles were concluded, the resistances of the ground screen connections were measured with the micro-ohm meter.

J.1 Measurement before heat cycles

J.1.1 Reference tests

The resistances of the ground screen connections were measured with the micro-ohm meter set to the "10 A, 2.5 mΩ" setting.

Table J.1: Type I

Joint no	$R_{measured}$ [mΩ]	T [°C]	R_a [mΩ]	R_b [mΩ]	R_{joint} [mΩ]	$R_{average}$ [mΩ]	R_{median} [mΩ]	R_{joint} [Ω/km]	$R_{average}$ [Ω/km]	R_{median} [Ω/km]
1	0.132	20.00	0.072	0.036	0.024	0.033	0.028	0.970	1.330	1.131
2	0.152				0.044			1.755		
3	0.159				0.051			2.037		
4	0.140				0.032			1.292		
5	0.132				0.024			0.954		
6	0.132				0.024			0.970		

Table J.2: Type II

Joint no	$R_{measured}$ [mΩ]	T [°C]	R_a [mΩ]	R_b [mΩ]	R_{joint} [mΩ]	$R_{average}$ [mΩ]	R_{median} [mΩ]	R_{joint} [Ω/km]	$R_{average}$ [Ω/km]	R_{median} [Ω/km]
1	0.175	20.00	0.073	0.053	0.049	0.022	0.018	3.090	1.378	1.134
2	0.136				0.010			0.642		
3	0.139				0.014			0.866		
4	0.145				0.019			1.214		
5	0.142				0.017			1.053		
6	0.148				0.022			1.402		

J.1.2 Main tests

For the measuring of the ground screen connections, the micro-ohm meter was set to the "1 A, 25 mΩ" setting.

Table J.3: Type I

Joint no	$R_{measured}$ [mΩ]	T [°C]	R_a [mΩ]	R_b [mΩ]	R_{joint} [mΩ]	$R_{average}$ [mΩ]	R_{median} [mΩ]	R_{joint} [Ω/km]	$R_{average}$ [Ω/km]	R_{median} [Ω/km]
1	1.203	20.40	0.072	0.036	1.095	2.119	1.655	43.79	84.74	66.21
2	1.779				1.671			66.83		
3	4.985				4.877			195.1		
4	2.567				2.458			98.33		
5	1.748				1.640			65.59		
6	1.080				0.971			38.85		

Table J.4: Type II

Joint no	$R_{measured}$ [mΩ]	T [°C]	R_a [mΩ]	R_b [mΩ]	R_{joint} [mΩ]	$R_{average}$ [Ω/km]	R_{median} [mΩ]	R_{joint} [Ω/km]	$R_{average}$ [Ω/km]	R_{median} [Ω/km]
1	5.124	20.4	0.073	0.053	4.999	2.337	2.290	312.4	146.1	143.1
2	1.005				0.879			54.95		
3	0.882				0.756			47.26		
4	2.321				2.196			137.2		
5	2.510				2.384			149.0		
6	2.936				2.811			175.7		

J.2 Measurements after heat cycles

Due to the loosening of the voltage measuring points on the cable side of the ground screen connections during the heat cycles, the measurements were performed both with the old and with new measuring points.

J.2.1 Reference tests

Old measuring points

Table J.5: Type I

Joint no	$R_{measured}$ [mΩ]	T [°C]	R_a [mΩ]	R_b [mΩ]	R_{joint} [mΩ]	$R_{average}$ [mΩ]	R_{median} [mΩ]	R_{joint} [Ω/km]	$R_{average}$ [Ω/km]	R_{median} [Ω/km]
1	0.144	20.50	0.072	0.036	0.035	0.206	0.133	1.420	8.255	5.305
2	0.642				0.534			21.34		
3	0.476				0.368			14.71		
4	0.223				0.115			4.599		
5	0.259				0.150			6.012		
6	0.145				0.036			1.450		

Table J.6: Type II

Joint no	$R_{measured}$ [mΩ]	T [°C]	R_a [mΩ]	R_b [mΩ]	R_{joint} [mΩ]	$R_{average}$ [mΩ]	R_{median} [mΩ]	R_{joint} [Ω/km]	$R_{average}$ [Ω/km]	R_{median} [Ω/km]
1	0.328	20.50	0.073	0.053	0.202	0.113	0.113	12.64	7.075	7.068
2	0.156				0.031			1.932		
3	0.235				0.109			6.840		
4	0.224				0.098			6.145		
5	0.247				0.122			7.602		
6	0.242				0.117			7.295		

New measuring points

Table J.7: Type I

Joint no	$R_{measured}$ [mΩ]	T [°C]	R_a [mΩ]	R_b [mΩ]	R_{joint} [mΩ]	$R_{average}$ [mΩ]	R_{median} [mΩ]	R_{joint} [Ω/km]	$R_{average}$ [Ω/km]	R_{median} [Ω/km]
1	0.162	20.50	0.072	0.036	0.054	0.153	0.100	2.161	6.119	4.008
2	0.413				0.305			12.20		
3	0.420				0.312			12.48		
4	0.214				0.106			4.235		
5	0.203				0.095			3.781		
6	0.155				0.047			1.862		

Table J.8: Type II

Joint no	$R_{measured}$ [mΩ]	T [°C]	R_a [mΩ]	R_b [mΩ]	R_{joint} [mΩ]	$R_{average}$ [mΩ]	R_{median} [mΩ]	R_{joint} [Ω/km]	$R_{average}$ [Ω/km]	R_{median} [Ω/km]
1	0.272	20.50	0.073	0.053	0.146	0.094	0.090	9.144	5.869	5.634
2	0.173				0.047			2.960		
3	0.212				0.086			5.386		
4	0.232				0.107			6.664		
5	0.220				0.094			5.881		
6	0.208				0.083			5.180		

J.2.2 Main tests

Old measuring points

Table J.9: Type I

Joint no	$R_{measured}$ [mΩ]	T [°C]	R_a [mΩ]	R_b [mΩ]	R_{joint} [mΩ]	$R_{average}$ [mΩ]	R_{median} [mΩ]	R_{joint} [Ω/km]	$R_{average}$ [Ω/km]	R_{median} [Ω/km]
1	4.821	21.60	0.072	0.036	4.712	12.46	13.66	188.5	498.2	546.4
2	16.58				16.48			659.0		
3	22.03				21.92			876.9		
4	15.36				15.25			610.2		
5	12.17				12.06			482.5		
6	4.415				4.306			172.2		

Table J.10: Type II

Joint no	$R_{measured}$ [mΩ]	T [°C]	R_a [mΩ]	R_b [mΩ]	R_{joint} [mΩ]	$R_{average}$ [mΩ]	R_{median} [mΩ]	R_{joint} [Ω/km]	$R_{average}$ [Ω/km]	R_{median} [Ω/km]
1	5.459	21.60	0.073	0.053	5.333	15.24	13.62	333.3	952.3	851.4
2	1.761				1.635			102.2		
3	6.720				6.593			412.1		
4	32.01				31.89			1993		
5	25.45				25.32			1582		
6	20.78				20.65			1291		

New measuring points

Table J.11 and J.12 shows the resistance measured with new voltage measuring points on the cable side.

As seen in the tables, the actual measuring with new voltage points were only performed on type II. The values obtained in the column R_{joint} of table J.11 for type I was found by taking the measured values with the old voltage points for type I, and then subtracting the mean difference between the resistance results of the 25th heat cycle of type II and the measured resistances with new measuring points for type II.

Although only being good enough to serve as an approximation, it was seen as sufficient since the difference between the resistance measurements with the new voltage measuring points and the 25th heat cycle of type II showed good coherence.

Table J.11: Type I

Joint no	$R_{measured}$ [mΩ]	T [°C]	R_a [mΩ]	R_b [mΩ]	R_{joint} [mΩ]	$R_{average}$ [mΩ]	R_{median} [mΩ]	R_{joint} [Ω/km]	$R_{average}$ [Ω/km]	R_{median} [Ω/km]
1	-	21.60	-	-	3.012	3.141	2.694	120.5	125.6	107.8
2	-				2.765			110.6		
3	-				6.417			256.7		
4	-				2.623			104.9		
5	-				2.606			104.3		
6	-				1.421			56.83		

Table J.12: Type II

Joint no	$R_{measured}$ [mΩ]	T [°C]	R_a [mΩ]	R_b [mΩ]	R_{joint} [mΩ]	$R_{average}$ [mΩ]	R_{median} [mΩ]	R_{joint} [Ω/km]	$R_{average}$ [Ω/km]	R_{median} [Ω/km]
1	4.600	21.60	0.073	0.053	4.473	4.291	4.359	279.6	268.2	272.4
2	1.073				0.947			59.17		
3	1.299				1.173			73.29		
4	10.27				10.14			633.9		
5	4.892				4.766			297.9		
6	4.371				4.245			265.3		

K Temperature development of the reference cables

K.1 Reference tests

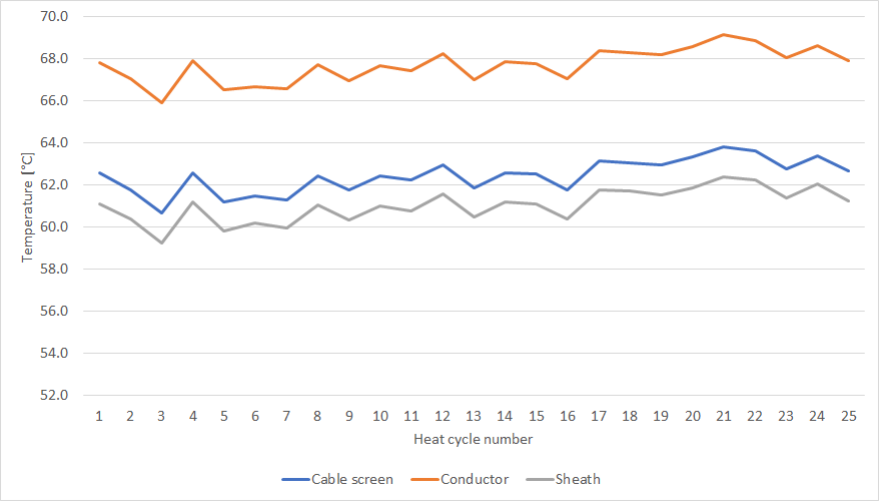

Figure K.1: Temperature development of the maximum temperature of ground screen, conductor and outer sheath in the reference cables during the reference tests. Each point is the average of the corresponding measurements for the two reference cables.

K.2 Main tests

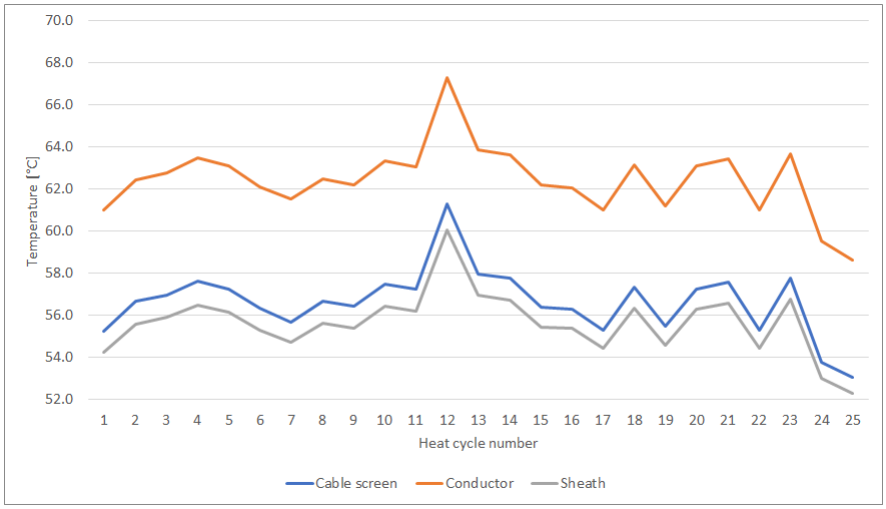

Figure K.2: Temperature development of the maximum temperature of ground screen, conductor and outer sheath in the reference cables during the main tests. Each point is the average of the corresponding measurements for the two reference cables.

L Resistance and temperature plots from the reference heat cycles

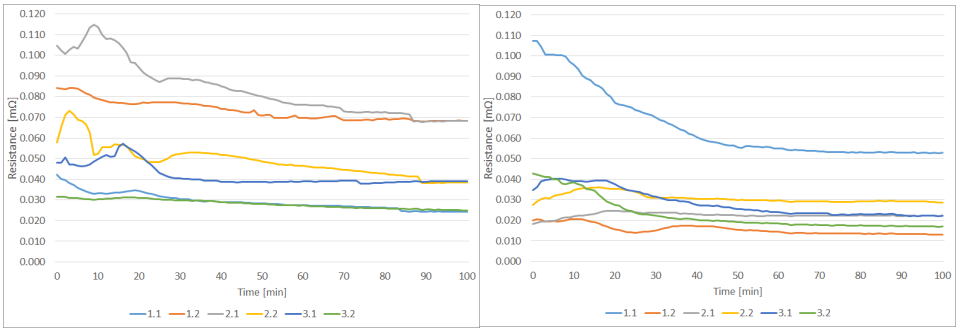

(a) Type I **(b)** Type II

Figure L.1: Cycle 1

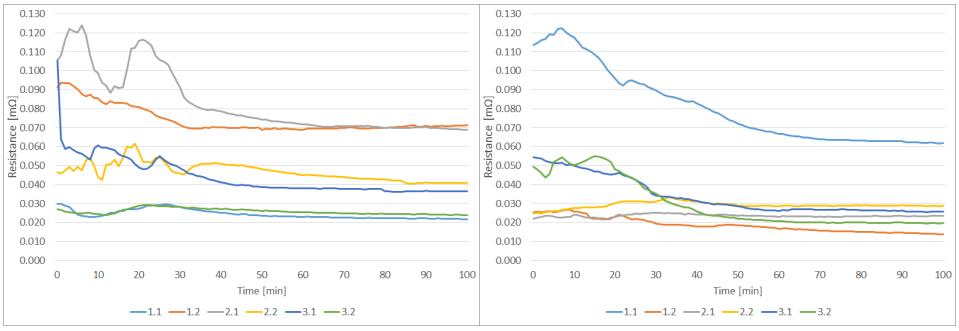

(a) Type I **(b)** Type II

Figure L.2: Cycle 2

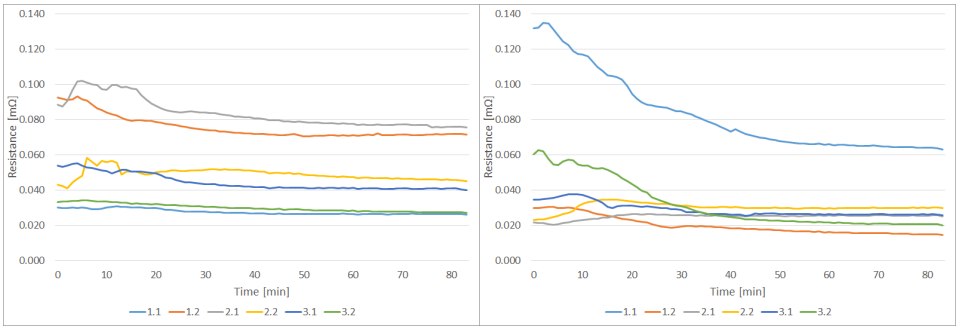

(a) Type I **(b)** Type II

Figure L.3: Cycle 3

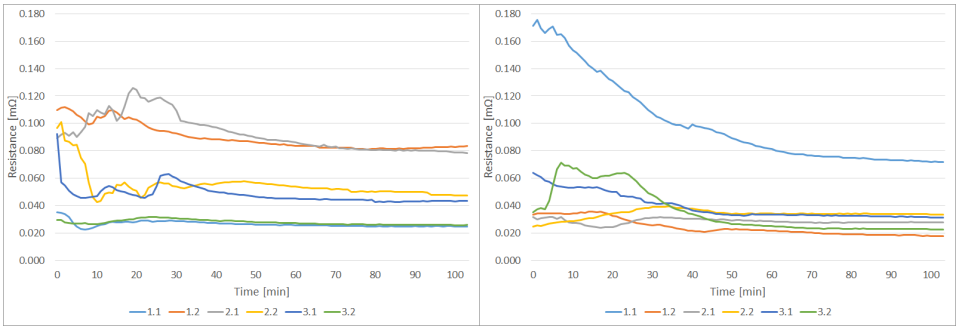

(a) Type I **(b)** Type II

Figure L.4: Cycle 4

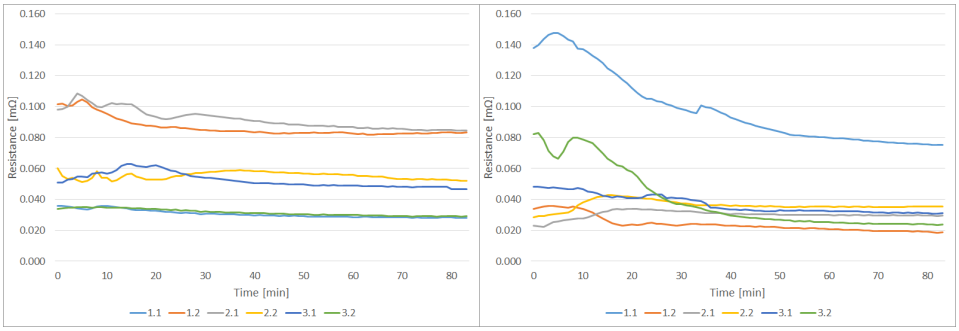

(a) Type I **(b)** Type II

Figure L.5: Cycle 5

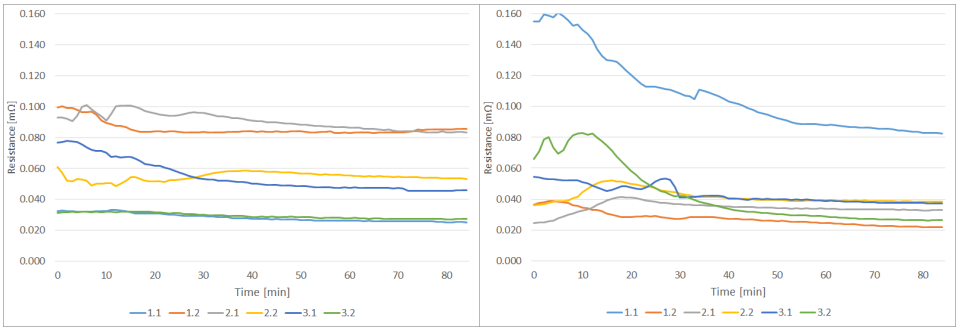

(a) Type I **(b)** Type II

Figure L.6: Cycle 6

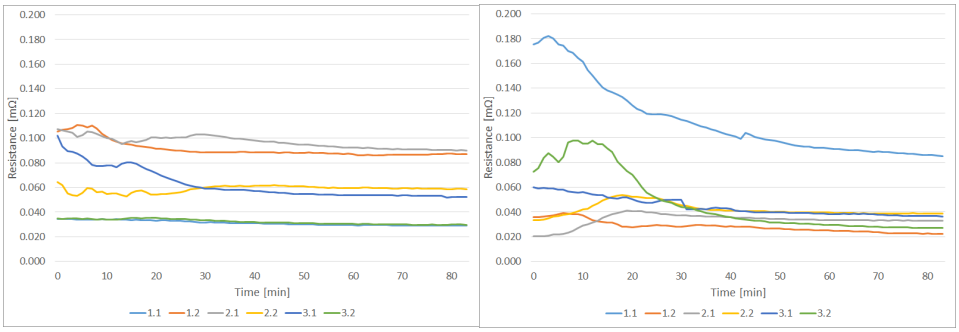

(a) Type I **(b)** Type II

Figure L.7: Cycle 7

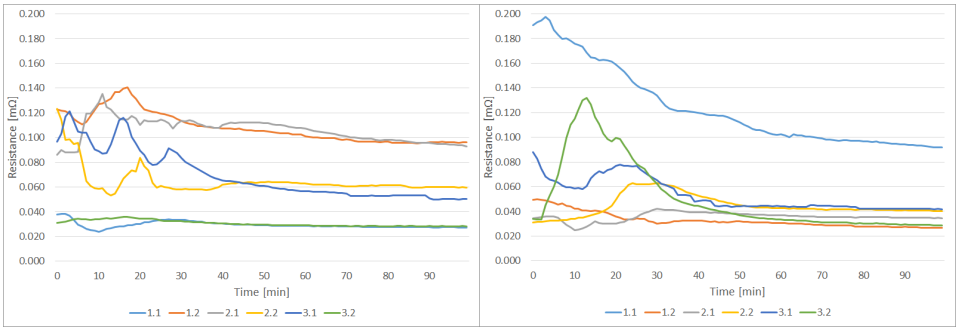

(a) Type I **(b)** Type II

Figure L.8: Cycle 8

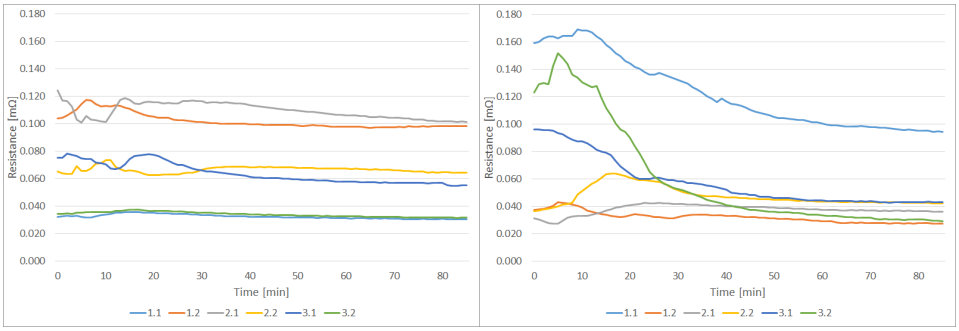

(a) Type I **(b)** Type II

Figure L.9: Cycle 9

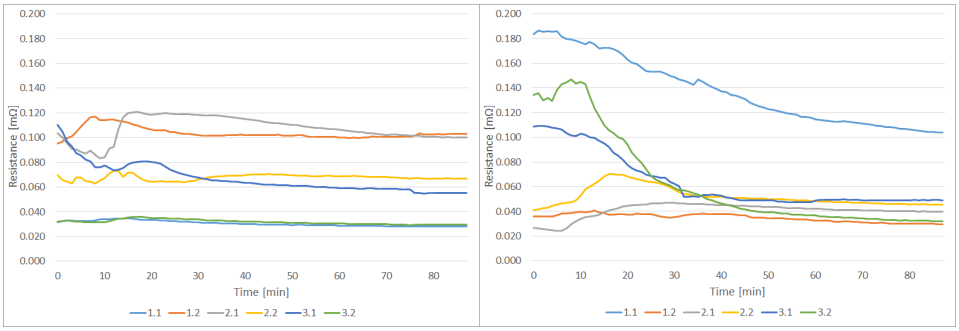

(a) Type I **(b)** Type II

Figure L.10: Cycle 10

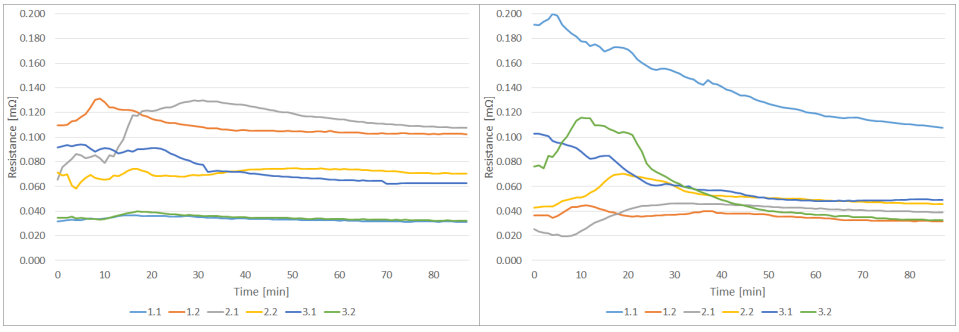

(a) Type I **(b)** Type II

Figure L.11: Cycle 11

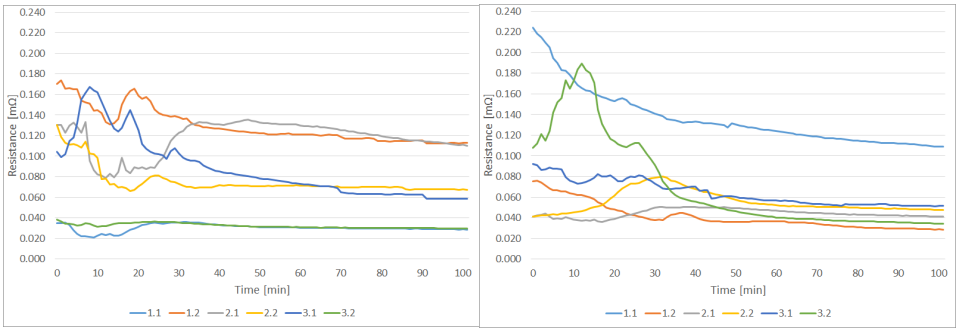

(a) Type I **(b)** Type II

Figure L.12: Cycle 12

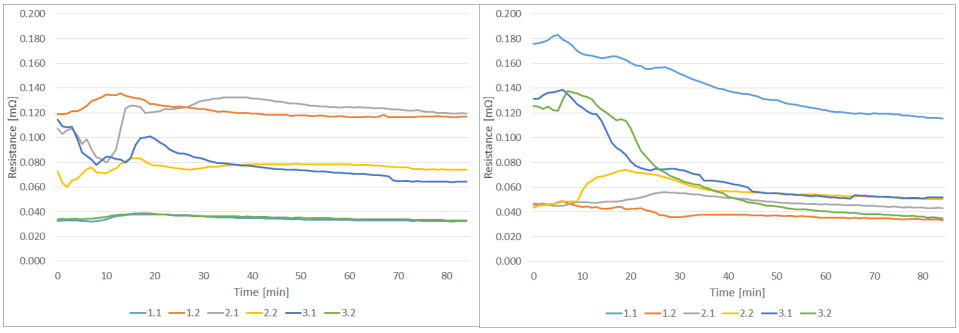

(a) Type I **(b)** Type II

Figure L.13: Cycle 13

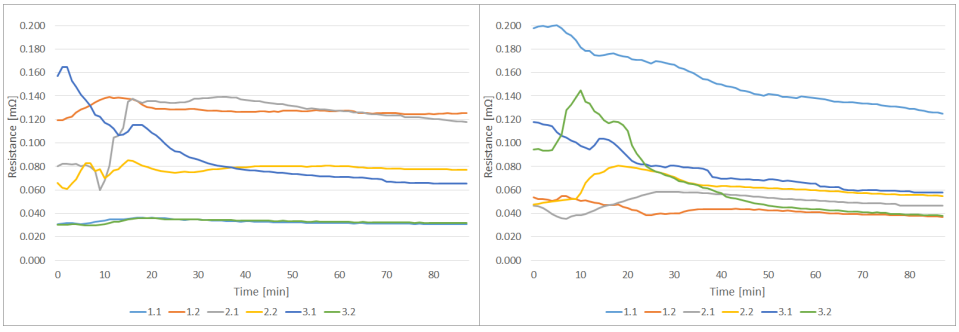

(a) Type I **(b)** Type II

Figure L.14: Cycle 14

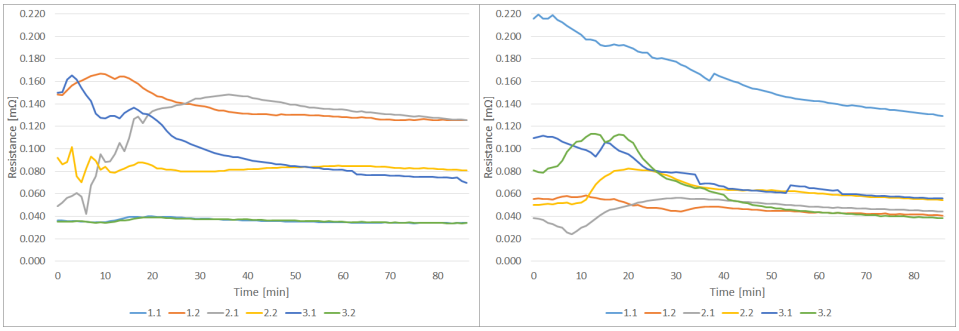

(a) Type I **(b)** Type II

Figure L.15: Cycle 15

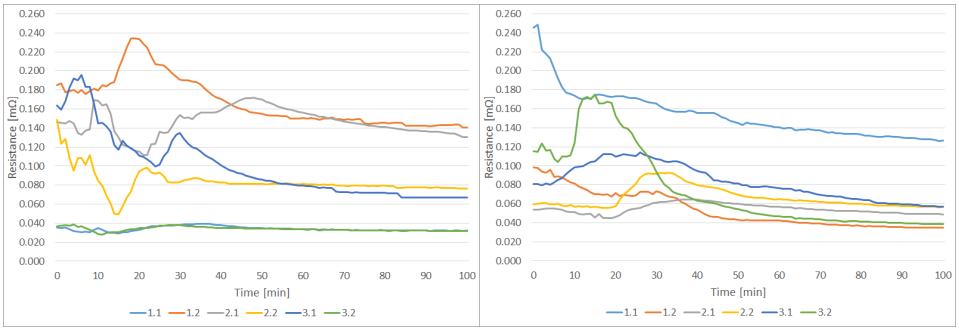

(a) Type I **(b)** Type II

Figure L.16: Cycle 16

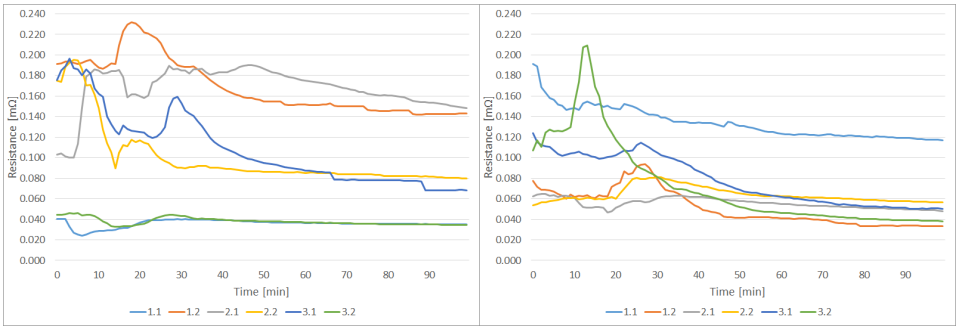

(a) Type I **(b)** Type II

Figure L.17: Cycle 17

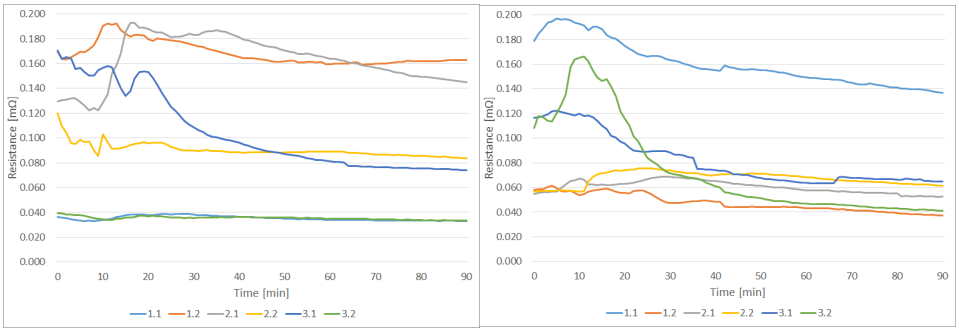

(a) Type I **(b)** Type II

Figure L.18: Cycle 18

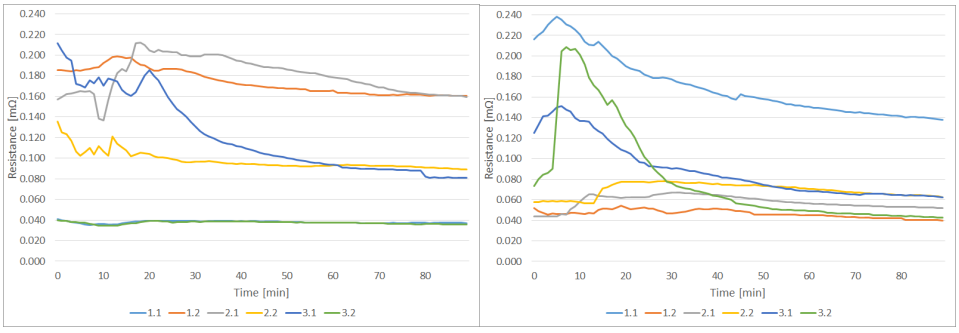

(a) Type I **(b)** Type II

Figure L.19: Cycle 19

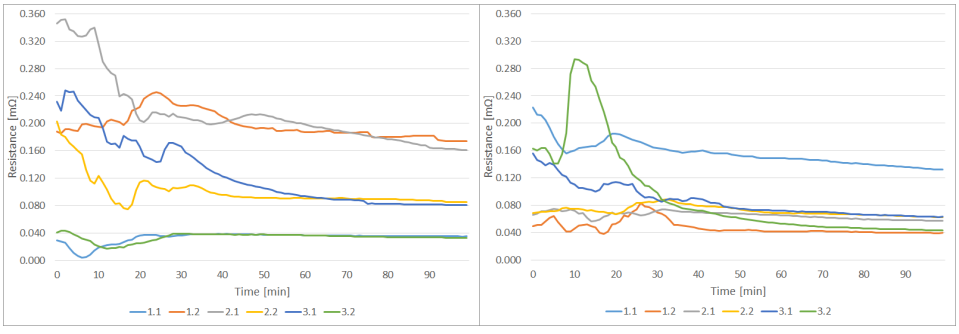

(a) Type I **(b)** Type II

Figure L.20: Cycle 20

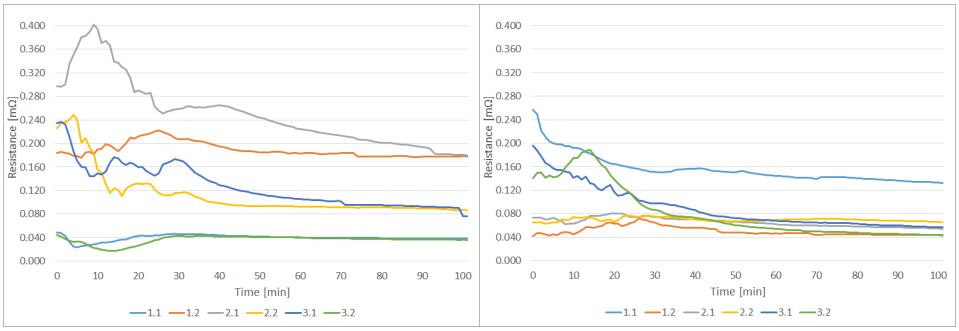

(a) Type I **(b)** Type II

Figure L.21: Cycle 21

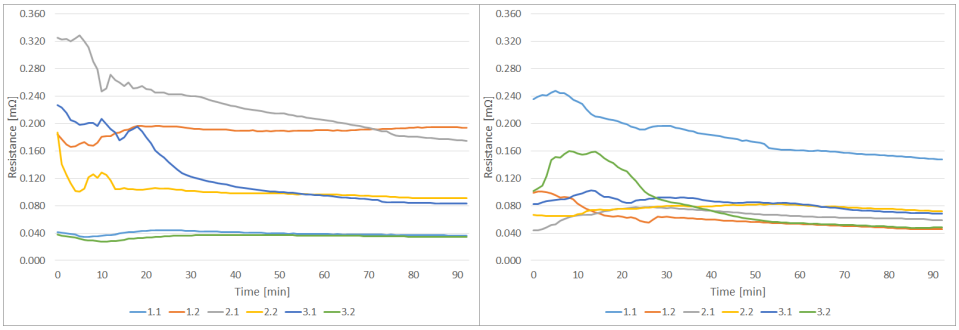

(a) Type I **(b)** Type II

Figure L.22: Cycle 22

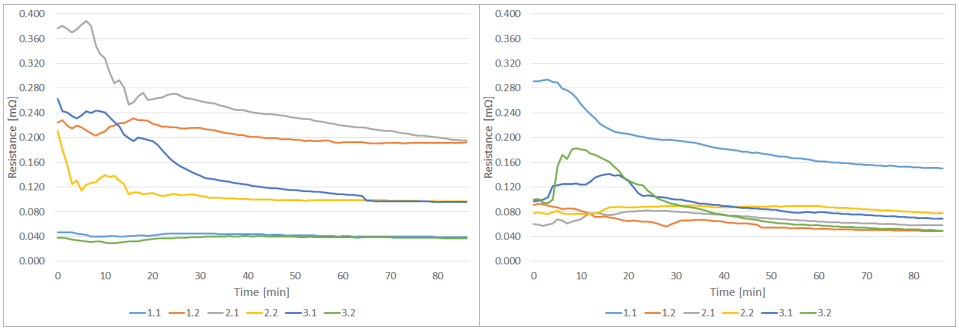

(a) Type I **(b)** Type II

Figure L.23: Cycle 23

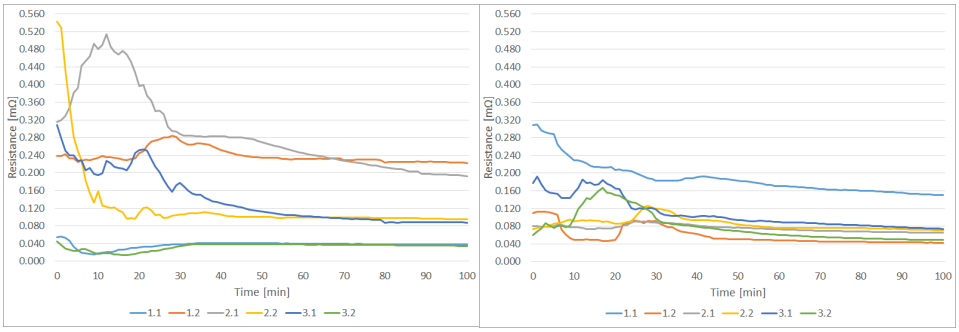

(a) Type I **(b)** Type II

Figure L.24: Cycle 24

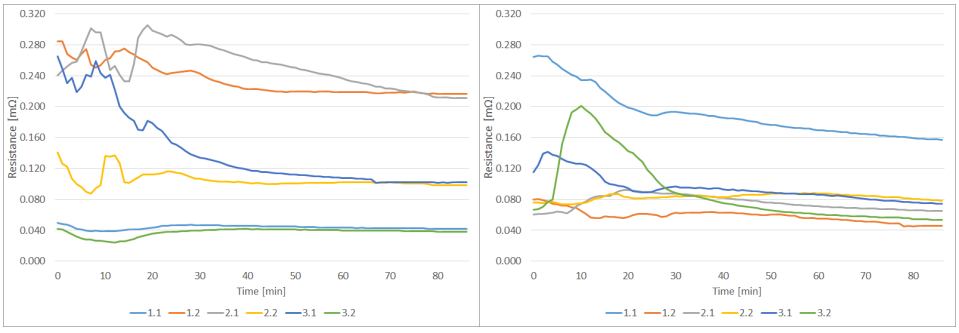

(a) Type I **(b)** Type II

Figure L.25: Cycle 25

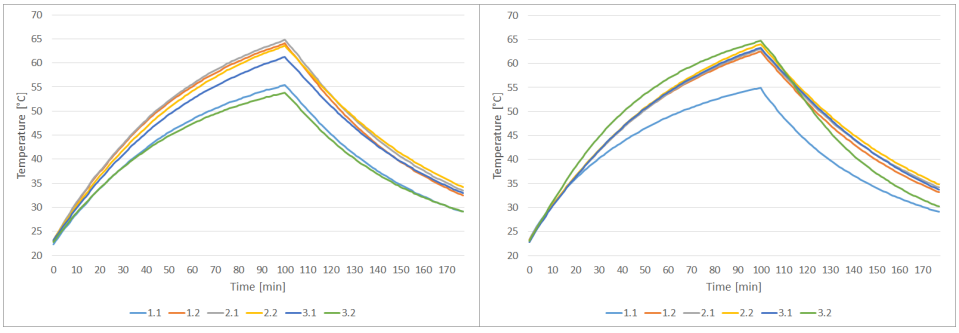

(a) Type I **(b)** Type II

Figure L.26: Cycle 1

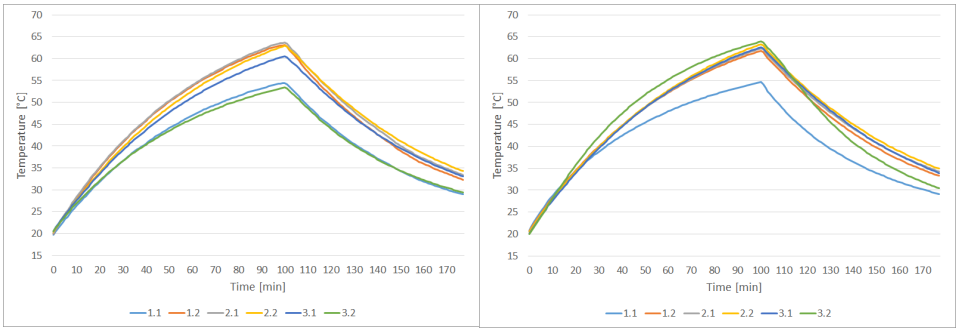

(a) Type I **(b)** Type II

Figure L.27: Cycle 2

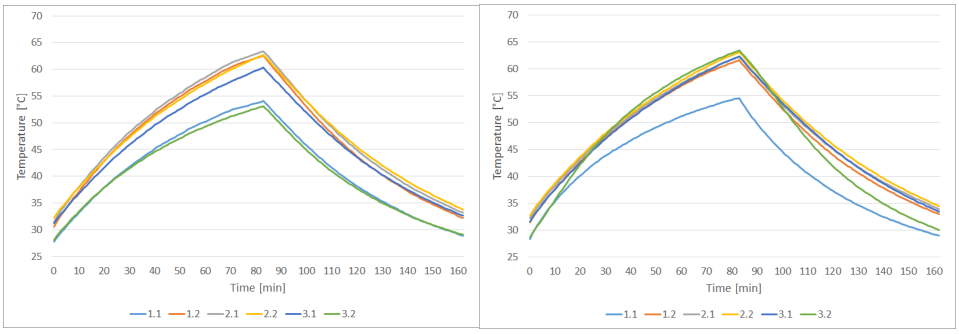

(a) Type I **(b)** Type II

Figure L.28: Cycle 3

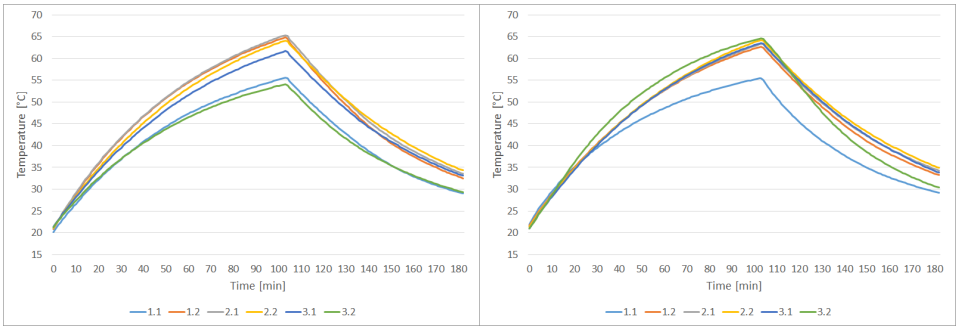

(a) Type I **(b)** Type II

Figure L.29: Cycle 4

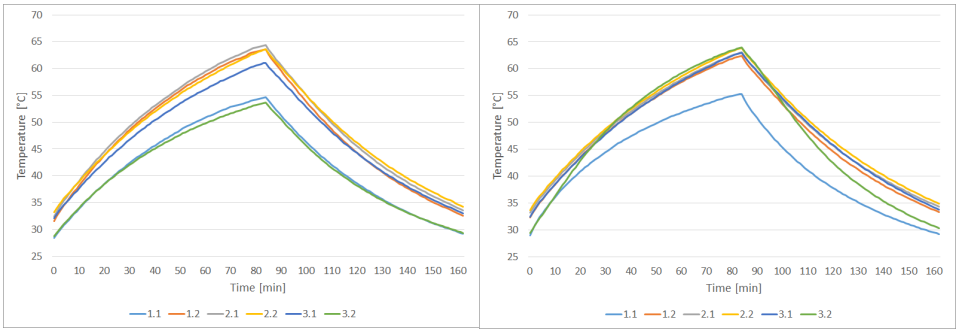

(a) Type I **(b)** Type II

Figure L.30: Cycle 5

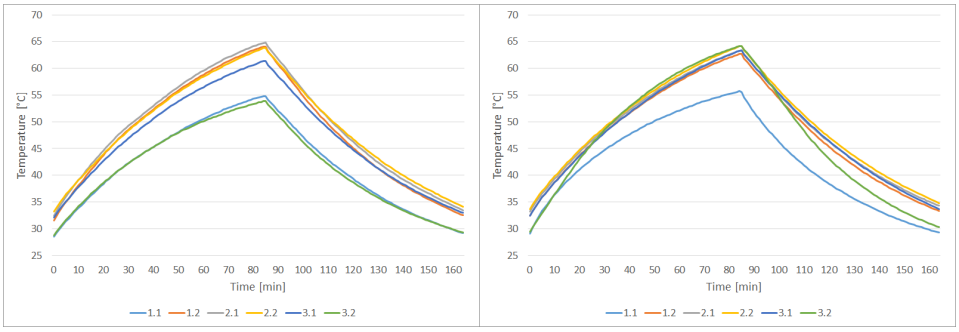

(a) Type I **(b)** Type II

Figure L.31: Cycle 6

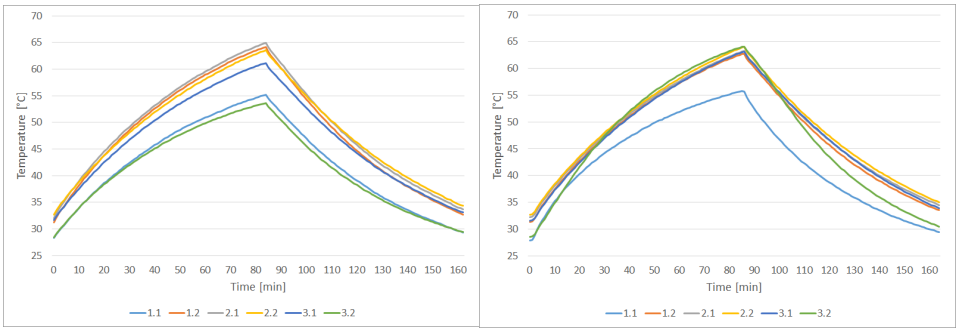

(a) Type I **(b)** Type II

Figure L.32: Cycle 7

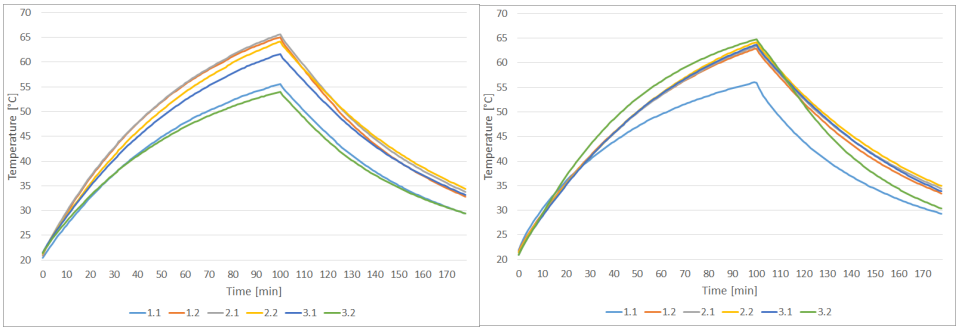

(a) Type I **(b)** Type II

Figure L.33: Cycle 8

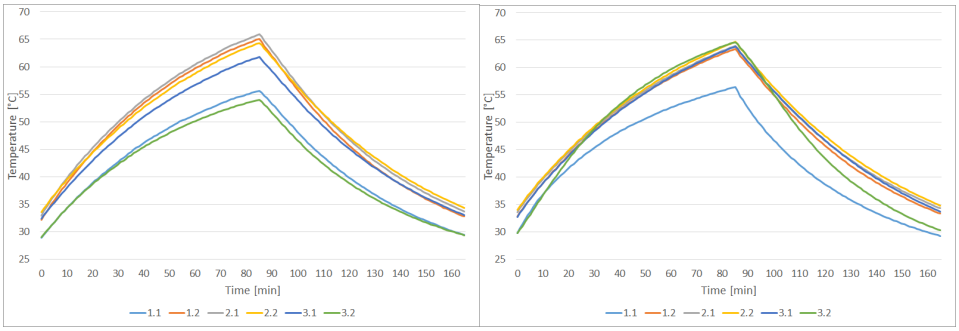

(a) Type I **(b)** Type II

Figure L.34: Cycle 9

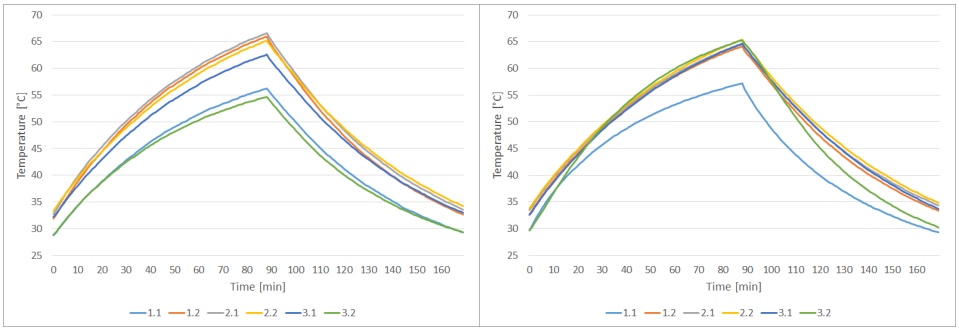

(a) Type I **(b)** Type II

Figure L.35: Cycle 10

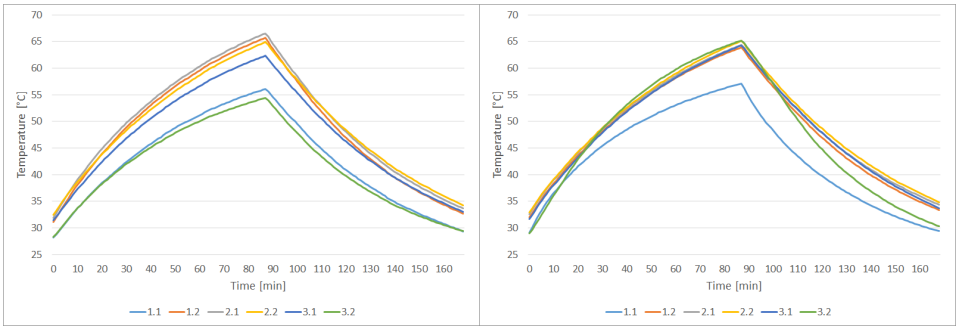

(a) Type I **(b)** Type II

Figure L.36: Cycle 11

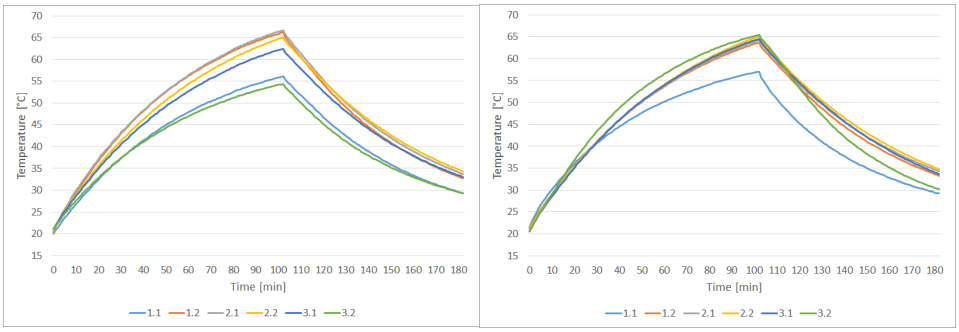

(a) Type I **(b)** Type II

Figure L.37: Cycle 12

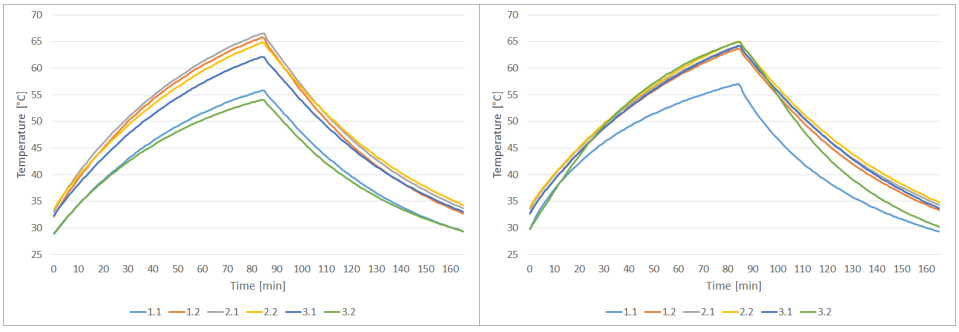

(a) Type I **(b)** Type II

Figure L.38: Cycle 13

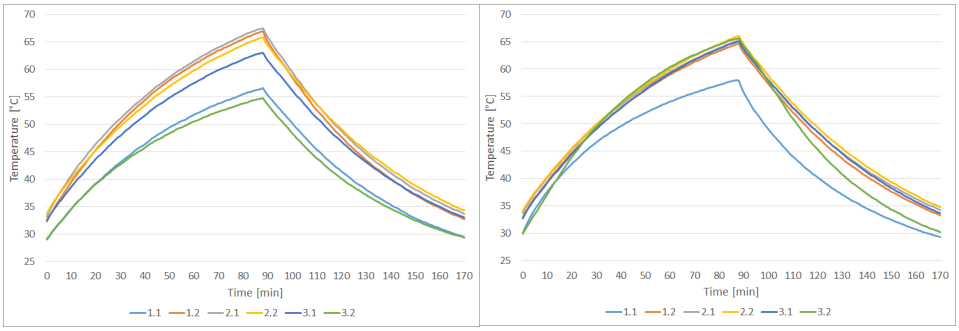

(a) Type I **(b)** Type II

Figure L.39: Cycle 14

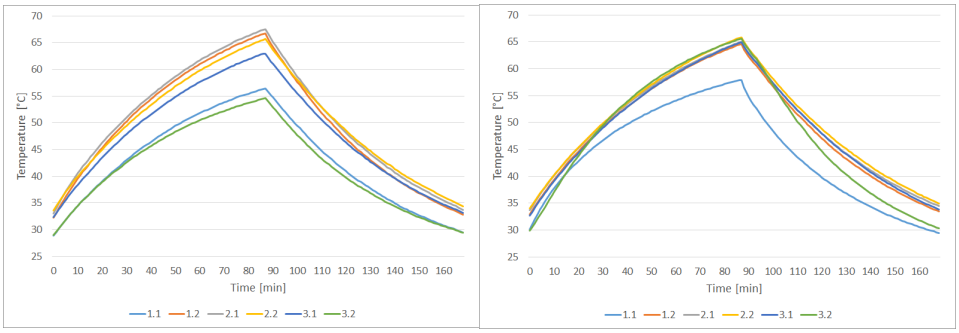

(a) Type I **(b)** Type II

Figure L.40: Cycle 15

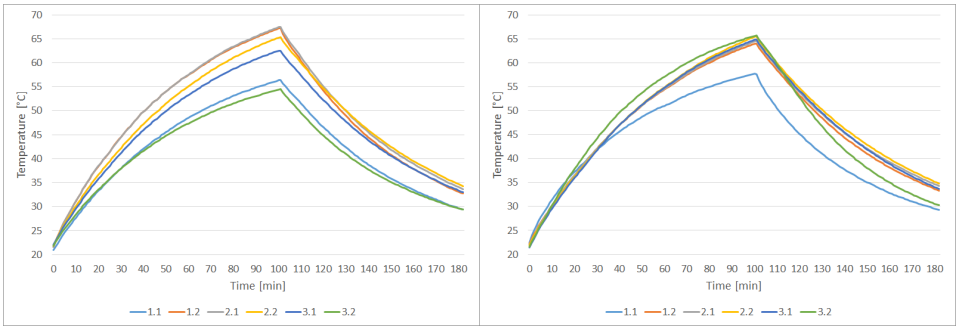

(a) Type I **(b)** Type II

Figure L.41: Cycle 16

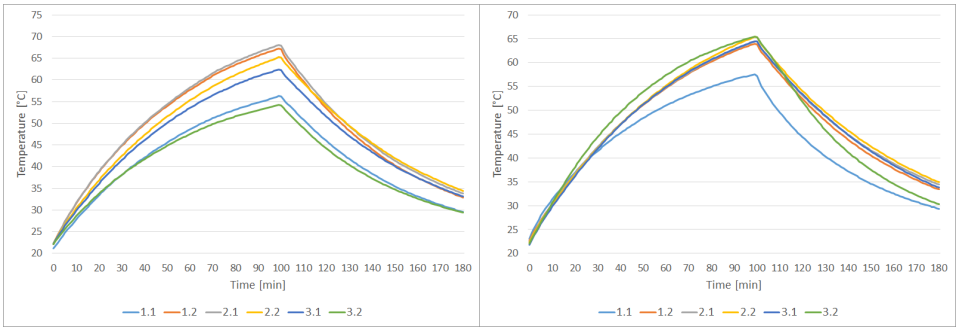

(a) Type I **(b)** Type II

Figure L.42: Cycle 17

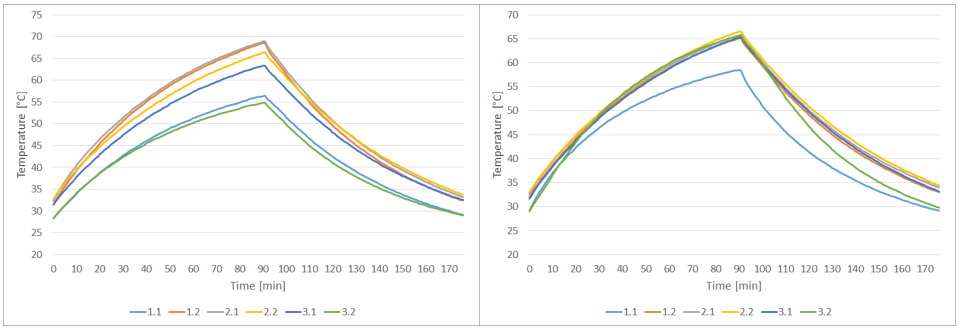

(a) Type I **(b)** Type II

Figure L.43: Cycle 18

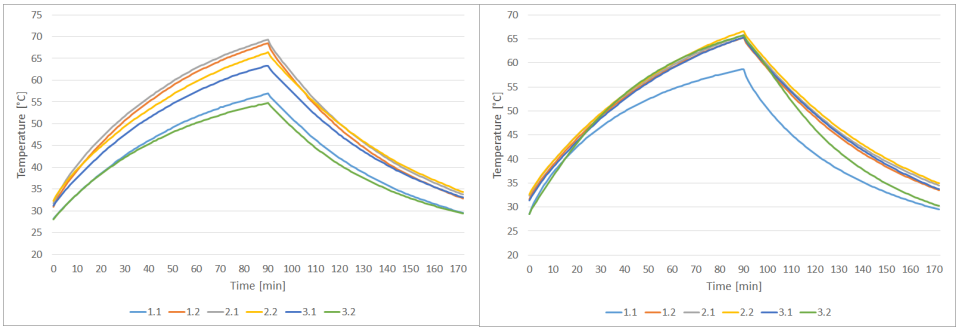

(a) Type I **(b)** Type II

Figure L.44: Cycle 19

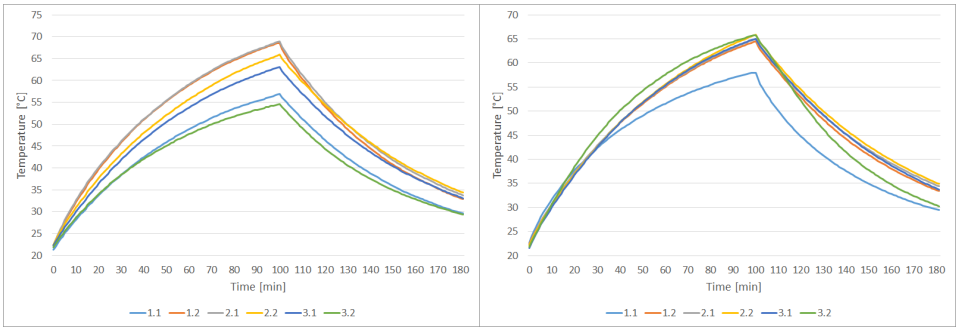

(a) Type I **(b)** Type II

Figure L.45: Cycle 20

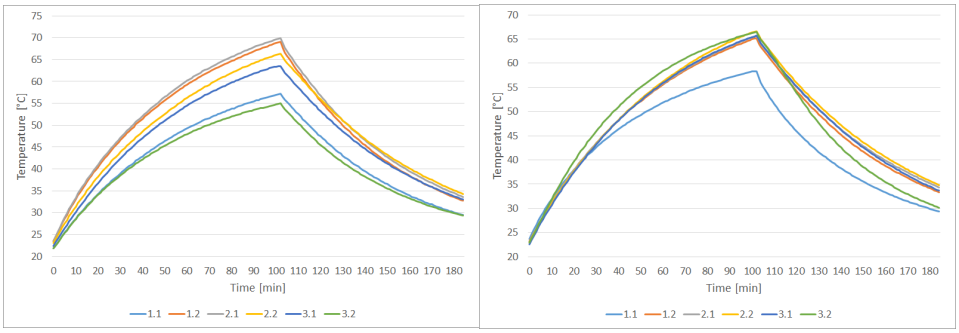

(a) Type I **(b)** Type II

Figure L.46: Cycle 21

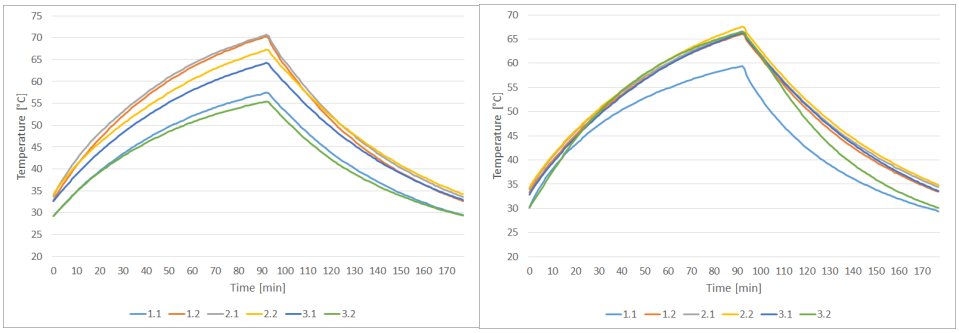

(a) Type I **(b)** Type II

Figure L.47: Cycle 22

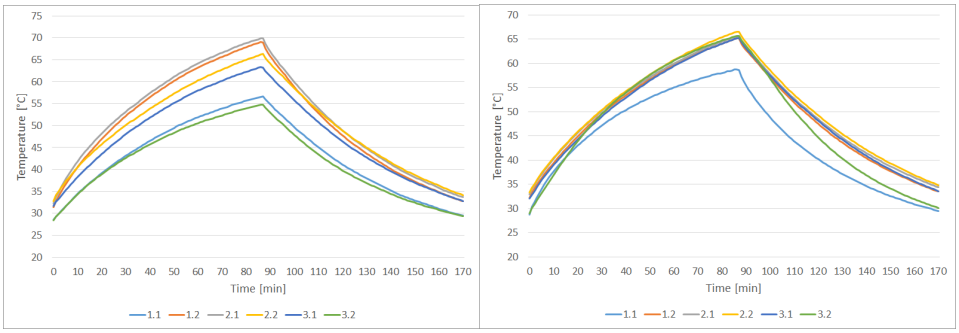

(a) Type I **(b)** Type II

Figure L.48: Cycle 23

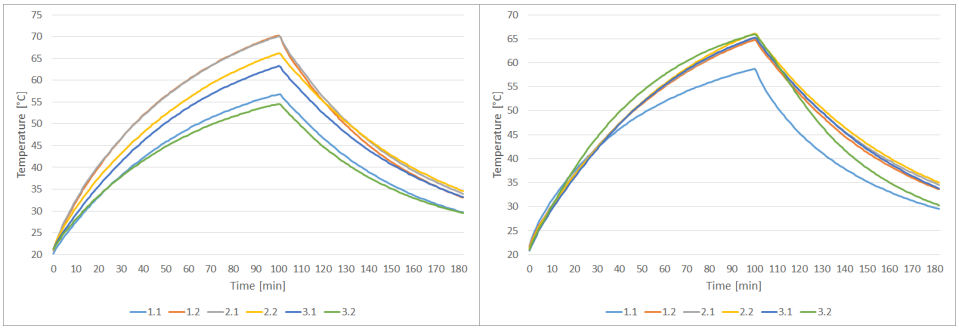

(a) Type I **(b)** Type II

Figure L.49: Cycle 24

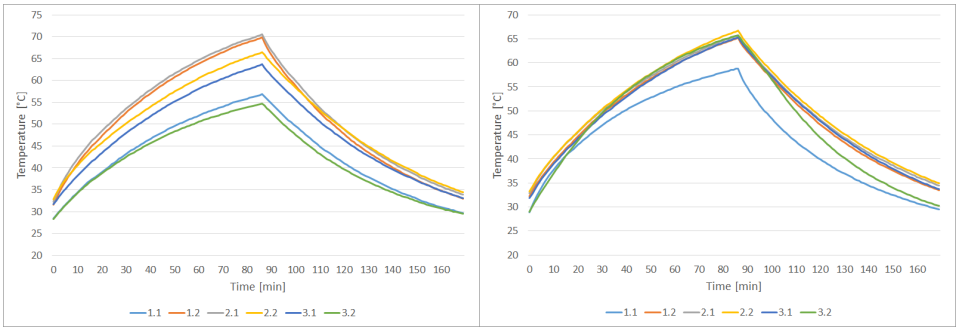

(a) Type I **(b)** Type II

Figure L.50: Cycle 25

M Resistance and temperature plots from the main heat cycles

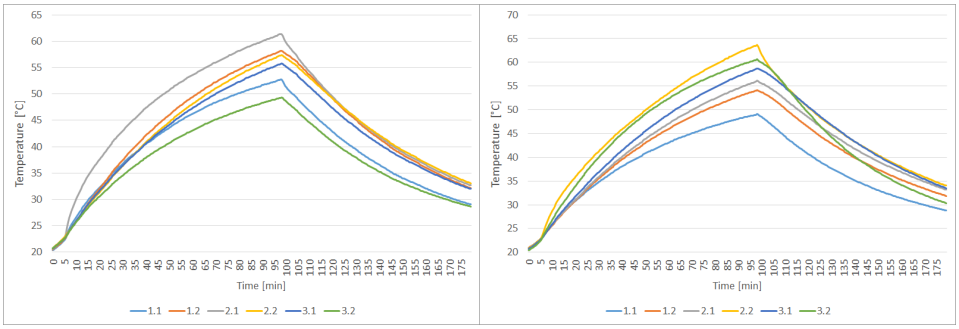

(a) Type I **(b)** Type II

Figure M.1: 30 A

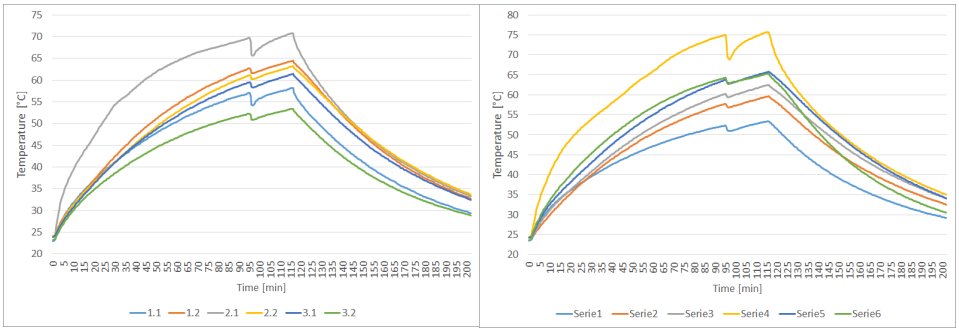

(a) Type I **(b)** Type II

Figure M.2: 40 A

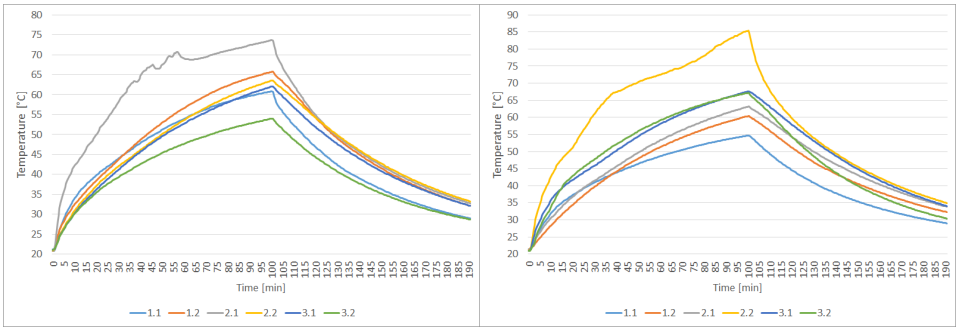

(a) Type I **(b)** Type II

Figure M.3: 45 A

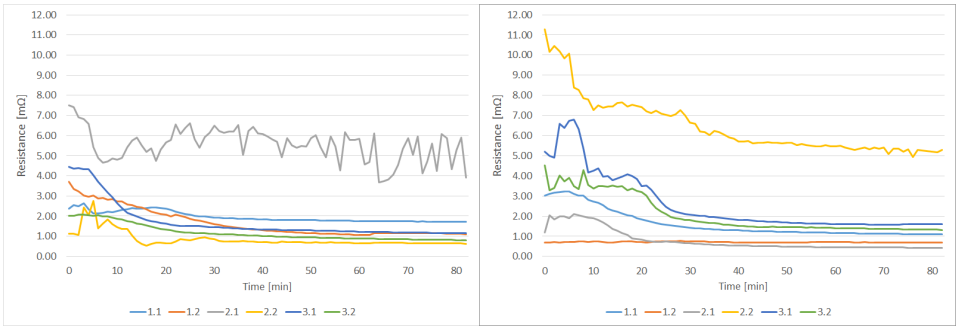

(a) Type I **(b)** Type II

Figure M.4: Cycle 1

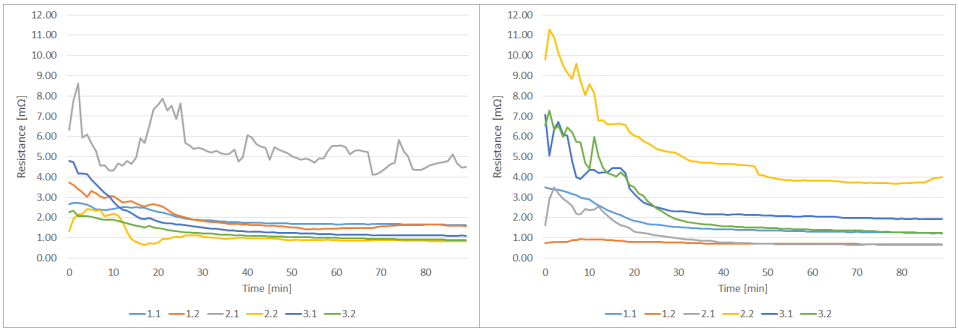

(a) Type I **(b)** Type II

Figure M.5: Cycle 2

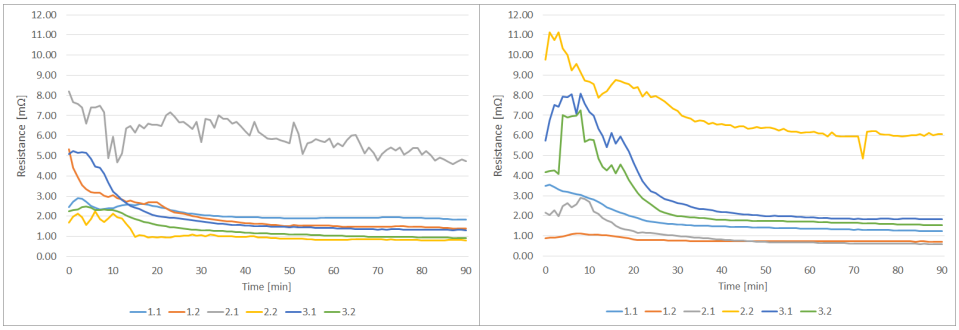

(a) Type I **(b)** Type II

Figure M.6: Cycle 3

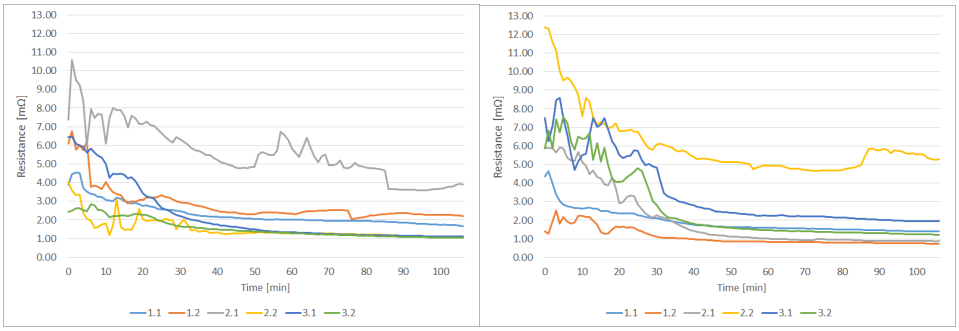

(a) Type I **(b)** Type II

Figure M.7: Cycle 4

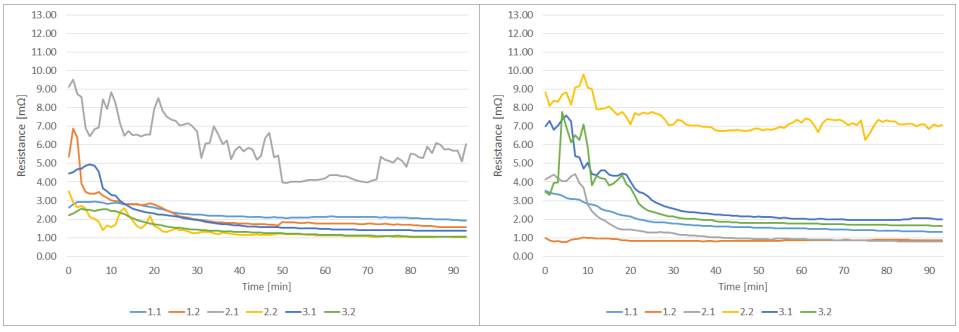

(a) Type I **(b)** Type II

Figure M.8: Cycle 5

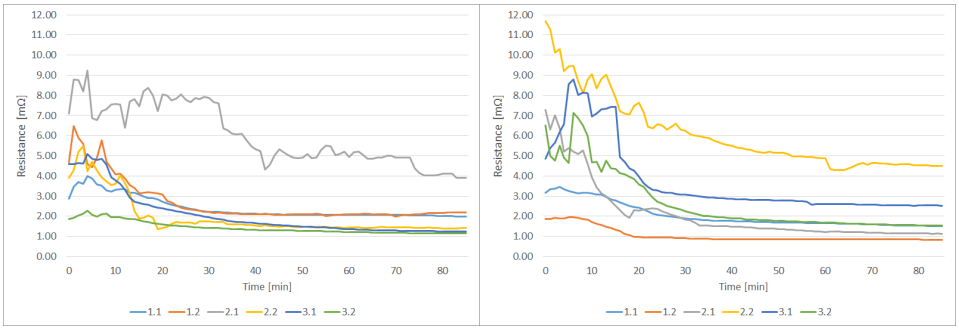

(a) Type I **(b)** Type II

Figure M.9: Cycle 6

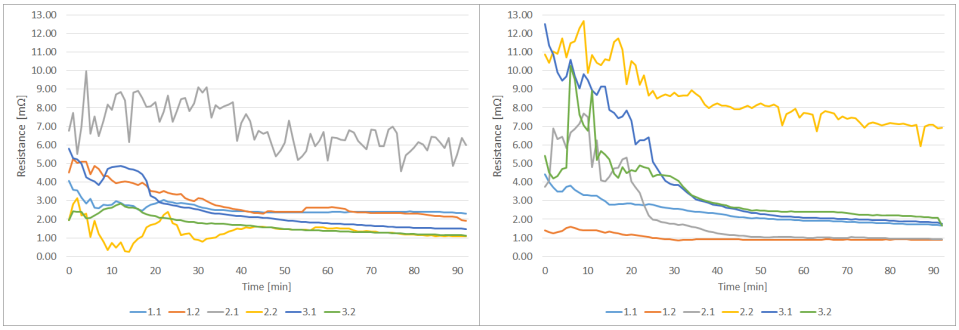

(a) Type I **(b)** Type II

Figure M.10: Cycle 7

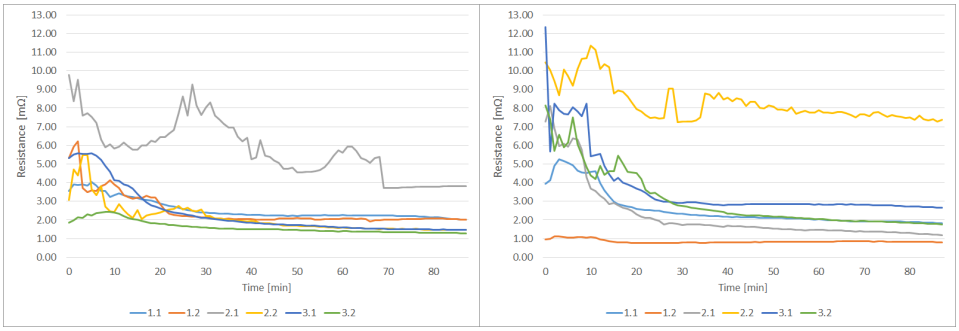

(a) Type I **(b)** Type II

Figure M.11: Cycle 8

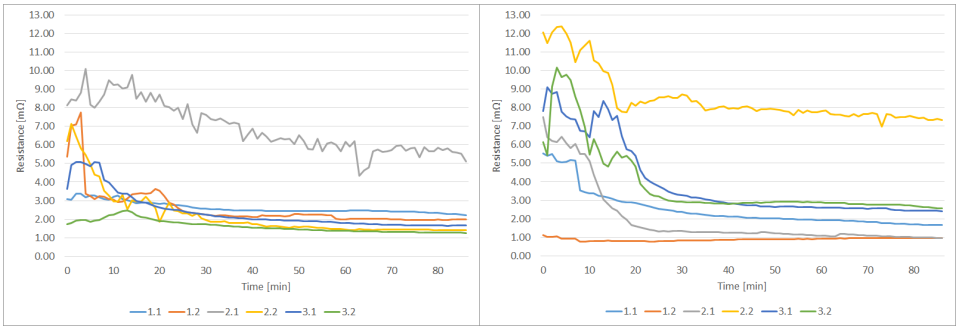

(a) Type I **(b)** Type II

Figure M.12: Cycle 9

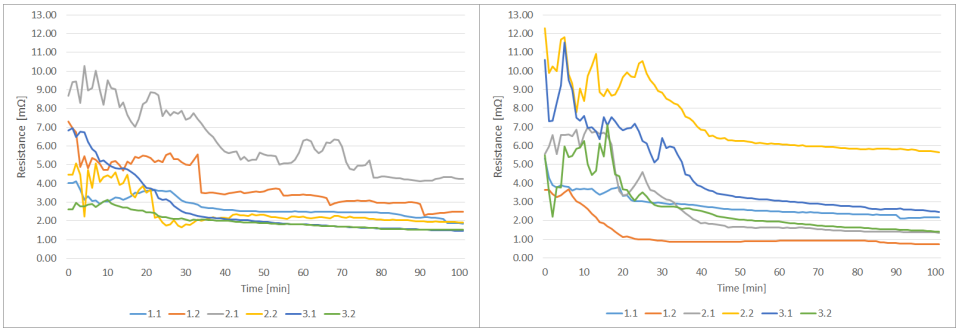

(a) Type I **(b)** Type II

Figure M.13: Cycle 10

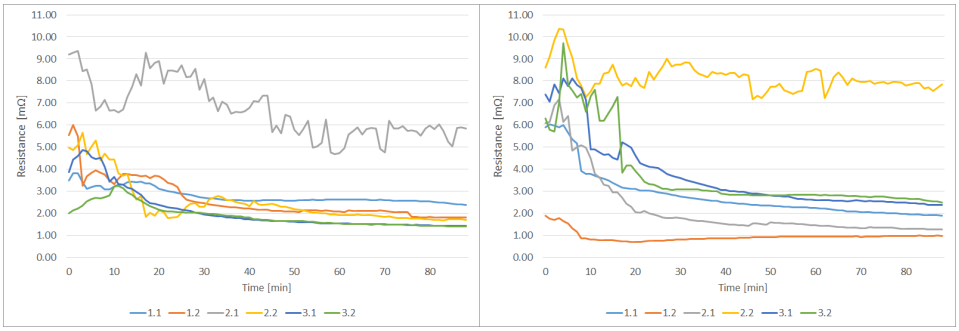

(a) Type I **(b)** Type II

Figure M.14: Cycle 11

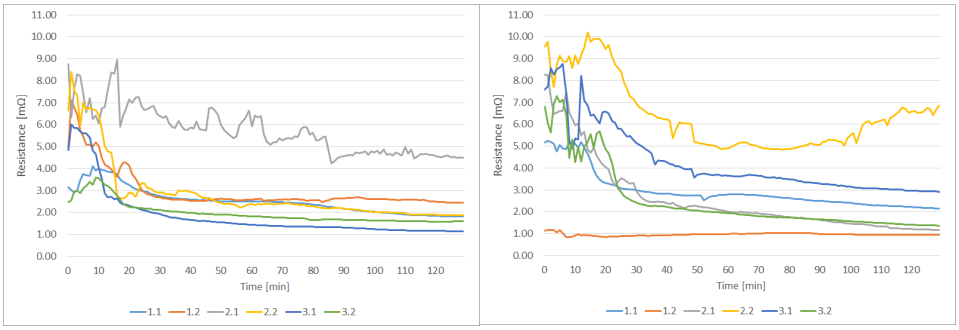

(a) Type I **(b)** Type II

Figure M.15: Cycle 12

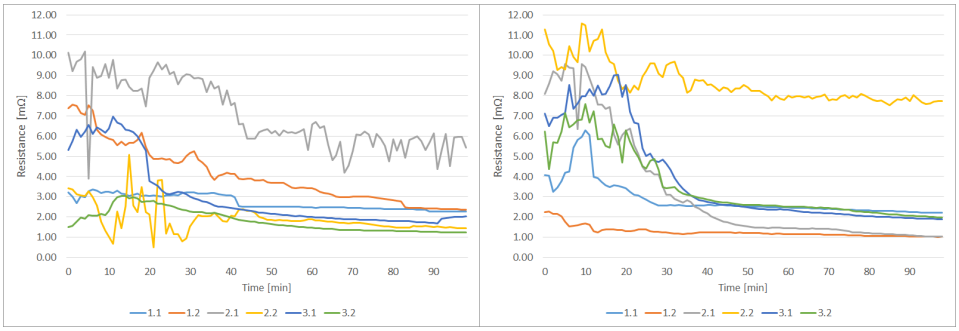

(a) Type I **(b)** Type II

Figure M.16: Cycle 13

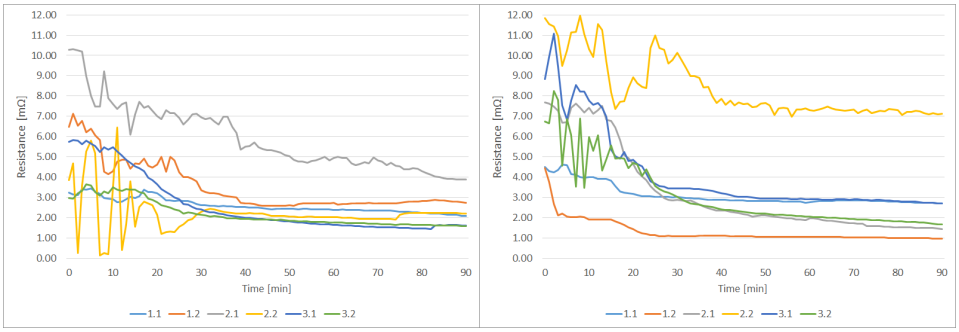

(a) Type I **(b)** Type II

Figure M.17: Cycle 14

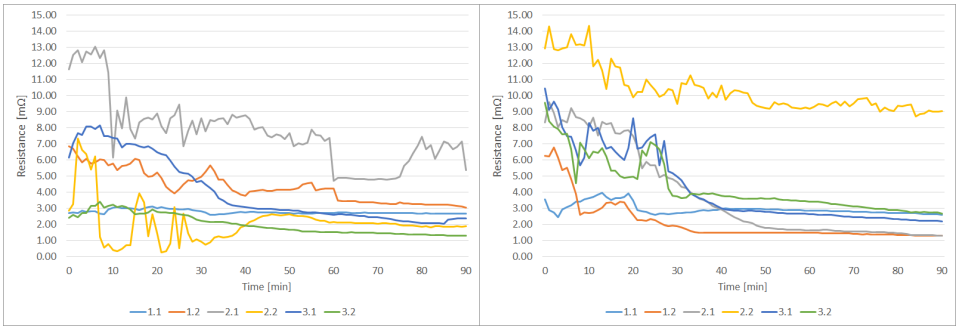

(a) Type I **(b)** Type II

Figure M.18: Cycle 15

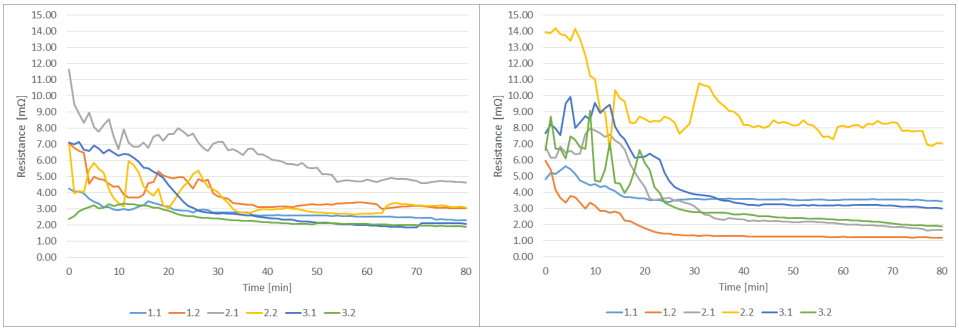

(a) Type I **(b)** Type II

Figure M.19: Cycle 16

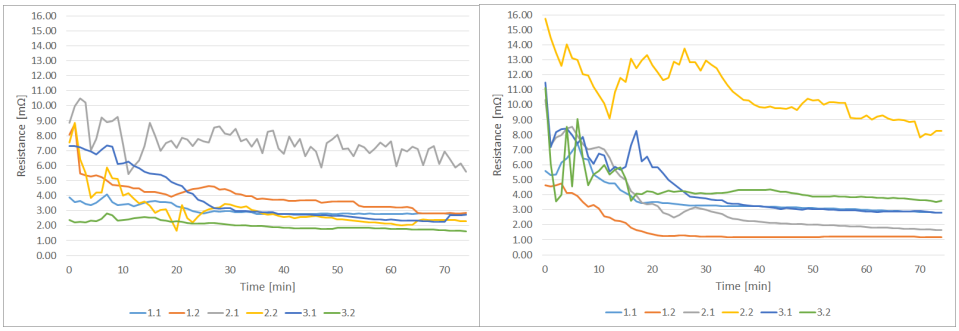

(a) Type I **(b)** Type II

Figure M.20: Cycle 17

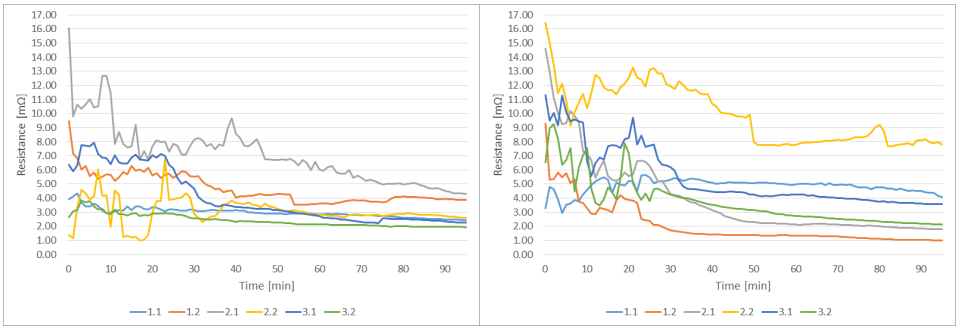

(a) Type I **(b)** Type II

Figure M.21: Cycle 18

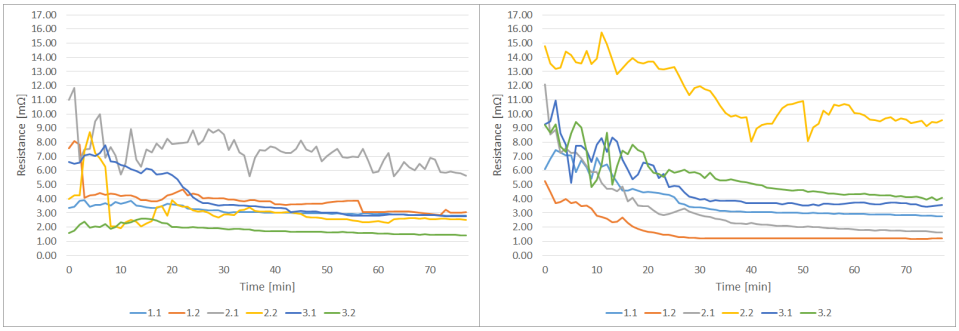

(a) Type I **(b)** Type II

Figure M.22: Cycle 19

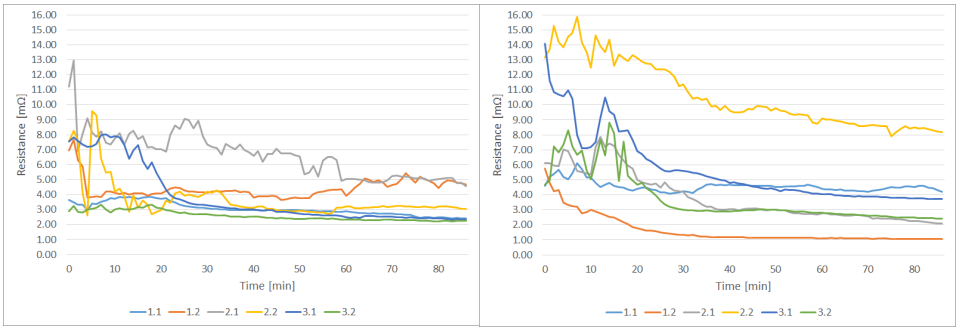

(a) Type I **(b)** Type II

Figure M.23: Cycle 20

(a) Type I **(b)** Type II

Figure M.24: Cycle 21

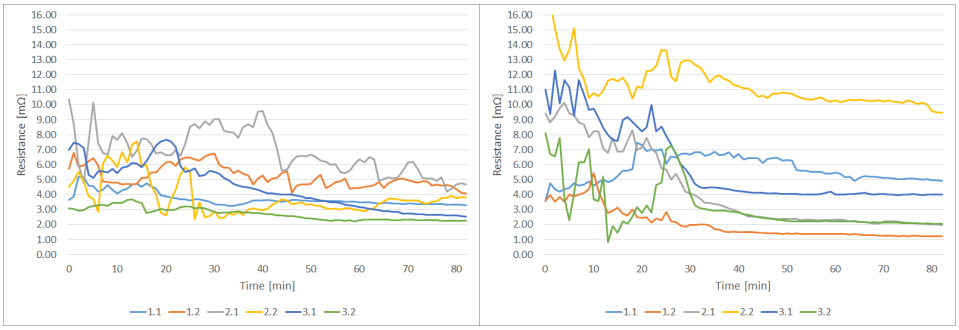

(a) Type I **(b)** Type II

Figure M.25: Cycle 22

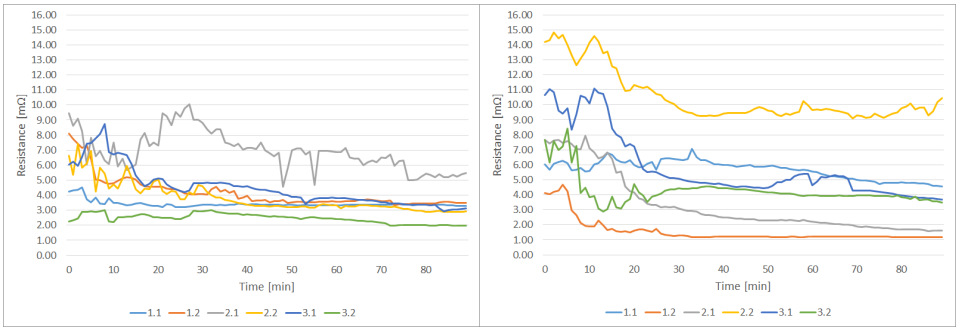

(a) Type I **(b)** Type II

Figure M.26: Cycle 23

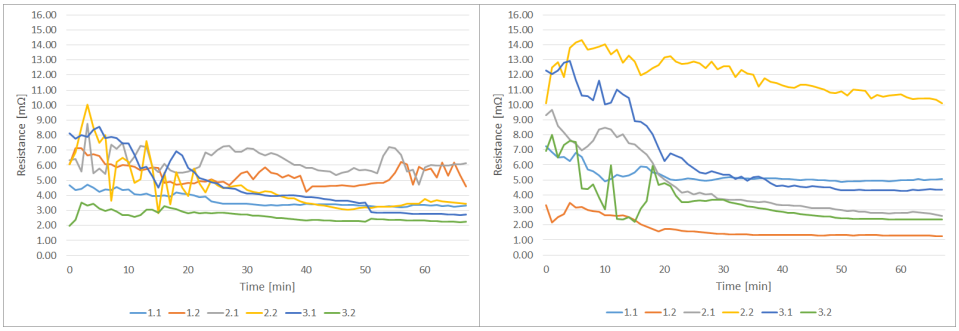

(a) Type I **(b)** Type II

Figure M.27: Cycle 24

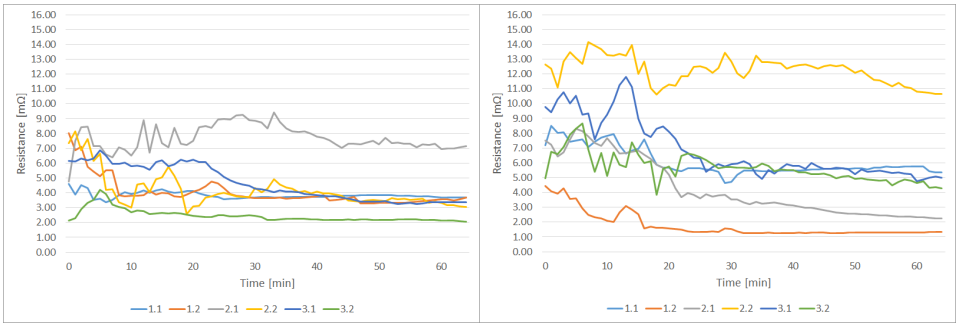

(a) Type I **(b)** Type II

Figure M.28: Cycle 25

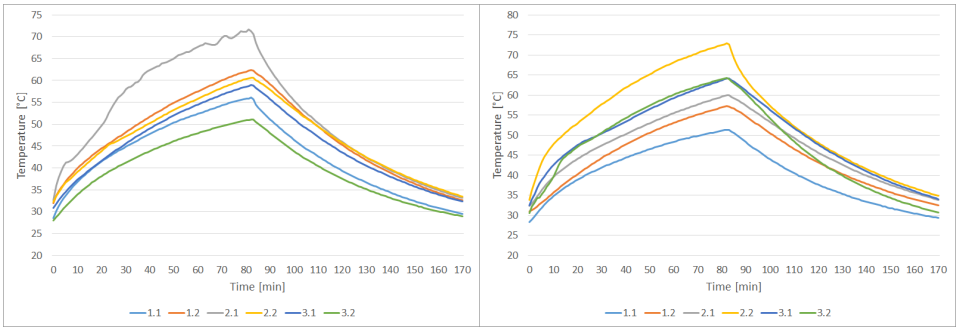

(a) Type I **(b)** Type II

Figure M.29: Cycle 1

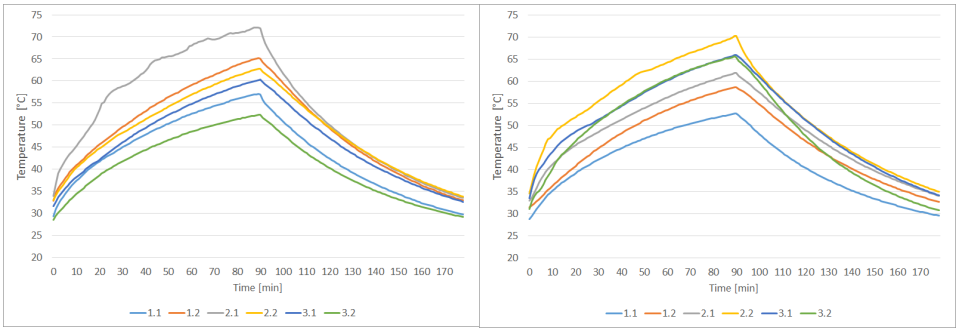

(a) Type I **(b)** Type II

Figure M.30: Cycle 2

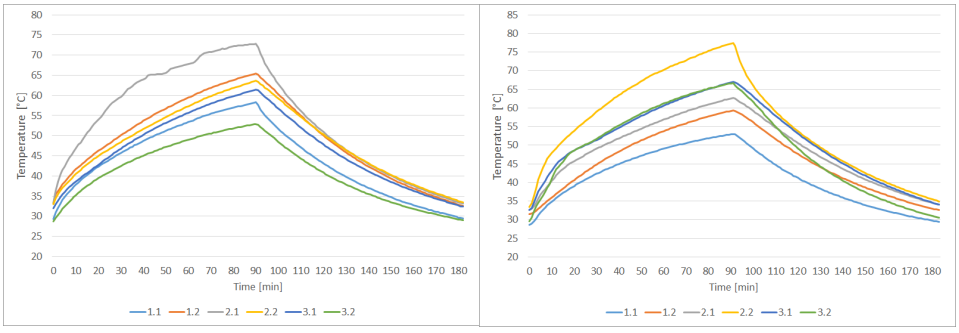

(a) Type I **(b)** Type II

Figure M.31: Cycle 3

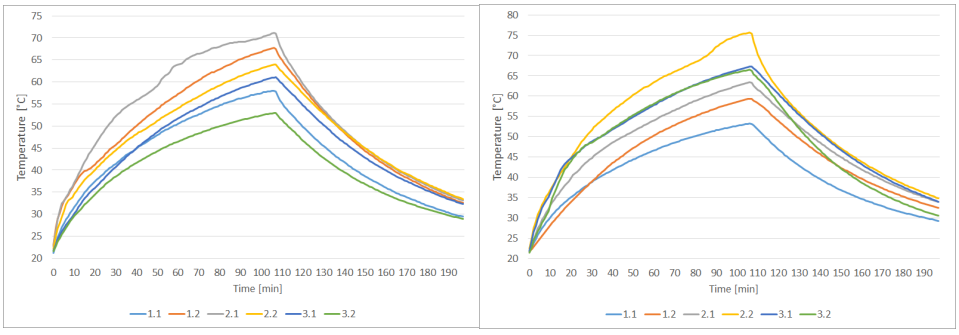

(a) Type I **(b)** Type II

Figure M.32: Cycle 4

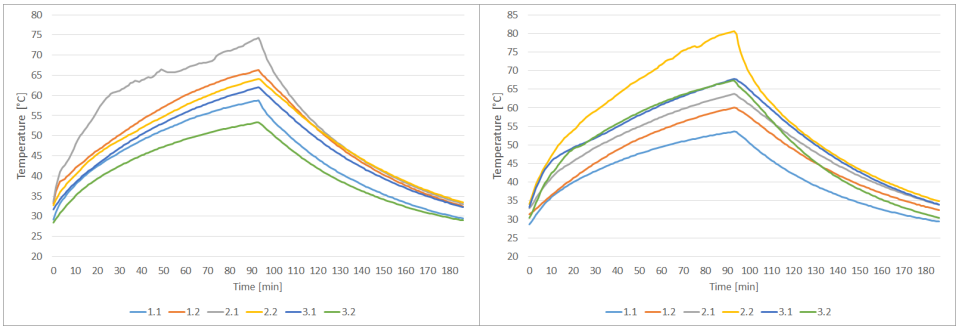

(a) Type I **(b)** Type II

Figure M.33: Cycle 5

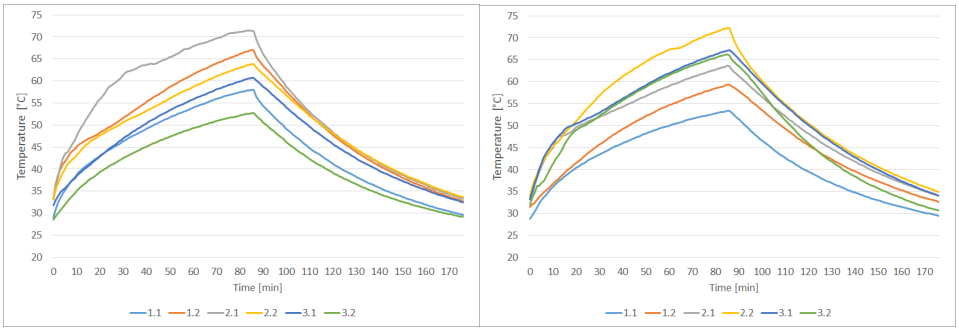

(a) Type I **(b)** Type II

Figure M.34: Cycle 6

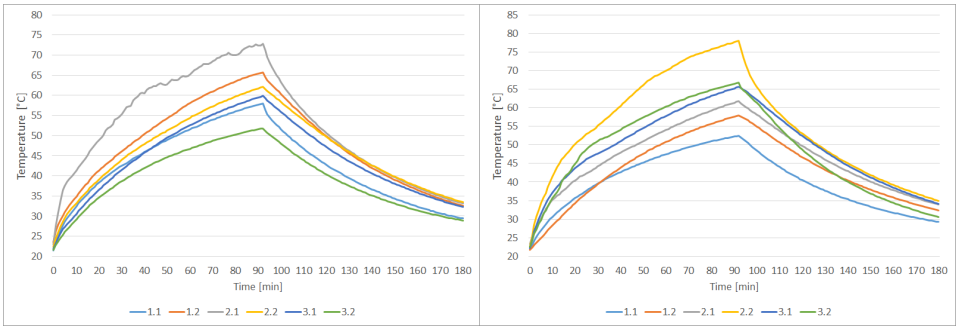

(a) Type I **(b)** Type II

Figure M.35: Cycle 7

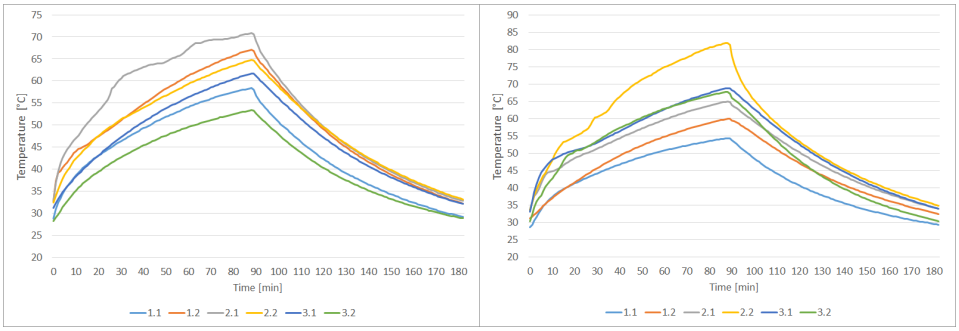

(a) Type I **(b)** Type II

Figure M.36: Cycle 8

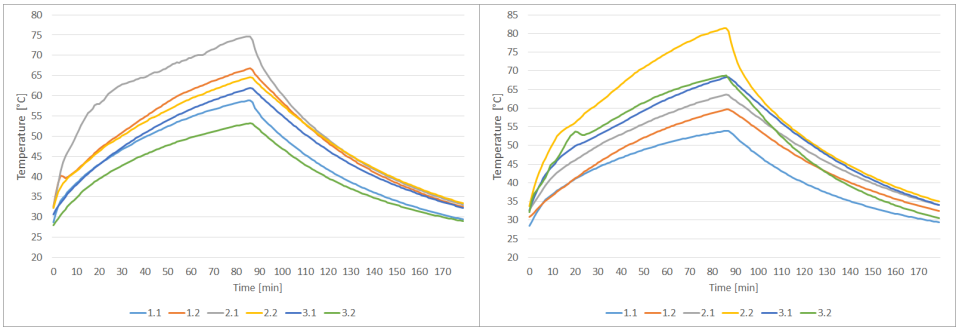

(a) Type I **(b)** Type II

Figure M.37: Cycle 9

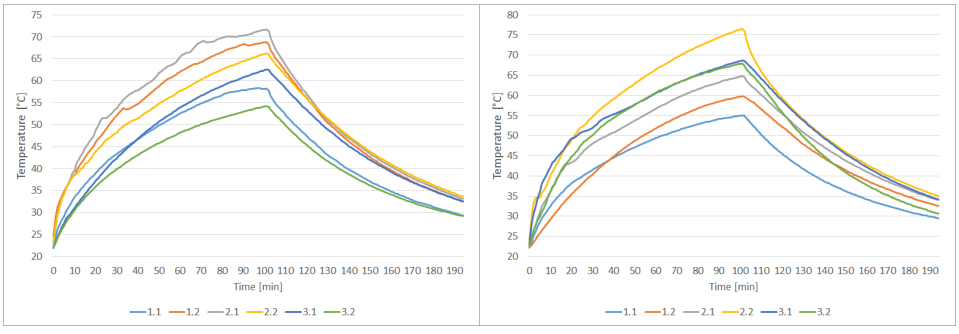

(a) Type I **(b)** Type II

Figure M.38: Cycle 10

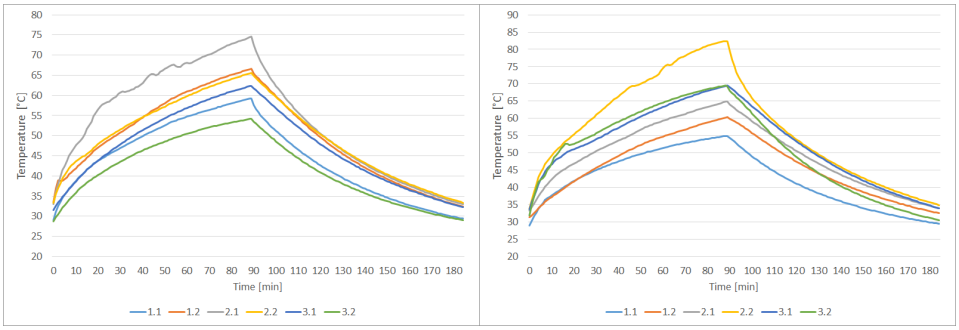

(a) Type I **(b)** Type II

Figure M.39: Cycle 11

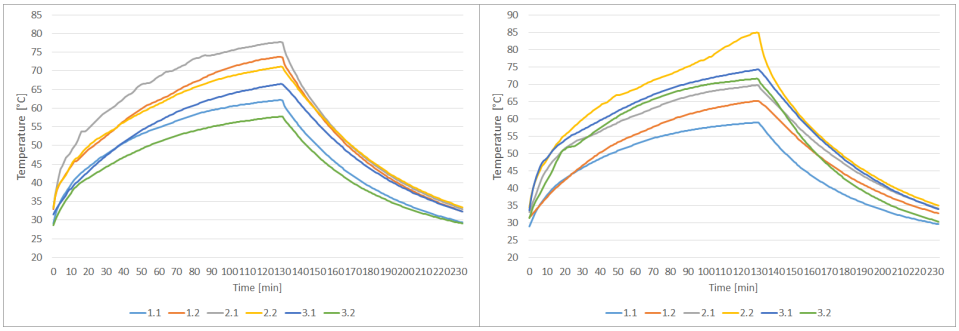

(a) Type I **(b)** Type II

Figure M.40: Cycle 12

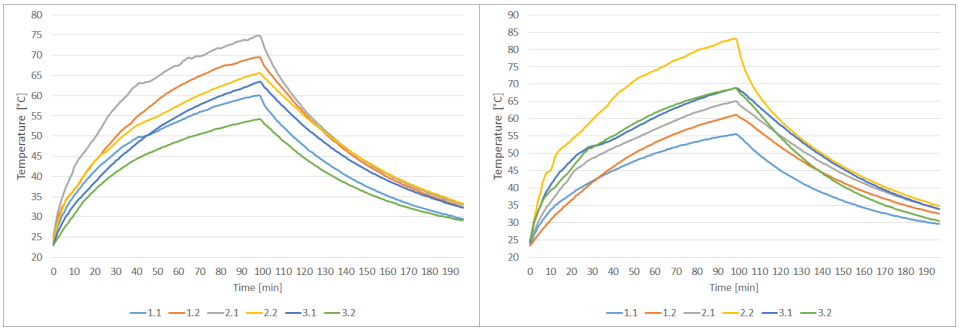

(a) Type I **(b)** Type II

Figure M.41: Cycle 13

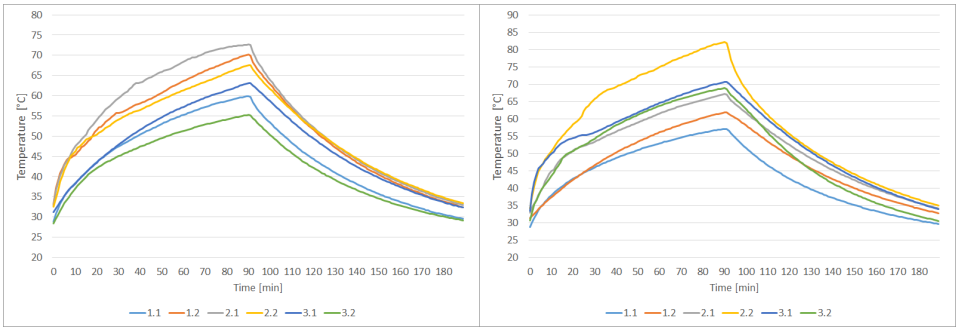

(a) Type I **(b)** Type II

Figure M.42: Cycle 14

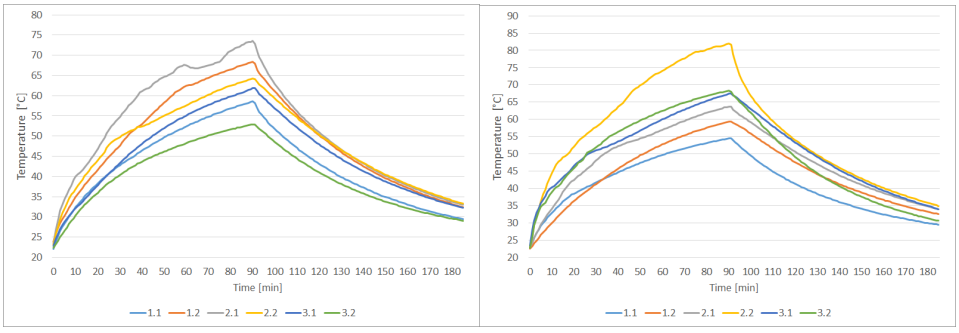

(a) Type I **(b)** Type II

Figure M.43: Cycle 15

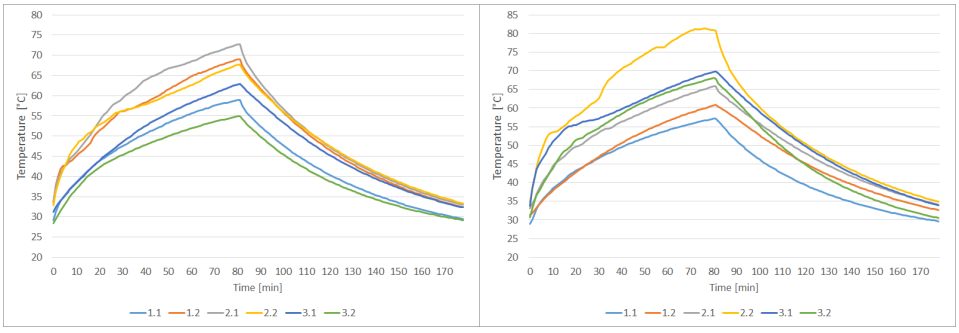

(a) Type I **(b)** Type II

Figure M.44: Cycle 16

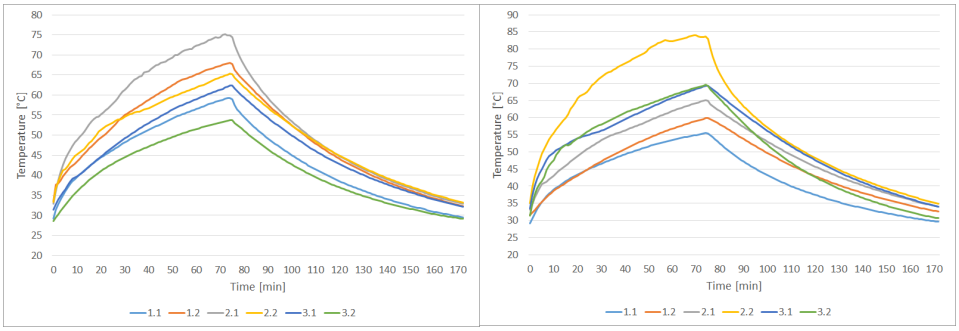

(a) Type I **(b)** Type II

Figure M.45: Cycle 17

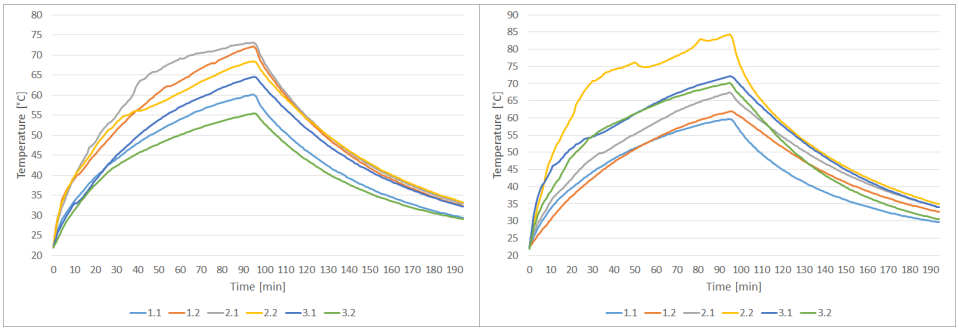

(a) Type I **(b)** Type II

Figure M.46: Cycle 18

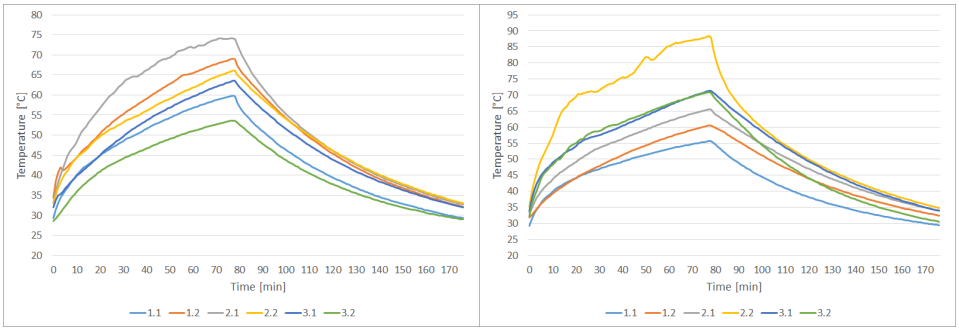

(a) Type I **(b)** Type II

Figure M.47: Cycle 19

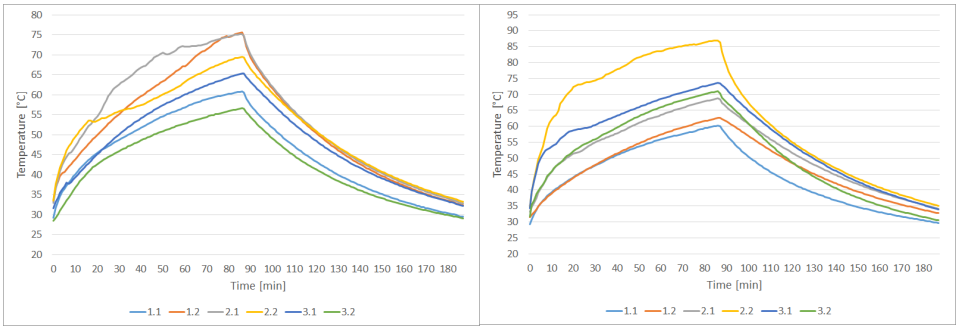

(a) Type I **(b)** Type II

Figure M.48: Cycle 20

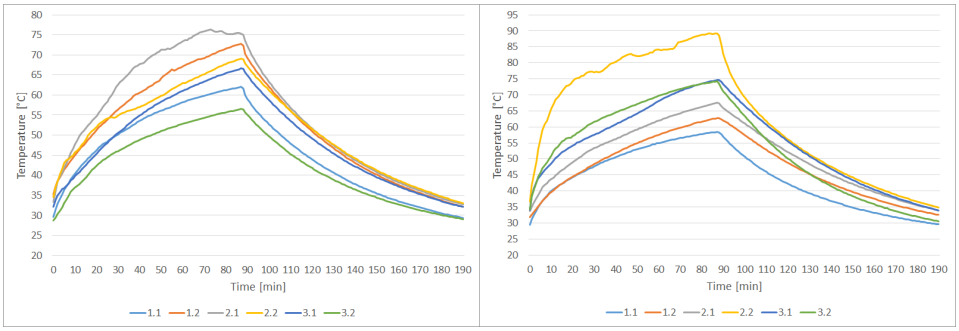

(a) Type I **(b)** Type II

Figure M.49: Cycle 21

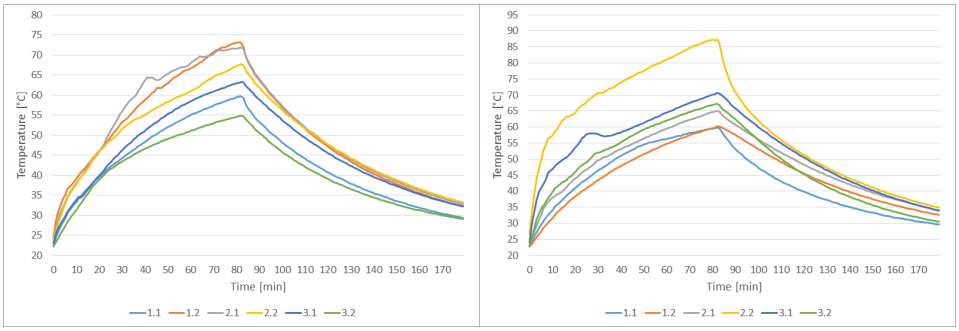

(a) Type I **(b)** Type II

Figure M.50: Cycle 22

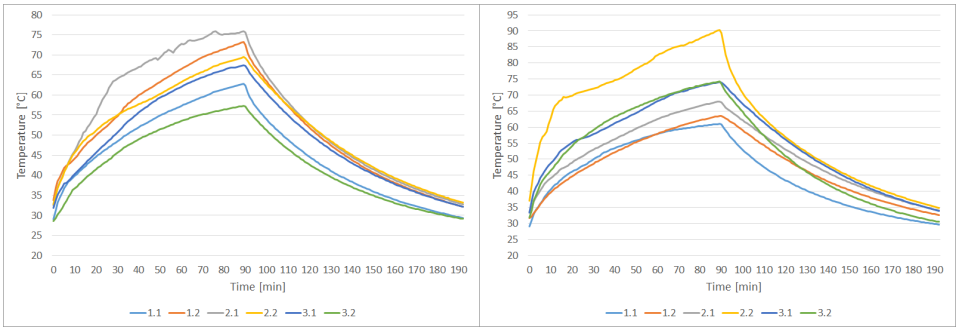

(a) Type I **(b)** Type II

Figure M.51: Cycle 23

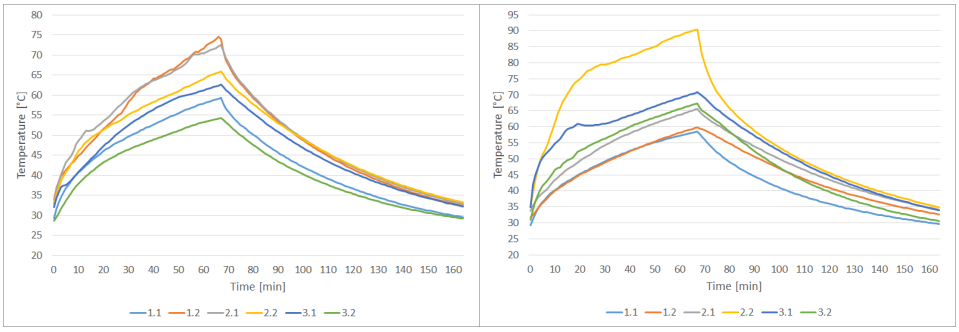

(a) Type I **(b)** Type II

Figure M.52: Cycle 24

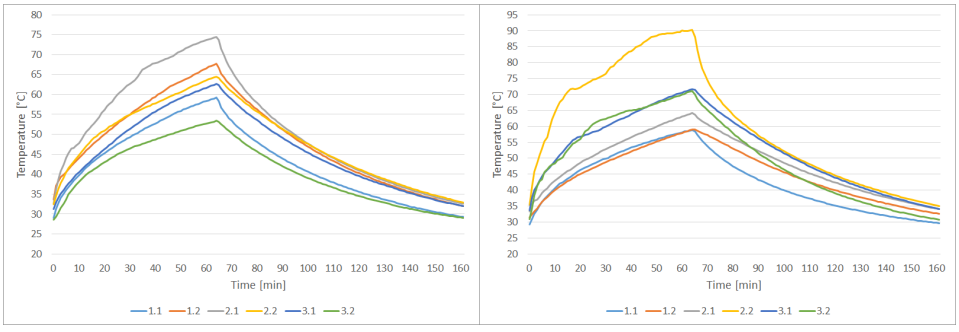

(a) Type I **(b)** Type II

Figure M.53: Cycle 25